INFLUENCE OF ADDITIVES ON THE PHYSCIOCHEMICAL PROPERTIES IN AMORPHOUS FOOD MATRICES

By

JUN LIANG

A Dissertation submitted to the

Graduate School-New Brunswick

Rutgers, The State University of New Jersey

in partial fulfillment of the requirements

for the degree of

Doctor of Philosophy

Graduate Program in Food Science

Written under the direction of

Dr. Richard D. Ludescher

And approved by

_____

_____

_____

_____

New Brunswick, New Jersey

October, 2014

ABSTRACT OF THE DISSERTATION

Influence of Additives on the Physicochemical Properties in Amorphous Food Matrices

By JUN LIANG

Dissertation Director: Richard D. Ludescher

There is lot of literature on the physico-chemical changes occurring in the ingredients (mainly starches, proteins) during food processing, but there is a need to understand how these biopolymers interact with the minor ingredients (plasticizer, sugars, emulsifiers, antioxidants, etc) during processing and thus their impact on the final product quality.

Phosphorescence spectroscopy allows us to monitor the modes, rates, and distribution of molecular mobility in complex foods, providing the molecular detail necessary to connect food quality and stability to molecular structure and mobility. The mobility contours generated from this research provided us with information about the onset temperature and level of molecular mobility required to support permeability of atmospheric oxygen. The phosphorescence emission spectra and lifetimes of the triplet probe Erythrosin B and Tryptophan embedded in the biomaterial films provide measures of the modes, rates, and distribution of molecular mobility in the film, providing the molecular detail necessary to connect food quality and stability to molecular structure and mobility. The interactions between the biopolymers with food additives depend on the molecular weight and structures of biopolymers. In this research, we have used embedded triplet probes (erythrosin B, tryptophan) to provide a facile and sensitive measure of matrix molecular mobility and oxygen permeability, AFM to imagine the matrix microstructure,

IR to detect the hydrogen bond network and protein structure changes, fluorescence spectroscopy to determine the rate of browning reaction, X-ray to measure the crystallinity index and DSC to measure the T_g of matrices in the food systems including sugars, starch and proteins. By comparing those data we acquired a detailed concept-map about the mechanism how the interactions between the biopolymers and food additives could influence the physico-chemical properties of amorphous food matrices.

ACKNOWLEDGEMENT

I would sincerely like to articulate my heartfelt thanks to my advisor Dr. Ludescher, whose thought-provoking suggestions and directions have kept me on task and have challenged me to think, reflect, and act to find my own voices in research. His kindness and patient tutoring helped me to achieve my ultimate education goal. His advices on research direction and methodologies are precious for me in my scientific career.

I would like to thank my dissertation committee members, Dr. Alan, H. King, Dr. Paul Takhistov, and Dr. Yoke-chen Chang for their guidance and suggestions.

I would like to express my appreciation to Andrew Draganski, Sanaz Jalalian, Ping Wang, Melinda Ligneres, Maria D. Corradini and Yan, Wang for their help on the lab work.

I dedicate this dissertation to my family whose adamant support and trust allowed me to fulfill my intellectual inspirations. Lina Sun, the most devoted wife, spiritual and affectionate mother I know, your insights have helped me grow and mature academically. Thank you for all you love and guidance. Benjamin, whose angelic smile and silvery laughter made this journey tolerable and joyous, you are my proudest achievement and your sweetness and gentleness, is my biggest source of inspiration.

TABLE OF CONTENTS

LIST OF TABLES

LIST OF FIGURES

Chapter I: Introduction

1. Physicochemical properties in amorphous food matrices1

1.1 Molecular mobility

Molecular mobility is an important temperature dependent factor and is often considered to be one of the main factors that affect rates of deteriorative changes and shelf life of food materials. Below the normal glass transition amorphous or partially crystalline polymers also exhibit secondary relaxations. Amorphous solids may differ in terms of the number and modes of molecular mobility that are active under specified conditions of temperature and composition. These are normally given the notations β, γ, δ, etc., in decreasing order of occurrence (Figure 1).

Molecular mobility is related to phenomena such as diffusion, viscosity and the glass transition (Hancock, Shamblin & Zografi, 1995) and can be viewed as a fundamental molecular determinate of macroscopic physical, chemical, and sensory qualities of foods. It is now generally recognized that molecular mobility is associated with the stability and quality of amorphous biomaterials by modulating specific physical processes and chemical reactions involving the translational diffusion, rotational motions or intramolecular motions (Shalaev & Zografi, 1996). Physical processes such as crystallization and chemical reactions such as Maillard browning require molecular mobility; molecules must diffuse and orient to either crystallize or react. In fluid solutions, diffusion is typically orders of magnitude faster than reaction rate and thus changes in viscosity that influence diffusion do not affect rate. In amorphous solids, due to their high viscosity, diffusion is often the rate limiting step and changes

in viscosity that influence diffusion significantly influences the reaction rate. (Le Meste, Champion, Roudaut, Blond & Simatos, 2002)

Figure 1

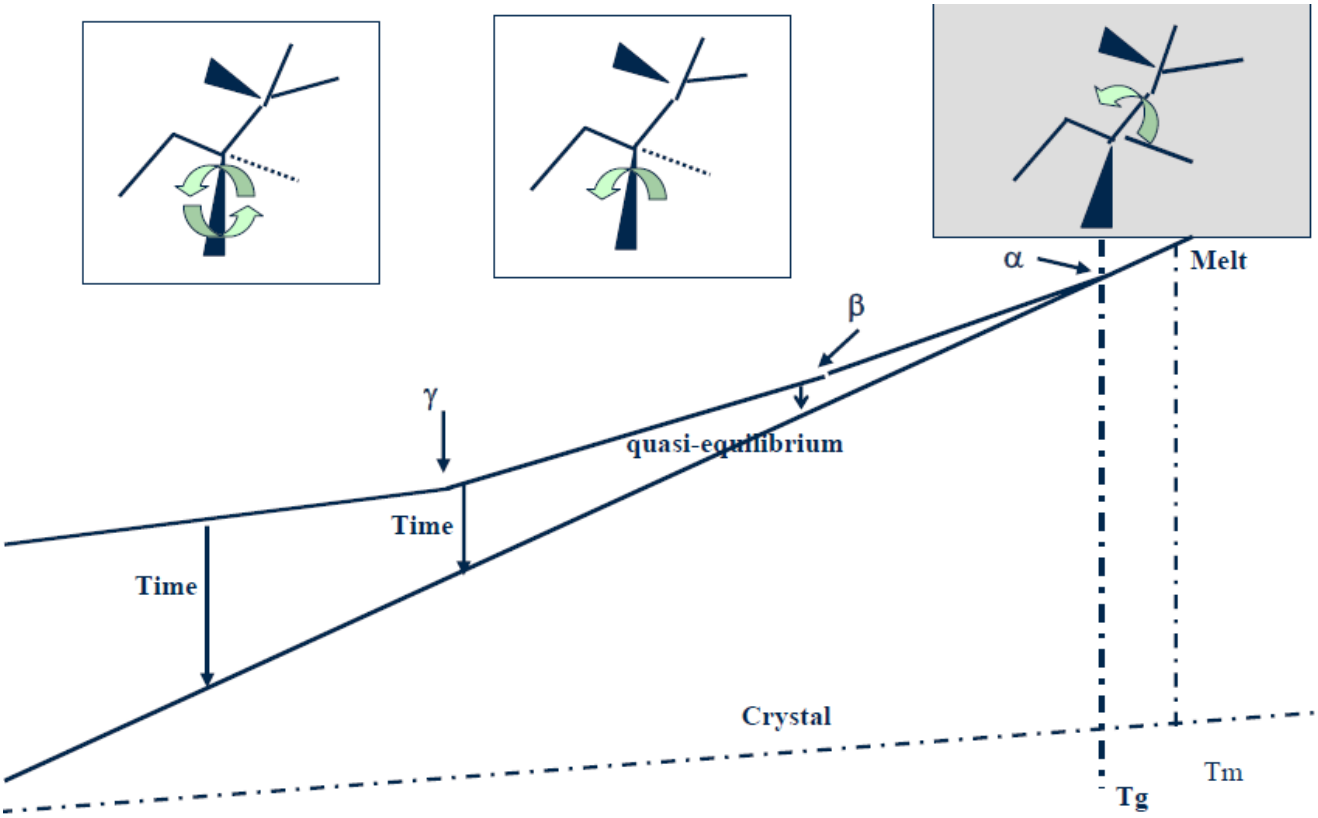

Reproduce from Lukasik, 2006

1.2.Importance of molecular mobility for matrices of solid food.

Molecules are considered to be rigid and less mobile at low temperature in glass and gain motion as temperature increases through the glass transition into the rubber/melt state. The transition from glass to liquid is termed as glass transition and occurs at a defined temperature called T_g. At low temperature, modes of vibrational mobility that require little free volume may be active; these may be limited to the coupled bond vibrations active in crystals and to hydroxyl rotations. At higher temperature the free volume increases sufficiently that more complex vibrational motions become activated; these may include rotations about the glycosidic bond or segmental motion(s) of one or more monomers within a polymer. At sufficiently high temperatures α-relaxations activated at the glass transition underlie the translational mobility associated with flow (McCrum, Read & Williams, 1967).

For almost 30 years, the influence of molecular mobility on the degradative reactions is simply incorporated into the thermodynamic phase transition phenomena. Slade and Levine (1991) suggested that diffusion in amorphous foods is governed by the glass transition. Their hypothesis assumed that at temperatures below the glass transition the rates of chemical reactions are extremely slow due to restricted molecular mobility and slow diffusion. The glass transition marks the onset of the α relaxation.

The glass transition temperature, T_g for pure matrix or T_g for freeze-dried matrix, is taken as a useful index temperature to indicate food stability: foods are thought stable at $T<T_g$; above T_g, physical changes or chemical reactions take place at a rate that varies with temperature difference ($\Delta T=T-T_g$). Plasticizers such as water and other small molecules modulate reaction rates by lowering T_g.

Undoubtedly T_g, as a simple and direct protocol for food stability, has significant impact on solid food: providing a straightforward method to evaluate the stability of food systems. Thus the complicated issue about how food quality attributes change during processing and storage is simplified to a process of determining T_g and storing the food at temperature below T_g to obtain a desirable shelf-life. Several excellent reviews have described the effort made in this field (Slade & Levine, 1991, 1995). But the glass transition cannot be considered the absolute threshold for molecular mobility. Molecular motions still persist in the glassy state with a lower amplitude and cooperativity than for above the glass transition. Transport of water and small molecules takes place even in the glassy state at a significant rate. Chang et al. (1996) examined the stability of freeze dried recombinant interleukin-1 receptor antagonist in a variety of matrices and found that protein de-amidation and aggregation occurred in some formulations below T_g. Srickley and Anderson (1996) studied the mechanism of insulin stability in amorphous freeze-dried powders. They found that hydrolytic de-amidation and dimerization proceeded in both the glassy and rubbery states, however they showed different sensitivity to mobility.

Carbohydrates and proteins can be found in almost all foods and there is some evidence of mobility in carbohydrate or protein matrices at temperature below T_g. For instance, sucrose was found to have significant molecular mobility in glass down to T_g-50K from enthalpy relaxation (Hancock, Shamblin & Zografi, 1995). It is now generally recognized that molecular mobility is associated with the stability of amorphous biomaterials. The stability and quality of amorphous solids are modulated by specific physical processes and chemical reactions involving the translational diffusion, rotational motions or intramolecular motions (Shalaev & Zografi, 1996).

Amorphous solids can be obtained through physical process such as rapid cooling, extrusion and drying. They can also be introduced unintentionally by routine manufacturing operations, such as coating, granulation, milling and lyophilization. The importance of molecular mobility for the stability of amorphous solid foods is widely recognized. The molecular mobility of the components of amorphous solid foods can be viewed as a fundamental molecular determinate of the macroscopic physical, chemical, and sensory qualities of foods.

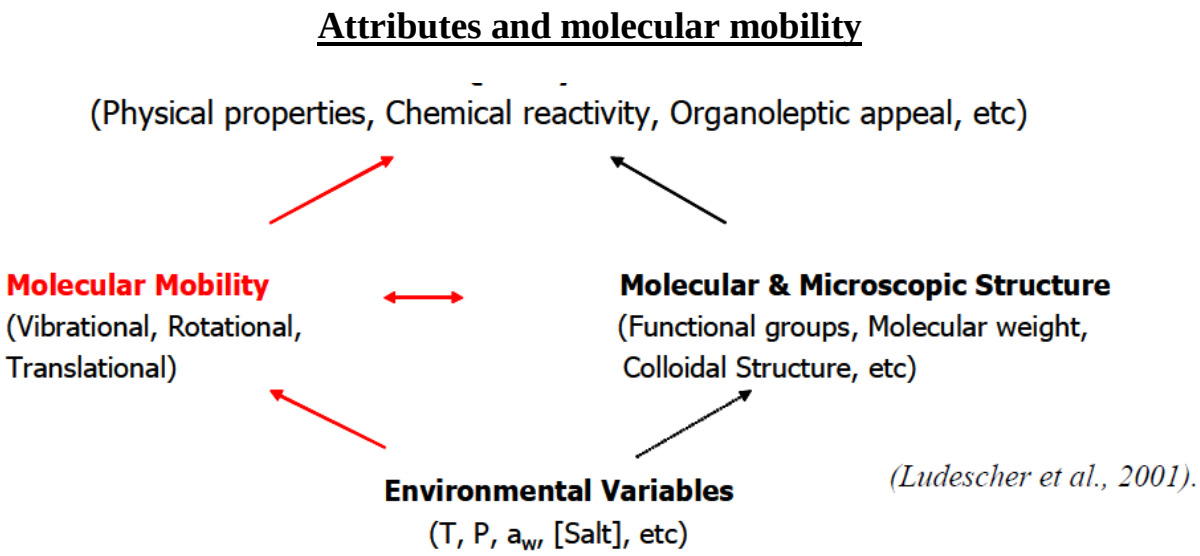

"Environmental variables such as temperature, pressure, water activity, salt concentration, as well as the presence of other solutes, affect the quality of amorphous foods primarily by modulating the molecular mobility of the components and only secondarily, if at all, by modulating their molecular and microscopic structure" (Ludescher, Shah, McCaul & Simon, 2001).

1.3 Oxygen diffusion

Oxygen is responsible for many degradative reactions in foods and pharmaceuticals including growth of microorganisms, enzymatic browning, and the oxidation of specific molecules

including proteins, vitamins, unsaturated fatty acids, and others. The permeability of oxygen in solid food is thus a fundamental aspect of their functionality. Gas permeability is an important property of food systems, and its exclusion or reduction in a food's internal environment is critical. Oxygen permeability (*P*) can be related to its diffusion coefficient (*D*) and solubility (*S*) in a particular material by the equation $P = DS$ (Crank &Park, 1968). Additives can affect the oxygen permeability in the food matrix in two distinct ways: (1) modulate the oxygen diffusion coefficient (D) by changing the matrix mobility as a plasticizer/ antiplasticizer, and (2) lower or raise the oxygen solubility (S) in the food matrix (Liang & Ludescher, 2012).

In addition, conditions also influence the rate of oxygen diffusion inside food. It's reported that oxygen permeability in amorphous solid increases dramatically with increases in temperature (Gennadios, Weller & Testin, 1993) and relative humidity (Simon-Lukasik & Ludescher, 2004). The development of strategies to reduce the oxidation or the respiration in food systems is important to prolong the shelf lives of foods. On the other hand, the permeability to oxygen and carbon dioxide is essential for respiration in living tissues such as fresh fruits and vegetables. So, moderate barrier coatings like edible films are more appropriate.

1.4 Hydrogen bond and microstructure

Glassy carbohydrates and proteins are hydrogen bonded solids and the properties of the matrix are therefore modulated by hydrogen bonded interactions among the molecules in the matrix. Wolkers et al. (1998) established that the OH stretching vibration, ν_{OH}, at ~3300 cm^{-1} increases with temperature in seven amorphous sugars and that ν_{OH} (T) displayed a characteristic change in slope at the sugar T_g. The slope of ν_{OH}(T) in the glass, the wavenumber-temperature coefficient WTC (in cm^{-1}/ ℃), was higher in glasses with higher T_g; since larger values of WTC

indicate weaker hydrogen bonds, this indicates that glasses with higher T_g are more loosely packed with weaker hydrogen bonds. Another study of mobility of maltose-water mixture with NMR suggested the formation of a stable hydrogen-bond network between sugar molecules in the glassy state, while water molecules weaken this network and increase the mobility of the hydroxyl protons of maltose (Van den Dries, Besseling, van Dusschoten , Hemminga, & van der linden, 2000). Ekdawi-Sever et al. (2003) compared the diffusive behavior of sucrose and α, α-trehalose in aqueous solutions by means of pulsed-gradient-spin-echo NMR, and they found that when dissolved in water, sucrose shows higher mobility due to its small hydration number and more compact shape. These interactions present in aqueous solutions may also exist in amorphous glasses and influence the mobility.

The interaction of food additives will also influence the microstructure of food matrices. Food structures vary enormously from relatively homogenous liquids to complex, multiphase solids containing fats, proteins, polysaccharides, salts and water in the form of fibers, aggregates, droplets, crystals, glasses or networks. The size, shape and distribution of these structures greatly influence product stability as well as sensory properties and even bio-absorption. Observing microstructure and changes in it with perturbations of composition or physical forces can reveal parameters directly related to texture. In fact, it is the microstructure that actually determines the sensory and mechanical characteristics of a food. A variety of microscopic techniques are available to examine food microstructure. These include light microscopy, scanning electron microscopy (SEM), transmission electron microscopy (TEM) and confocal laser scanning microscopy (CLSM). SEM and TEM offer the advantage of high resolution, but sample preparation procedures are laborious and may lead to artifacts. CLSM offers an alternative method to observe food structure without disturbing the internal structure. Recently, Dr. Huang

in the Department of Food Science, Rutgers University has used AFM to extensively study the influence of food additives on the food matrices like zein and sugar polymers.

1.5 Browning Reaction

Non-enzymatic browning reaction (NBR) is one of the most important chemical reactions affecting food quality during processing and in storage. Browning reactions, for example, generate the flavor, aroma, and color typical of baked cereal and meat products, modulate the functionality of proteins, and can generate off flavors and odors. In dehydrated foods, NBR often results in product deterioration, mainly by generating off-flavors and colors, and by lowering nutritional value (Shallenberger & Smith, 1959; Burin, Buera, Hough & Chirife, 2002; Kawai, Hagiwara, Kakai&Suzuki, 2004). NBR is an amino-carbonyl reaction whose mechanism and kinetics in real foods, and in models containing reducing sugars and amino compounds as reactants, have been studied extensively (Sumaya-Martinez, Thomas, Linard, Binet & Guerard, 2005; Schebor, Burin & Chirife, 1999; Ajandouz & Puigserver, 1999). These studies have revealed the various stages of NBR and shown that the rate of the reaction is strongly dependent on material composition, temperature, moisture content and pH.

The physical state of foods may determine rates of NBR. The physical stability of amorphous foods is often related to their glass transition temperature (T_g). The glass transition can affect rates of reaction by modulating the diffusion rate of the chemical components; diffusion rate is modulated by the matrix molecular mobility, which is likely to be extremely slow below the glass transition (Lievonen, Laaksonen & Roos, 1998). In an early study correlating the non-enzymatic browning reaction with matrix properties, Karmas and coworkers (Karmas, Buera & Karel, 1992) found that browning rates in different food models were strongly

dependent on moisture, temperature, and on the glass transition. Roos and Himberg (Roos & Himberg, 1994) came to similar conclusions from measurements of non-enzyme browning as a function of water content, water activity, and glass transition at chilling temperatures. However, several studies have stressed the effects of other physical characteristics of the matrix such as crystallization and collapse, often coinciding with the glass transition, should also be considered. Kawai and coauthors, for example, have reported faster rates of NBR in amorphous polyvinylpyrrolidone (PVP) than in amorphous trehalose or maltose, despite the much higher T_g value of PVP (Kawai, Hagiwara, Rikuo & Suzuki, 2005); they proposed that hydrogen bonding plays an important role in modulating the browning reaction in glassy matrixes. It is thus important to systemically identify those matrix properties that influence NBR in solid food systems.

2. Materials and methods

2.1 Preparation of amorphous thin films

We prepared amorphous carbohydrate or protein films containing varying content of additives (glycerol, sugars, methylcellulose, or antioxidants) by using a slightly modified version of our published methods for making sucrose/glycerol films (You & Ludescher, 2009). The mixture solutions were stirred at room temperature for at least half an hour to make sure the additives was totally blended with carbohydrate or proteins. For the luminescence experiments, mixtures were prepared from solutions containing Ery B or tryptophan at the appropriate concentration. Erythrosin B or tryptophan was dissolved in deionized water to prepare a 10 mM stock solution; an aliquot from this solution was added to the starch solution to obtain a mole ratio of $1{:}10^4$ (erythrosin B) or $1{:}10^3$ (tryptophan) for dye/molecule unit in the matrices.

The mixture solutions were spread 15 μl on approximately one third of a quartz slide (30 × 13.5 × 0.6 mm, custom made by NSG Precision Cells, Farmingdale, NY). The slides were placed under a gentle warm air stream using an air gun to rapidly (within 5 min) evaporate the moisture.

Slides were soaked in Terg-A-Zyme (Alconox, Inc., NY) soap solution over 24 h to remove surface impurities, then washed with deionized water, and finally rinsed with ethanol and dried with acetone before using.

For the experiment of IR, AFM and X-ray, the films were prepared with the same method as that for luminescence except that the sample solutions were spread on ATR plates for the IR experiment, mica chips for AFM or glass slides for the X-ray experiment. The quartz slides, ATR plates, mica chips and glass slides with film were stored at room temperature against the desiccant Drierite for at least 1 week and kept in an atmosphere of P_2O_5 in order to maintain 0% RH. The desiccant P_2O_5 was refreshed as necessary.

2.2 Technique of luminescence to measure the molecular mobility and oxygen permeability

2.2.1 Probe

Luminescence spectroscopy uses optical probes, organic molecules with well-characterized spectroscopic properties that "report" on the properties of the molecular environment. In this study, I have used erythrosin B and tryptophan (Figure 2) depending on the food matrices studied.

Erythrosin B has phosphorescence emission time scale of 10^{-5} to 10^{-3}s corresponding to motion in glassy environment and is sensitive to oxygen (Lam et al., 2001). Numerous studies in our lab have used Erythrosin B and shown it to be sensitive in monitoring molecular mobility in

many simple model amorphous systems and thus it definitely offers a good choice as a probe. However the maximum excited state lifetime of erythrosin B is approximately ~1ms thus restricting its application to longer time range (Thomas, 1986).

Tryptophan has been shown to exhibit strong room temperature phosphorescence emission after excluding oxygen in many proteins (Vanderkooi, Maniara, Green &Wilson, 1987). Its phosphorescence lifetime at 77K is 5-6s (Strambini & Gonnelli, 1995). Tryptophan phosphorescence can be as long as 1-2 s in proteins and thus could measure slower motions that are un-measurable with most other triplet probes (Thomas, 1986). Phosphorescence emission from intrinsic tryptophan has been used to monitor the effect of hydration on the internal molecular mobility of the protein lysozyme (Shah & Ludescher, 1993). Tryptophan has also been used as a dispersed probe in studying molecular mobility in amorphous sucrose (Shah & Ludescher, 1995).

Figure 2

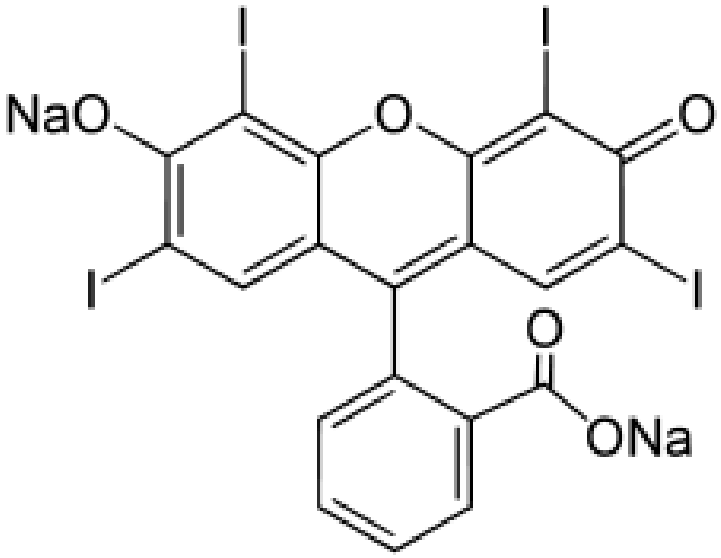

Erythrosin B

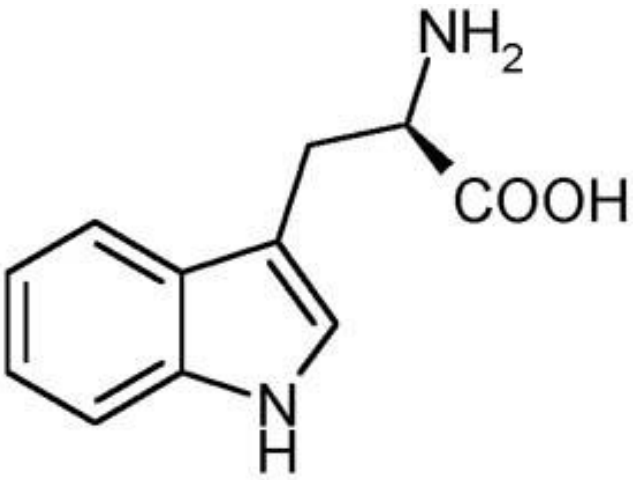

Tryptophan

Luminescence is characterized by its lifetime (intensity), polarity and energy (wavelength), each signal providing distinct information about matrix mobility and the rate of oxygen diffusion inside the food matrices. The different time scales of molecular motions demand different probes; for example slower motions like the ones that occur in viscous glass demand using long-lifetime chromophores as compared to say if the medium was liquid (Lakowicz, 1999).

The energy (inverse of wavelength) of the excited state is modulated by dipolar interaction between the probe and the matrix. Prior to excitation, the ground state of the probe is effectively stabilized by dipolar (or more generally dielectric) interactions between the probe and the matrix (Lakowicz, 1999). Upon photo-excitation, a new excited state with novel electronic distribution is rapidly (10^{-15} s) created within an environment optimized for the ground state. The newly formed excited state, which is at higher energy due to these unfavorable interactions, can be stabilized by dipolar reorientation (dipolar relaxation) in the matrix that generates new interactions that specifically stabilize the excited state (Demchenko, 1988a, b). This dipolar relaxation, however, can only influence the emission energy if it occurs on the time scale of the excited state lifetime. Therefore, a fluorescence spectrum is only affected by fast dipolar relaxation while a phosphorescence spectrum is affected by much slow dipolar relaxation rates. Thus, an analysis of probe fluorescence or phosphorescence emission spectra as a function of excitation wavelength can indicate the presence of matrix dipolar relaxation on the time scale of the probe emission lifetime.

2.2.2 Emission energy (wavelength)

Both absorption and emission are distributed over a wide range of energies and thus wavelengths. The energy of an electronic transition is also quite sensitive to dipolar interactions

between a polar chromophore and the molecules in its immediate environment (the solvent/matrix shell) (Ludescher, Shah, McCaul & Simon, 2001). Because both absorption and emission occur on time scales (10^{-15} s) much faster than the molecular motions of solvent molecules (10^{-12} s), the non-equilibrium solvent shells surrounding the newly formed excited or ground states raise the energies of these states; the rate and extent of dipolar relaxation due to molecular motion in the non-equilibrium solvent shells thus has a dramatic effect on the emission energy (wavelength) distribution. In solutions of high viscosity, and especially in amorphous rubbery and glassy solids, solvent relaxation is slow because molecular mobility is slow; solvent relaxation may occur on the microsecond time scale or longer. The time scale for relaxation in such cases is often comparable to or longer than the phosphorescence lifetime. So phosphorescence spectroscopy can be an effective tool to study the dipolar relaxation in a protein matrix (Ludescher, Shah, McCaul & Simon, 2001).

Figure 3

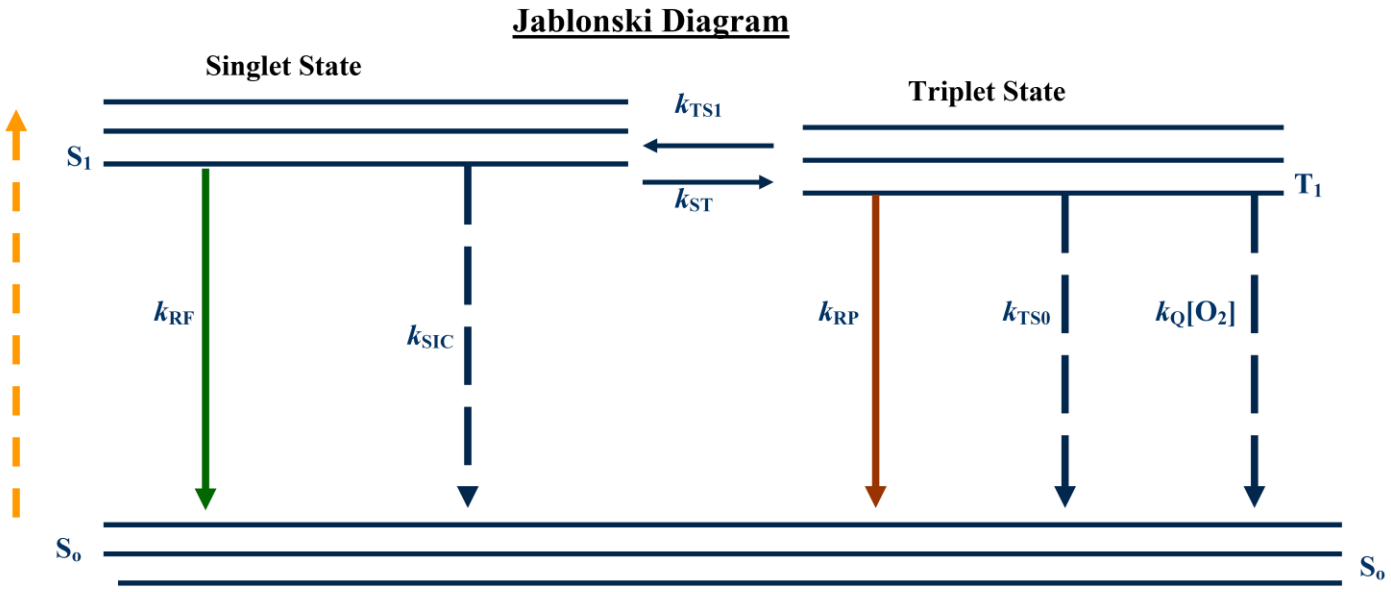

Abbreviations used:-

k_{RF} - Rate of fluorescence emission

k_{RP} - Rate of phosphorescence emission

k_{ST} – Rate of intersystem crossing from singlet to triplet state.

k_{TS1} - Rate of intersystem crossing from triplet to singlet state.

k_{SIC}- Rate of interval conversion from S_1 to S_0

k_{TS0}- Rate of intersystem crossing from triplet state T to ground state S_0

$k_{Q[O_2]}$- Rate of collisional quenching due to oxygen

2.2.3 Intensity

Phosphorescence intensity can be monitored by measuring the intensity decay as function of time. The phosphorescence lifetime can be expressed in terms of the de-excitation rate constants. In a complex amorphous matrix, there may be several different environments and hence several different lifetimes of the triplet probe. The phosphorescence intensity decay could be fitted with either stretched exponential function or multi-exponential functions (Chen, 2003; Shamblin, Hancock, Dupuis & Pikal, 2000). In case of erythrosin B, as shown in Equation 1, phosphorescence intensity decays are often non-exponential and a stretched exponential decay function has being shown to describe the wide distribution of relaxation times (Champion, Le Meste & Simatos, 2000; Lee et al., 2001), where I(t) is the intensity as a function of time following pulsed excitation, I(0) is the initial intensity at time zero, τ is the lifetime, and β is the stretching exponent which characterizes the distribution of the decay times. For tryptophan as shown in Equation 2 in absence of any external quenchers, in a multi-exponential model the intensity is assumed to be decaying as the sum of individual single-exponential decays; τ_i are decay times, α_i represent the amplitudes of the components at t = 0 and n is the number of decay times.

$$I(t) = I(0) \exp\left[-(t/\tau)^{\beta}\right] \quad (1)$$

$$I(t) = \sum_{i=1}^{n} \alpha_i \exp(-t/\tau_i) \quad (2)$$

Emission intensity is directly proportional to quantum yield. The phosphorescence lifetime can be expressed in terms of the de-excitation rate constants. In case of erythrosin B, the decay

rate $k_P(T)$ is given as shown in equation 3 and for tryptophan is given in equation 4 in absence of external quenchers.

$$k_P(T) = k_{RP} + k_{TS0}(T) + k_{TS1}(T) \quad (3)$$

$$k_P(T) = k_{RP} + k_{TS0}(T) \quad (4)$$

The process of quenching causes reduction in the phosphorescence intensity. Oxygen is the most effective quencher of the triplet state (Vanderkooi, Maniara, Green & Wilson, 1987). For erythrosine B, when oxygen is present, the equation can be expressed as equation 5 and for tryptophan can be given as in equation 6.

$$K_P(T) = K_{RP} + K_{TS0}(T) + K_{TS1}(T) + K_{O2}[O_2] \quad (5)$$

$$K_P(T) = K_{RP} + K_{TS0}(T) + K_{O2}[O_2] \quad (6)$$

Measurements of +/- oxygen thus can be used to monitor the extent of oxygen diffusion through the matrix.

3. Goal, hypothesis, and specific objectives

The goal of this project is to determine how food additives with different chemical structures and molecular weights can influence the shelf-life of solid foods, food ingredients, agricultural products and related biomaterials. We hypothesize that composition of the amorphous matrix modulates the molecular mobility of the matrix and that the rates of specific degradative processes are controlled in part by the matrix molecular mobility and intermolecular forces in the food matrices. The specific objectives driven by our hypotheses and designed to accomplish this goal are:

Objective one. Investigate how different food additives modulate the molecular mobility of amorphous solid sugar, protein and carbohydrate matrixes; composite matrixes investigated will include protein and carbohydrate polymers plus plasticizers (glycerol, oligosaccharide), antioxidants (gallate derivatives) and thickeners (methylcellulose).

Objective two. Investigate the molecular mechanism(s) underlying changes in mobility though studies of how composition modulates the local hydrogen bonding network and microstructures of the amorphous matrix.

Objective three. Determine how food additives modulate the rates of specific chemical reactions (Maillard browning) and physical processes (oxygen diffusion) within the amorphous solid matrix.

The research will deepen our understanding of how variations in the composition (plasticizer, sugars, protein, antioxidants, starch, and polymer) modulate physical properties and influence the reaction in the model of non-enzyme browning reaction in the amorphous carbohydrate and protein matrices. It should result in the development of a set of "molecular rules" that could be used to guide formulation of products for extended shelf-life. By comparing those data we generated a detailed concept-map about the mechanisms controlling the interactions between the biopolymers and food additives and how they influence the physico-chemical properties of amorphous food matrices. A detailed study of the effect of composition on molecular mobility, local structure, and the rates of chemical reaction and physical change in amorphous sugars and carbohydrates is thus clarified.

We will use embedded triplet probes (erythrosin B and tryptophan) to provide a facile and sensitive measure of matrix molecular mobility and oxygen permeability, atomic force microscopy to imagine matrix microstructure, IR spectroscopy to detect the hydrogen bond

network and protein structure changes, fluorescence spectroscopy to determine the rate of browning reaction, and DSC to measure the Tg of matrices in amorphous food system models including sugars, starches and proteins. Maillard browning will be monitored using optical spectroscopy; oxygen diffusion will be measured by monitoring oxygen quenching of long-lived triplet probes (tryptophan and other food grade chromophores) embedded within the amorphous matrix. The specific targeted systems and research to be done are shown below:

1) Investigated the effect of glycerol on the molecular mobility and hydrogen bond network in glucose matrix using the methods of luminescence and IR.
2) Investigated the effects of glycerol on the mobility, hydrogen bond network, and microstructure of potato starch matrix using the methods of luminescence, AFM, IR and X-ray.
3) Investigated the effect of physical changes on the rates of non-enzymatic browning reaction in the starch-based amorphous matrices using the methods of luminescence and IR.
4) Investigated the relation of molecular mobility and browning reaction in matrixes of glucose oligomer mixed with BSA using the methods of luminescence and IR.
5) Investigated the effects of antioxidant on the molecular mobility and hydrogen bond network of sucrose matrix using the methods of luminescence and IR.

References:

Ajandouz, E. H., Puigserver, A. (1999) Nonenzymatic browning reaction of essential amino acids: effect of pH on caramelization and maillard reaction kinetics. *Journal of Agricultural and Food Chemistry*, 47, 1786-1793.

Burin, L., Buera, M. P., Hough, G., Chirife, J. (2002) Thermal resistance of β-galactosidase in dehydrated dairy model systems as affected by physical and chemical changes. *Food Chemistry*,

76,423-430.

Champion, D., Le Meste, M., Simatos, D. (2000) Towards an improved understanding of glass transition and relaxations in foods: molecular mobility in the glass transition range. *Trends in Food Science & Technology*, 11, 41-55.

Chang, B.S., Beauvais, R.M., Dong, A., Carpenter, J.F. (1996) Physical factors affecting storage stability of freeze-dried interleukin-1 receptor antagonist: glass transition and protein conformation. *Archives of Biochemistry and Biophysics*, 331, 249-258.

Chen, R. (2003) Apparent stretched exponential luminescence decay in crystalline solids. *Journal of Luminescence*, 102, 510-518.

Crank, J., Park, G. S. (1968) Diffusion in polymers, Academic Press, New York, 1-39.

Demchenko, A.P. (1988a) Site-selective excitation: a new dimension in protein and membrane spectroscopy. *Trends in Biochemical Sciences,* 13,374-377.

Demchenko, A.P. (1988b) Red-edge excitation fluorescence spectroscopy of single-tryptophan proteins. *European Biophysics Journal*, 16, 121-129.

Ekdawi-Sever, N., de Pablo, J.J., Feick, E., von Meerwall, E. (2003) Diffusion of sucrose and α, α-trehalose in aqueous solutions. *The Journal of Physical Chemistry A*, 107, 936-943.

Gennadios, A., Weller, C.L., Testin, R.F. (1993) Temperature effect on oxygen permeability of edible protein-based films. *Journal of Food Science*, 58, 212-14, 219.

Hancock, B.C., Shamblin, S.L., Zografi, G. (1995) Molecular mobility of amorphous pharmaceutical solids below their glass transition temperatures. *Pharmaceutical Research*, 12, 799-806.

Karmas, R., Buera, M. P., Karel, M. (1992) Effect of glass transition on rates of nonenzymatic browning in food systems. *Journal of Agricultural and Food Chemistry*, 40, 873-879.

Kawai, K., Hagiwara, T., Rikuo, T., Suzuki, T. (2005) The rate of non-enzymatic browning reaction in model freeze-dried food system in the glassy state. *Innovative Food Science & Emerging Technologies,* 6, 346-350.

Kawai, K., Hagiwara, T., Takai, R., Suzuki, T. (2004) Maillard reaction rate in various matrices.

Bioscience, Biotechnology, and Biochemistry, 68, 2285-2288.

Lakowicz, J. R. Principles of Fluorescence Spectroscopy. Second ed. New York: Kluwer Academic/Plenum Press. 1999.

Lee, K.C.B., Siegel, J., Webb, S.E.D., Leveque-Fort, S., Cole, M.J., Jones, R., Dowling, K., Leve, M.J., French, P.M.W. (2001) Applications of the stretched exponential function to fluorescence lifetime imaging. *Biophysical Journal.* 8, 1265-1274.

Le Meste, M., Champion, D., Roudaut, G., Blond, G., Simatos, D. Glass transition and food technology: a critical appraisal. *Journal of Food Sci*ence, 2002, 67, 2444-2458.

Liang, J., Ludescher, R. D. (2012) Influence of Glycerol on the Molecular Mobility and Hydrogen Bond Network in the Glucose-Based Matrix. *Carbohydrate Research*, *361*, 120-126.

Lievonen, S. M., Laaksonen, T. J., Roos, Y. H. (1998) Glass transition and reaction rates: nonenzymatic browning in glassy and liquid systems. *Journal of Agricultural and Food Chemistry*, 46, 2778-2784.

Ludescher, R.D., Shah, N.K., McCaul, C.P., Simon, K.V. (2001) Beyond *T*g: opticalluminescence measurements of molecular mobility in amorphous solid foods. *Food Hydrocolloids*, 15, 331-339.

McCrum, N.G., Read, B.E., Williams, G. (1967) Anelastic and Dielectric Effects in Polymeric Solids. John Wiley & Sons, Limited, Toronto.

Roos, Y. H., Himberg, M. J. (1994) Nonenzymatic browning behavior, as related to glass transition, of a food model at chilling temperature. *Journal of Agricultural and Food Chemistry*, 42, 893-898.

Schebor, C., Burin, L., Buera, M. P., Chirife, J. (1999) Stability to hydrolysis and browning of trehalose, sucrose and raffinose in low-moisture systems in relation to their use as protectants of dry biomaterials. *Lebensm-Wiss. U.-Technol.*, 32, 481-485.

Shah, N. K., Ludescher, R. D. (1993) Influence of hydration on the internal dynamics of hen egg white lysozyme in the dry state. *Photochemistry and Photobiology*, 58 169-174.

Shah, N. K., Ludescher, R. D. (1995) Phosphorescence of probes of the glassy state in amorphous sucrose. *Biotechnology Progress,* 11 540-544.

Shalaev, E.Y., Zografi, G. (1996) How does residual water affect the solid-state degradation of drugs in the amorphous state? *Journal of Pharmaceutical Sci*ence 85(11), 1137-1141.

Shallenberger, R. S., Smith, O. (1959) Food color changes, role of the sugars in the browning reaction in potato chips. *Journal of Agricultural and Food Chemistry*, 7, 274-277.

Shamblin, S., Hancock, B.C., Dupuis, Y., Pikal, M.J. Interpretation of relaxation time constants for amorphous pharmaceutical systems. (2000) *Journal of Pharmaceutical Sciences,* 89, 417-427.

Shi, K., Kokini, J. L., Huang, Q. (2009) Engineering Zein Films with Controlled Surface Morphology and Hydrophilicity. *Journal of Agricultural and Food Chemistry,* 57, 2186-2192.

Shirke, S (2005) Molecular Mobility in Amorphous Sugars and Sugar A lcohols as Detected by Phosphorescence of Erythrosin B. MS dissertation, Department of Food Science, Rutgers, the state University of New Jersey

Simon-Lukasik, K. V., Ludescher, R.D. (2004) Erythrosin B phosphorescence as a probe of oxygen diffusion in amorphous gelatin films. *Food Hydrocolloids*, 18, 621-630.

Slade, L., Levine, H. (1991) A food polymer science approach to structure-property relationships in aqueous food systems: non-equilibrium behavior of carbohydrate-water systems. *Advances in Experimental Medicine and Biology***,** 302, 29-101.

Slade, L., Levine, H. (1995) Glass transitions and water-food structure interactions. *Advances in Food and Nutrition Research*, 38, 103-269.

Slade, L., Levine, H., Finley, J. (1989) Protein-water interactions: water as a plasticizer of gluten and other proteins. In *Protein Quality and the Effects of Processing* (D.C. Phillios & J. Finley, editors), pp9-124. Marcel Dekker, Inc.

Srickley, R. G., Anderson, B.D. (1996) Solid-state stability of human insulin I. mechanism and the effect of water on the kinetics of degradation in lyophiles from pH 2-5 solutions. *Pharmaceutical Research,* 13, 1142-1153.

Strambini, G.B., Gonnelli, M. (1995) Tryptophan phosphorescence in fluid solution. *Journal of American Chemical Society*, 117 7646-7651.

Sumaya-Martinez, M. T., Thomas, S., Linard, B., Binet, L., Guerard, F. (2005) Effect of maillard reaction conditions on browning and antiradical activity of sugar-tuna stomach hy

Van den Dries, I. J., Besseli drolysate model systems. *Food Research International*, 1045-1050.

Thomas, D. Rotational Diffusion of Membranes. Ragan, C.I., Cherry, R.J. (1986).Techinques for Analysis of membrane proteins. Chapman and Hall, London. 377-394.

Van den Dries, I. J., Blesseling, N. A. M., van Dusschoten , D., Hemminga, M . A., van der linden, E. (2000) Relation between a transition in molecular mobility and collapse phenomena in glucose-water system. *The Journal of Physical Chemistry B,* 1004, 9260-9266.

Vanderkooi, J. M., Maniara, G., Green, T. J., Wilson, D. F. (1987) An optical method for measurement of dioxygen concentration based upon quenching of phosphorescence. *The Journal of Biological Chemistry,* 262, 5476-5482.

Wolkers, W.F., Oldenhof, H., Alberda, M., Hoekstra, F.A. (1998) A fourier transform infrared microspectroscopy study of sugar glasses: application to anhydrobiotic higher plant cells. *Biochimica et Biophysica Acta*, 1379, 83-96.

You, Y. M., Ludescher, R. D. (2009) Effect of xanthan on the molecular mobility of amorphous sucrose detected by erythrosin B phosphorescence. *Journal of Agricultural and Food Chemistry*, 57, 709-716.

Chapter II: Influence of Glycerol on Molecular Mobility and Hydrogen Bond Network in Amorphous Glucose Matrix

A paper published in *Carbohydrate Research*

Jun Liang, Richard. D. Ludescher

1. Introduction

Glucose, one of the most widely distributed and important sugars in nature, possesses considerable application value for the food and pharmaceutical industries. It is used in abundance as food additive, filler, and as a component in tablet coatings. As an amorphous (noncrystalline) solid, glucose can also act as an effective protectant against lipid oxidation and bacterial growth (Romero-Bastida, Flores-Huicochea, Martin-Polo, Velazquez & Torres, 2004). The stability and properties of amorphous biomaterials are modulated by specific physical processes and chemical reactions that are directly modulated by the molecular mobility of the amorphous matrix (You & Ludescher, 2008). Thus, it is of primary importance to understand the molecular mobility of amorphous solids containing glucose and its response to changes in composition and environmental conditions. Experimental techniques such as NMR, DSC and fluorescence have been extensively used to evaluate the mobility of amorphous biomaterials (Vittadini, Dickinson, Lavoie, Pham & Chinachotti, 2003;Sonar, Singh, Sudhakar, Dodabalapur & Sellinger, 2008; Liang, et al, 2008; Liang, Tian, Yang, Zhang & Skibsted, 2009; Andronis & Zografi, 1997). We have systemically used phosphorescence of Erythrosin B (Ery B), a triplet state molecular probe, to monitor the molecular properties of protein and oligosaccharide matrixes (Shirke & Ludescher, 2005; Simon-Lukasik & Ludescher, 2004; You & Ludescher, 2009; Sundaresan & Ludescher, 2008).

Glycerol is widely used as a humectant and cryoprotectant as well as a softener or texture modifier to improve the properties and stability of many foods and pharmaceutical preparations. Small molecules such as glycerol and water can enhance the flexibility and ductility of polymeric materials, an effect termed plasticization (Gao, et al, 2006; Sun, 1997; Teixeira, Da RÓZ, Carvalho & Curvelo, 2007). The effects of those small molecules on the physical properties of amorphous solids have also been studied. It has been reported that glycerol can exert different effects depending on its concentration. In sucrose, for example, the rate and extent of matrix relaxation decreased at temperatures below the matrix T_g when the ratio of glycerol/sucrose (mole/mole) was lower than 0.27, indicating that glycerol was acting as an antiplasticizer at low concentrations (You & Ludescher, 2007). Different, concentration-dependent effects of glycerol were also found in other amorphous solids. Lourdin and colleagues reported that glycerol at a content below 12% could increase the ductility of potato starch film; when the amount of glycerol exceeded 12%, however, the ductility decreased (Lourdin, Bizot & Colonna, 1997). Similar antiplasticizing effects of glycerol were also found in the matrixes of trehalose and maltodextrin (Anopchenko, Psurek, VanderHart, Douglas & Obrzut, 2006; Roussenova, Murith, Alam & Ubbink, 2010). In most cases, there exists a critical content that marks the onset of a change in functionality from antiplasticizer to plasticizer.

The role of glycerol in films is determined by its effect on at least two types of molecule motions in matrix: large-scale molecular motions (α-relaxations) and localized molecular motions (β-relaxations). The molecular mobility at any temperature relative to the glass transition is greatly influenced by molecular weight of the compound forming the matrix. Previously we have reported that matrix molecular mobility varies in the order glucose < maltose

< maltrotriose in the region from 40 ℃ below to 40 ℃ above the glass-transition temperature, indicating that the molecular mobility is actually higher in sugars with compounds with higher molecular weight (Shirke & Ludescher2005). The hydrogen bond network is an important factor modulating those molecular motions in amorphous solids. The number, length and strength of hydrogen bonds within the matrix will inevitably affect interactions between the molecules in the matrix, consequently affecting the molecular mobility. FTIR, an effective chemical analysis method, is widely used to detect the status of hydrogen bonds in amorphous carbohydrate glasses (Pivonka, 2003; Rozenberg, 1996; Kim & Hochstrasser, 2005).

Although there have been extensive studies about the effect of glycerol on polymeric materials (Suyatma, Tighzert & Copinet, 2005; Cuq, Gontard, Cuq & Guilbert, 1997; Fairley, Monahan, German & Krochta, 1996). The effects of glycerol on glucose, a simple but extremely important sugar, have not yet been reported. This study thus assessed the effects of glycerol on the mobility of amorphous glucose using phosphorescence from the triplet probe erythosin B (Ery B) dispersed in the matrix. Glycerol content was varied from 0 to 0.4 (mole ratio of glycerol/glucose) by adding glycerol to the glucose solution before film formation. The temperature-dependence of mobility was measured and analyzed at different glycerol contents, generating families of mobility versus temperature curves. Samples under the same conditions were measured by FTIR in a temperature range from 30 to 100 ℃. By studying the relation of mobility to hydrogen bond strength and network, we can better understand the mechanism of glucose mobility in the amorphous solid state.

2. Materials and methods

2.1 Sample preparation

About 3.1 g of D-glucose (99.5% pure; Sigma Chemical, St. Louis, Mo) was dissolved in about 5 mL of deionized water. Erythrosin B (Ery B; Sigma Chemical, St. Louis, MO) disodium salt was dissolved in deionized water to prepare a 10 mM stock solution. An aliquot from this solution was added to the glucose solution to obtain an Ery B: glucose mole ratio of $1:10^4$. For luminescence measurements, glucose-glycerol mixtures were prepared from solutions containing Ery B. Glycerol (99% GC pure; Sigma Chemical, St. Louis, MO) was added to glucose solutions to obtain a series of mixtures with glycerol: glucose mole ratios of 0.1, 0.2, 0.3, and 0.4. Before preparing glassy films, glycerol-glucose solutions were stirred on a stir plate (Nuova, Cologna Veneta, Italy) for at least half hour to ensure that glycerol was completely mixed with glucose.

To make glucose films for measuring luminescence and FTIR, 15 μl of the glucose/glycerol/probe solutions at room temperature were spread on approximately one third of a quartz slide ($30 \times 13.5 \times 0.6$ mm, custom made by NSG Precision Cells, Farmingdale, NY). Before preparing the films, the slides were soaked in Terg-A-Zyme (Alconox, Inc., NY) soap solution over 24 h to remove surface impurities, then washed with deionized water and dried with acetone. The films were stored at room temperature against the desiccants DrieRite and P_2O_5 in order to maintain 0% RH. The films were stored in the desiccator for at least one week and protected from light to prevent photobleaching of Ery B. The desiccant P_2O_5 was refreshed as necessary.

2.2 Glass transition temperature of glucose-glycerol films

The glass transition temperature (T_g) of all amorphous films were calculated based on composition. The T_g of a binary mixture depends on the mass fraction (χ_1 and χ_2), change in heat capacity at T_g (ΔC_{P1} and ΔC_{P2}), and glass transition temperature (T_{g1} and T_{g2}) of the components. The relation is given by the modified Couchman and Karasz equation (Couchman & Karasz, 1978):

$$T_g = (\chi_1 T_{g1} \Delta C_{P1} + \kappa \chi_2 T_{g2} \Delta C_{P2}) / (\chi_1 \Delta C_{P1} + \kappa \chi_2 \Delta C_{P2})$$

The ΔC_P's of glucose and glycerol are 0.78 J/g K (Nelson, Newton, 1941) and 1.05 J/ g K (You & Ludescher, 2007), respectively. The T_g's of glucose and glycerol are 38°C (Simperler, et al, 2006) and -83 ℃ (You & Ludescher, 2007), respectively.

2.3 Phosphorescence Measurement and Analysis

All luminescence measurements were conducted on a Cary Eclipse spectrophotometer (Varian Instruments, Walnut Creek, CA) equipped with a temperature controller and multicell holder. All measurements were made at least in triplicate and the slides were first heated and data were collected from 100 to -10 ℃ in all experiments.

High purity nitrogen or air was routed into the sample compartment and directly into the quartz fluorescence cuvette that held the slide. The cuvette was flushed for at least 30 min at 100 ℃ before beginning the measurement. The cuvette was capped with a lid having inlet and outlet ports for the gas line, so that all experiments were performed at constant pressure. Each intensity decay observation was the average of 50 cycles. For each cycle, data were collected from a single flash with a decay of 0.04 ms, a 0.05 ms gate time, and a total decay time of 10.0

ms. Phosphorescence and delayed fluorescence emission scans were collected over a range from 540 to 800 nm with an excitation wavelength of 520 nm. The excitation and emission monochromators were both set at 20 nm band pass. Each data point (collected at 1 nm intervals with a 0.1 s averaging time) was collected from a single flash with 0.2 ms delay and 5 ms gate time.

For lifetime measurements, because intensity decays were non-exponential, a stretched exponential function was selected to analyze the intensity decays:

$$I\,(t) = I\,(0)\,\exp\,[-(t/\tau)^{\beta}] + \text{constant} \qquad (1)$$

where $I(0)$ is the initial intensity, τ is the stretched exponential lifetime, and β is an exponent varying from 0 to 1 that characterizes the lifetime distribution. The use of stretched exponential model provides analysis of a continuous distribution of lifetimes, which is appropriate for describing a complex glass possessing a distribution of relaxation times for dynamic molecular processes. The smaller the β value, the more non-exponential are the intensity decays and the broader the distribution of lifetimes (Duchowicz, Ferrer & Acuña, 1998).

The energy of the emission maximum (ν_p) and FWHM of the emission band were determined by using a log-normal line shape function to fit both delayed fluorescence and phosphorescence.

$$I(\nu) = I_0\,\exp\left\{-\ln(2)\left(\frac{ln\left[1+2b\left(\nu-\nu_p\right)\right]/\Delta}{b}\right)^2\right\} \qquad (2)$$

where I_0 is the maximum emission intensity, ν_p is the peak frequency (cm^{-1}), Δ is a linewidth parameter, and b is an asymmetry parameter. The bandwidth Γ (FWHM) was calculated according to the following equation:

$$\Gamma = \Delta\left[\frac{\sinh(b)}{b}\right] \quad (3)$$

Delayed luminescence spectra collected from 540-750 nm were fit using a sum of log-normal functions for delayed fluorescence ($I_{DF}(\nu)$) and phosphorescence ($I_P(\nu)$). Each emission band was analyzed for independent fitting parameters using a sum of two functions as described in Eq. 2.

The phosphorescence lifetimes were used to calculate the rate constants associated with the various processes that depopulate the triplet state. Our analysis of the delayed emission is similar to the photophysical scheme for Ery B outlined by Duchowicz and colleagues using a slightly different nomenclature (Shirke & Ludescher, 2005). The measured phosphorescence lifetime (τ) is the inverse sum of all possible de-excitation rates (k_P) for the triplet state T_1

$$1/\tau = k_P = k_{RP} + k_{TS1} + k_{TS0} + k_Q[O_2] \quad (4)$$

where k_{RP} is the rate of radiative decay to the ground state, k_{TS1} is the rate of reverse intersystem crossing to the excited singlet state S_1, k_{TS0} is the rate of intersystem crossing to the singlet manifold followed by vibrational relaxation to the ground state S_0, and $k_Q[O_2]$ is the rate of oxygen quenching (assumed negligible in the absence of oxygen). The radiative decay rate has a value of 41 s^{-1} for Ery B (Shirke &Ludescher, 2005).

Reverse intersystem crossing is a thermally activated process that has an exponential dependence on the energy gap ΔE_{TS} between T_1 and S_1 (Lettinga, Zuihof & van Zandvoort, 2000):

$$k_{TS1}(T) = k^{o}_{TS1}\exp(-\Delta E_{TS}/RT) \quad (5)$$

The ratio of intensity of delay fluorescence (I_{DF}) to phosphorescence (I_P), where I_{DF} and I_P are determined from analysis of emission spectra using the log-normal function (Eq. 2), is proportional to the rate of reverse intersystem crossing. A plot of $\ln(I_{DF}/I_P)$ versus 1/T thus has a slope of $-\Delta E_{TS}/R$.

One of the non-radiative decay routes is through intersystem crossing to the ground state S_0. The decay rate is k_{TSO}, which reflects the rate of collisional quenching of the probe due to both internal and external factors. We assume that the term k_{TSO} primarily reflects the external environmental factors since the self-collisional quenching among probe molecules can be neglected within the extremely viscous amorphous solid. In this study, the temperature–dependent term k_{TSO} can be calculated using Eq 4 from the measured lifetimes using the known value of k_{TS0} and by estimating k_{TS1}.

2.4 Attenuated Total Reflectance Fourier Transform Infrared (ATR-FTIR) Spectroscopy

The ATR-FTIR spectra were collected by using a Thermal Nicolet Nexus 670 FT-IR spectrometer (Thermo Fisher Scientific Inc., Waltham, MA) equipped with a Smart ARK thermal accessory and analyzed using the associated EZ-OMNIC software. Each spectrum was the average of 512 scans with 4 cm^{-1} resolution in an atmosphere of P_2O_5 to minimize the

interference of moisture under ambient condition. The slides were placed on the heating plate and heated up to 100 ℃ to melt the matrix; then the melted matrix was laid on ATR crystal using a small spoon. The measurements were conducted from 100 ℃ down to 30 ℃.

2. Results and discussion

As a plasticizer, glycerol is added to change the properties of a material, primarily through depression of the glass transition temperature (T_g). The T_g values for amorphous dry glucose/glycerol binary mixtures calculated from the Couchman and Karasz equation were 38 ℃, 30 ℃, 23 ℃, 17 ℃, and 11 ℃ for mole ratios of 0.0, 0.1, 0.2, 0.3, and 0.4, respectively.

Figure 4

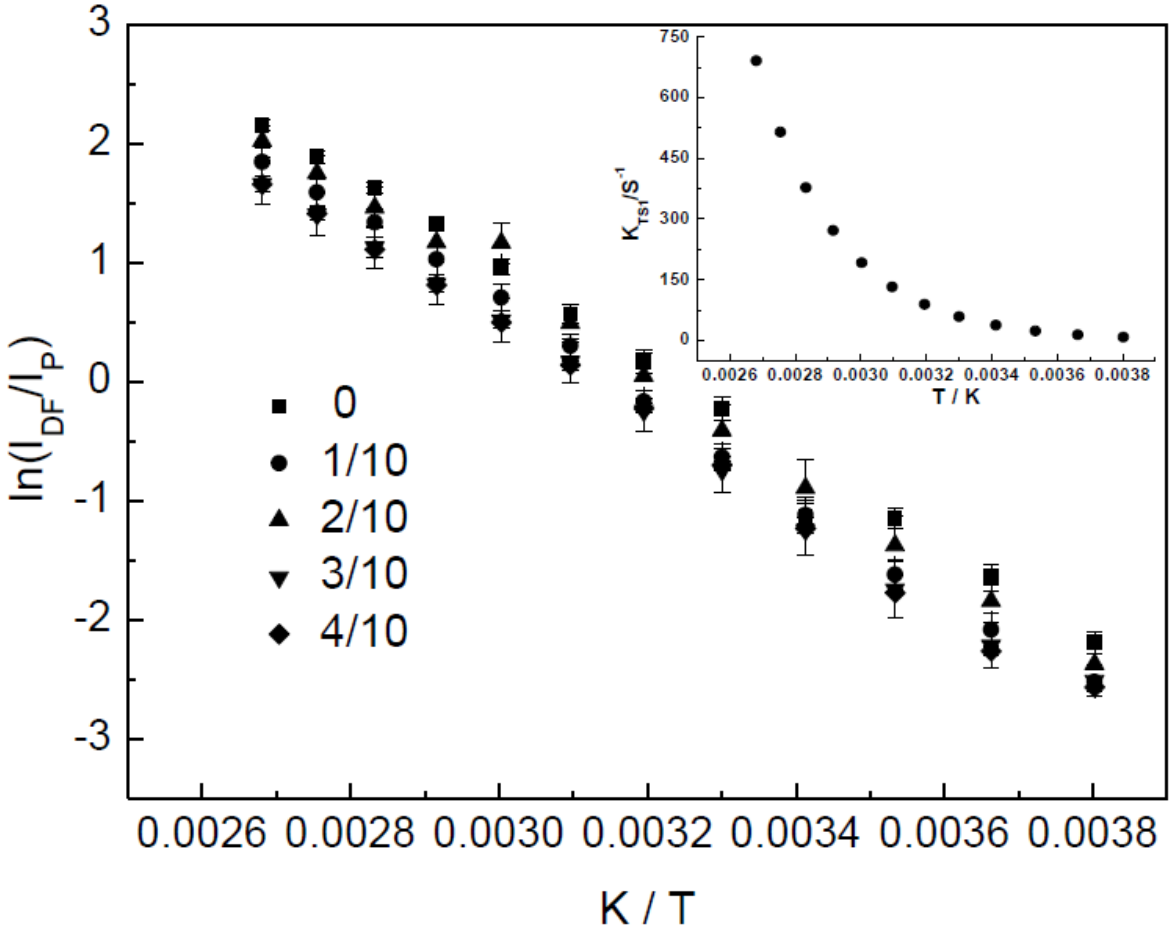

Figure 4. Natural log of ratio of peak intensity for delayed fluorescence (I_{DF}) to phosphorescence (I_P) ($\ln(I_{DF}/I_P)$) for Ery B in glucose films containing varying mole ratios of glycerol plotted versus inverse temperature. Insert shows the values for $k_{TS1}(T)$ in these films calculated as described in the text

3.1 Delayed emission spectra

The delayed emission spectra of Ery B in amorphous glucose/glycerol films displayed two bands: a longer wavelength phosphorescence band (maximum ~690 nm) due to emission from the lowest triplet state (T_1) and a shorter wavelength delayed fluorescence band (maximum ~555 nm) due to emission from the first excited singlet state (S_1) repopulated by thermally stimulated reverse intersystem crossing from T_1. Delayed emission spectra of Ery B in glucose with varying glycerol content collected over the temperature range from 100 to -10 ℃ showed an increase in phosphorescence (I_P) and an decrease in delayed fluorescence (I_{DF}) intensity with decreasing temperature as expected for this probe (Kondo, 1997) (data not shown). Both the delayed fluorescence and phosphorescence bands shifted to longer wavelength at higher temperature. The intensity ratio of delayed fluorescence to phosphorescence was analyzed as a van't Hoff plot of $\ln(I_{DF}/I_P)$ versus 1/T (Figure 4) and the linear slope was used to calculate the energy gap (ΔE_{TS}) between the T_1 and S_1 states. Van't Hoff plots were linear with $R^2 \geq 0.995$. The slopes of samples containing varying contents of glycerol showed negligible differences, indicating that ΔE_{TS} was not affected by addition of glycerol.

As reported in the literature, k^o_{TS1} for Ery B varies from 0.3×10^7 s^{-1} in ethanol and 6.5×10^7 s^{-1} in water to 111×10^7 s^{-1} in solid polyvinyl alcohol. (Kondo, 1997) We estimated the maximum possible value for k^o_{TS1} in glucose/glycerol by assuming that the values of $k_{TS1}(T)$ calculated using Eq. 5 cannot result in values for k_{TS0} (calculated from lifetimes using Eq. 4) that decrease with temperature; the values obtained are thus the minimum possible values of $k_{TS0}(T)$. The value of k^o_{TS1} used for this study was 3×10^7 s^{-1}; the insert in Figure 4 shows the values of $k_{TS1}(T)$ over the temperature range from -10 to 100 ℃ .

Figure 5

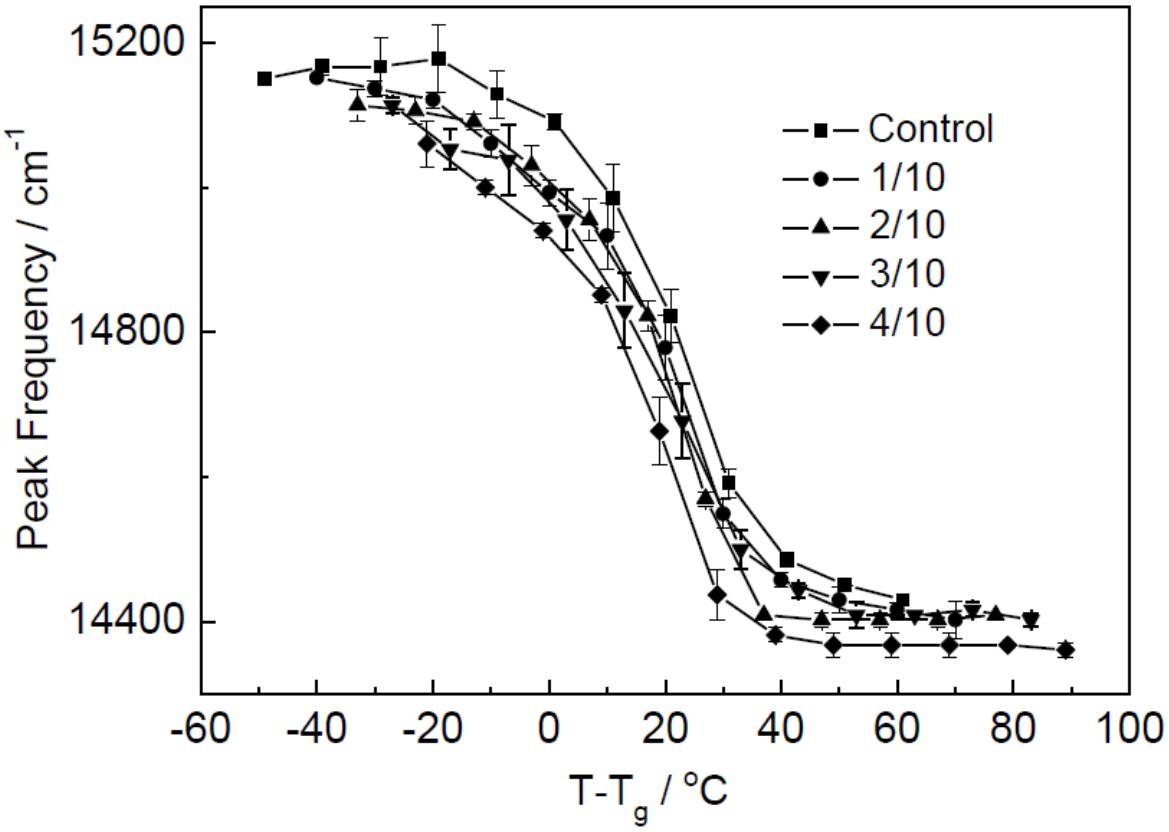

Figure 5. Temperature dependence of the peak frequency for phosphorescence emission from Ery B in amorphous glucose/glycerol films.

Figure 6

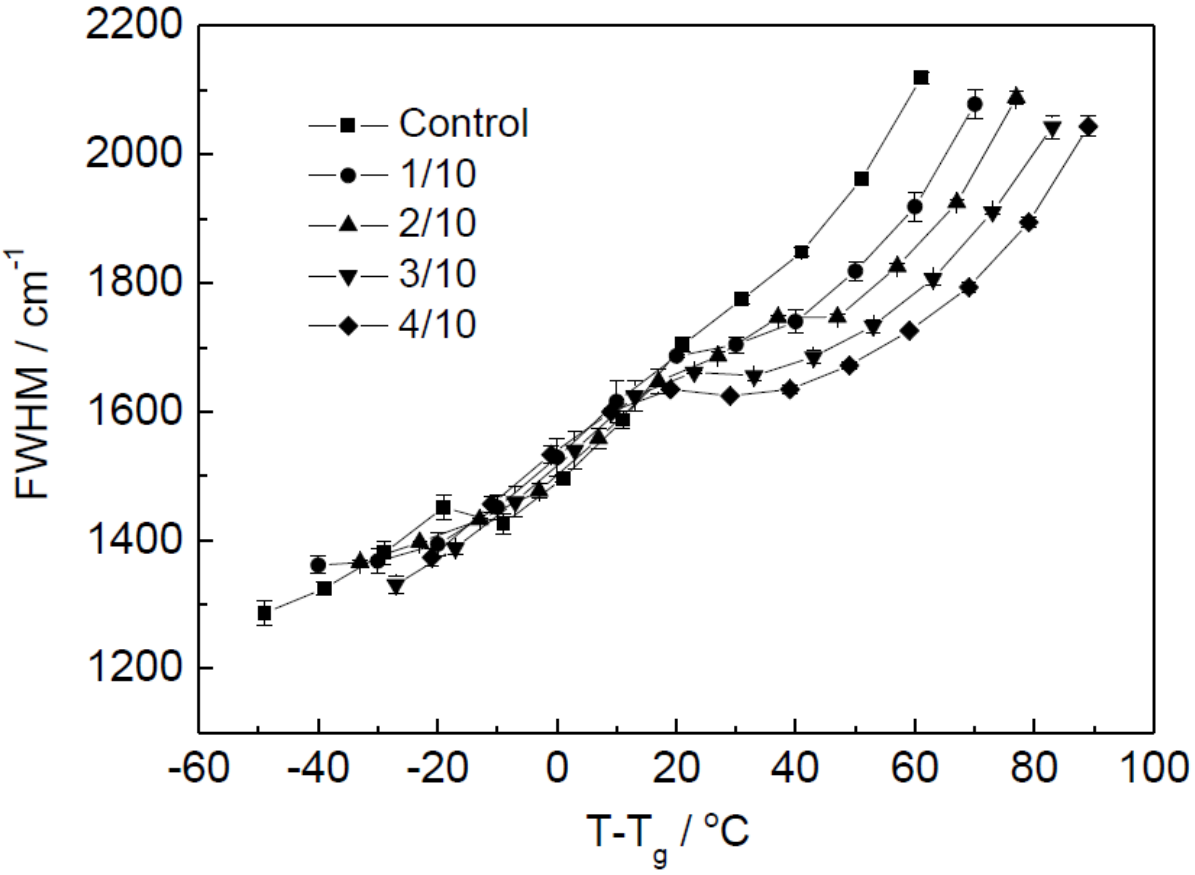

Figure 6. Temperature dependence of the bandwidth (FWHM) for phosphorescence emission from Ery B in amorphous glucose/glycerol films.

The peak frequency (ν_P) and bandwidth (r) for phosphorescence emission were determined by fitting emission spectra to a log-normal line shape function (Eq. 2 and 3) and plotted in Figures 5 and 6, respectively, as a function of T-T_g to emphasize their dependence on the physical state of the films. The peak frequency was approximately constant at low temperature and decreased dramatically at temperatures at and slightly above the matrix T_g to a significantly lower constant value. While all $\nu_P(T\text{-}T_g)$ curves were similar in shape, the presence of glycerol slightly lowered the peak frequency in a dose-dependent manner. The peak frequency provides a measure of the average energy of emission; consequently, a decrease in frequency reflects an increase in the average extent of dipolar relaxation around the excited triplet state prior to emission (Shirke & Ludescher, 2005). This mode of matrix relaxation thus increased dramatically with temperature at the T_g and to a much lesser extent with glycerol content at all temperatures.

The emission bandwidth increased with temperature in all samples. The bandwidth was largely unaffected by glycerol in the glass and at temperatures up to ~ T_g+20 ℃. In the sugar melt at higher temperatures, however, glycerol significantly lowered the bandwidth in a dose dependent manner. The phosphorescence bandwidth provides a measure of the range of energetically distinct matrix environments sampled by the Ery B probe within the amorphous matrix (You & Ludescher, 2007). The glycerol-induced decrease in inhomogeneous broadening at high temperatures indicates a corresponding decrease in the breadth of the distribution of energetically distinct matrix environments; glycerol thus appears to make the glucose melt, but not the glucose glass, more homogeneous.

Figure 7

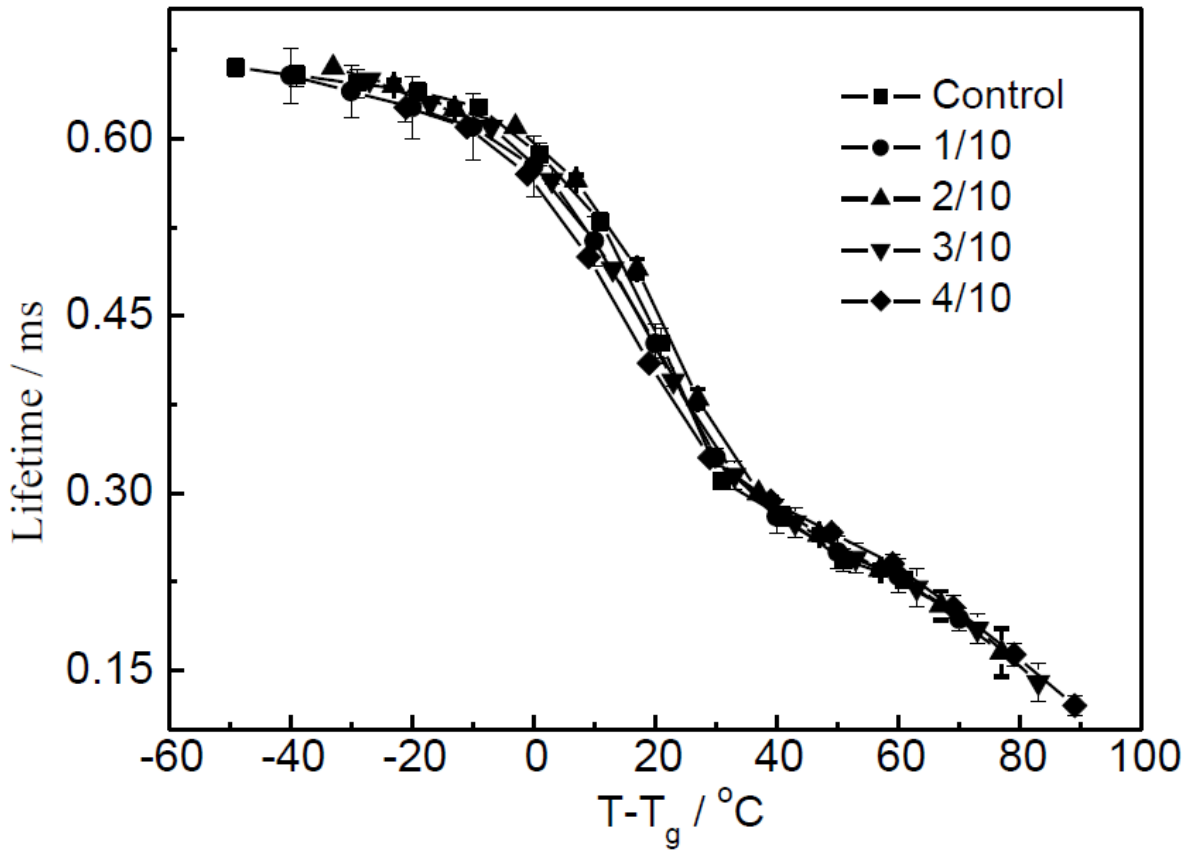

Figure 7. Temperature dependence of lifetime obtained from fits to a stretched exponential decay model of the intensity decay of Ery B in amorphous glucose/glycerol films.

Figure 8

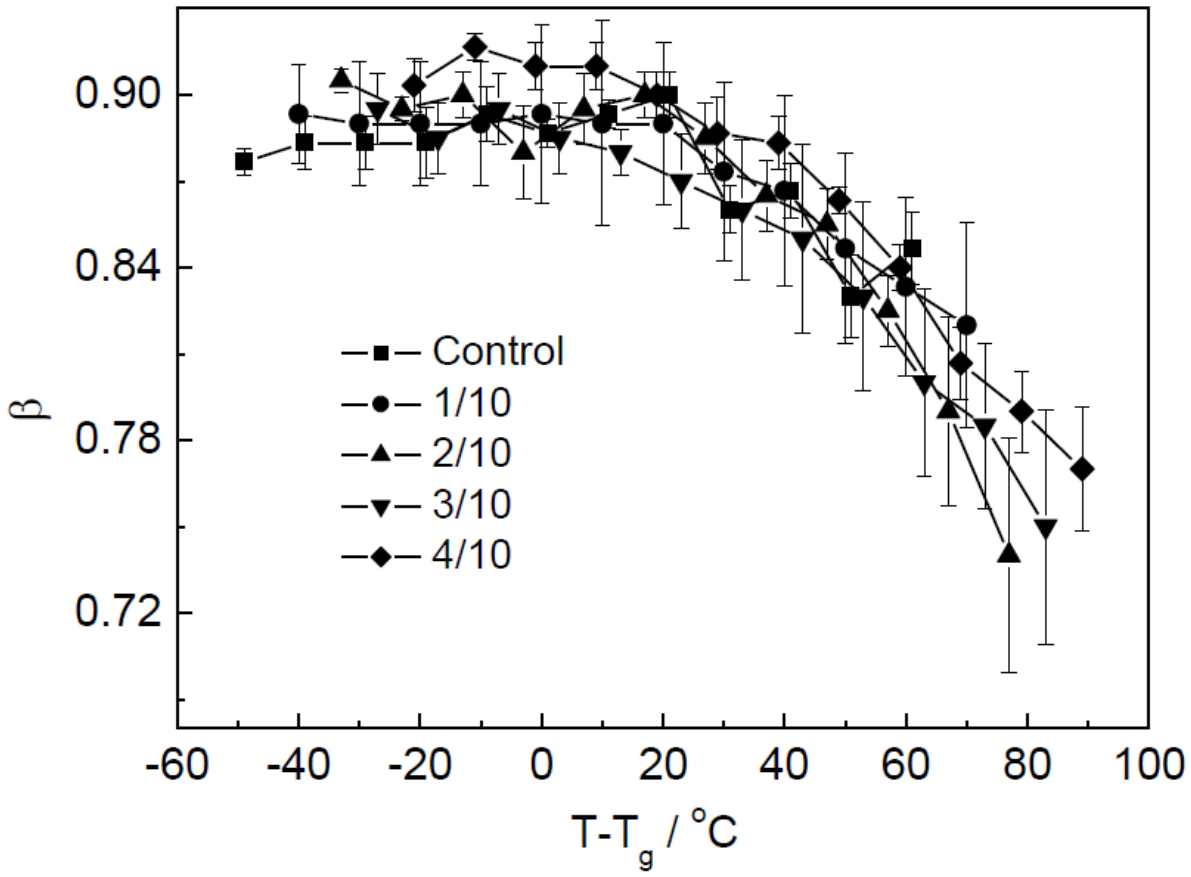

Figure 8. Stretching exponent β obtained from fits to a stretched exponential decay model of the intensity decay of Ery B in amorphous glucose/glycerol films.

3.2 Emission lifetimes

The phosphorescence emission intensity decays from Ery B in glucose/glycerol films under N_2 were collected from 100 to -10 ℃. All intensity decay transients were fit using a stretched exponential decay model (Eq. 1); R^2 was ≥ 0.995 for all fits. The stretched exponential lifetimes (τ) and stretching exponents (β) from these fits are plotted as a function of T-T_g in Figures 7 and 8, respectively. The lifetimes displayed a similar thermal behavior in all films, exhibiting a gradual linear decrease in the glass below T_g, a dramatic decrease at T_g, and a more gradual linear decrease beginning at ~ T_g+30 ℃. The lifetimes were comparable for all samples with varying content of glycerol, a distinctly different result from our previous results (Shirke & Ludescher, 2005), suggesting that the interaction of glucose and glycerol possesses different characteristics compared with other mixed sugar matrixes we have studied. The stretching exponent β was approximately constant in the matrix below ~ T_g+20 ℃ and decreased at higher temperature for all samples; there was no dose-dependent effect of glycerol.

The Ery B lifetimes in these samples were unaffected by oxygen (determined from data, not shown, collected in dry air) indicating that oxygen could not significantly permeate the glucose/glycerol matrix.

Figure 9

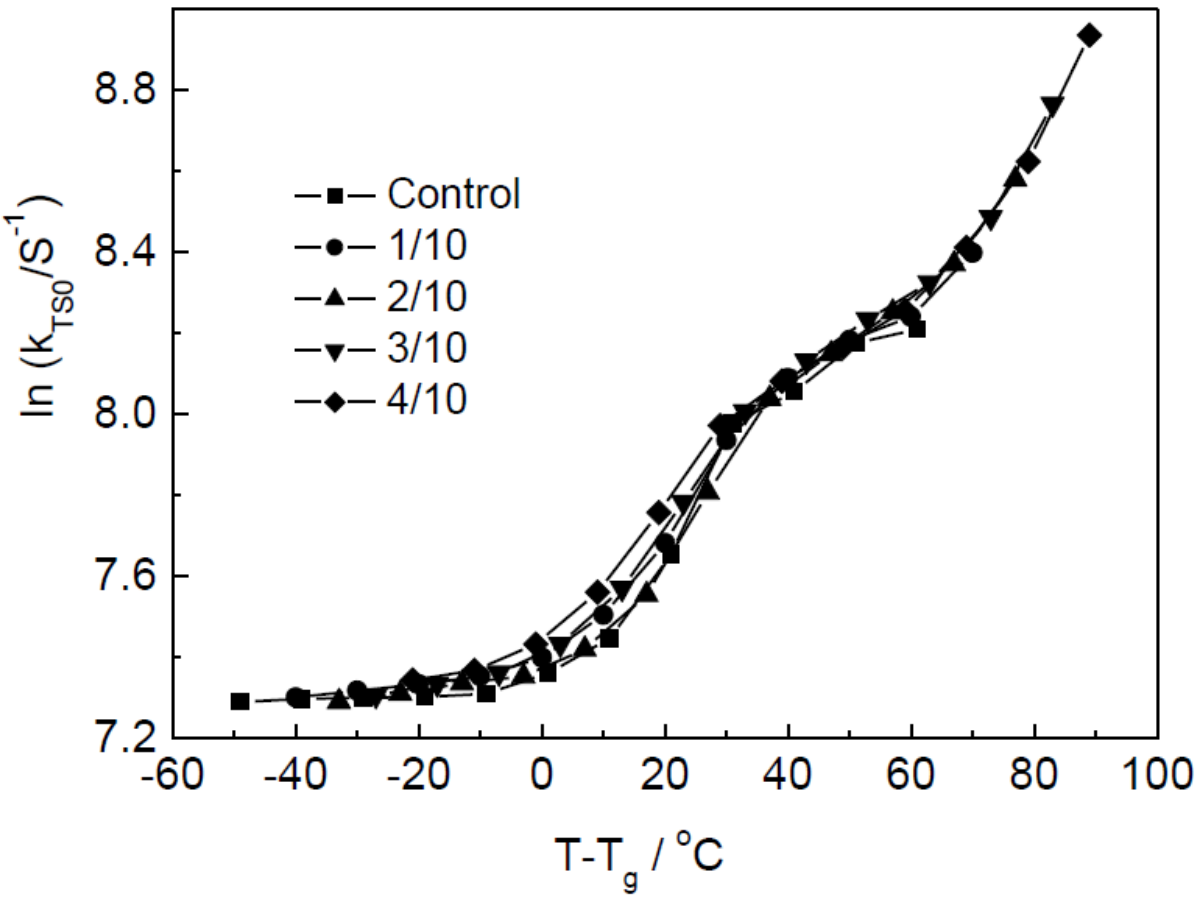

Figure 9. Effect of temperature on the rate constant for nonradioactive decay (k_{TS0}) of triplet state of Ery B in amorphous glucose/glycerol films. Data were calculated from the lifetime data of Figure 7.

In the absence of oxygen, the Ery B phosphorescence emission rate k_p (= 1/τ) is the sum of rates for radiative emission (k_{RP} = 41 s^{-1} for Ery B), reverse intersystem crossing k_{TS1}, and collisional quenching k_{TS0} (Eq. 4). The increase of k_p (decrease in lifetime) with temperature thus reflects an increase in k_{TS1} and k_{TS0}; the rate k_{TS1} follows Arrhenius kinetics (discussed above, Figure 4) while the rate k_{TS0} reflects the effect of temperature on the molecular mobility of the amorphous matrix (Pravinata, You & Ludescher, 2005). We calculated k_{TS0}(T) using Eq. 4, the literature value of k_{RP}, and our estimates of k_{TS1}(T). These values, plotted as ln(k_{TS0}) versus T-T_g in Figure 9, exhibit a quite complex temperature dependence. The values increased very gradually in the glass below T_g, increased dramatically over the temperature interval from T_g to T_g+30 ℃, and then exhibited a gradual increase that became more dramatic at temperatures above T_g+60 ℃.

Previous studies have indicated that glycerol can act as an antiplasticizer at low concentration and low temperature and as a plasticizer at high concentration and high temperature (You & Ludescher, 2007; Lourdin, Bizot & Colonna, 1997; Anopchenko, Psurek, VanderHart, Douglas & Obrzut, 2006; Roussenova, Murith, Alam & Ubbink, 2010). The concentration regimes over which glycerol acts as antiplasticizer or plasticizer are affected by experimental conditions and matrix composition. In amorphous sucrose (You & Ludescher, 2007), this changeover occurs at ~21 mol%. Since these mobility data collected at glycerol mole fraction from 0.1-0.4 scale nearly identically to T-T_g, it appears that glycerol acts only to plasticize the glucose matrix and does not have any antiplasticization effect. Data collected at very low glycerol concentration (1 wt%) further supported this conclusion.

Figure 10

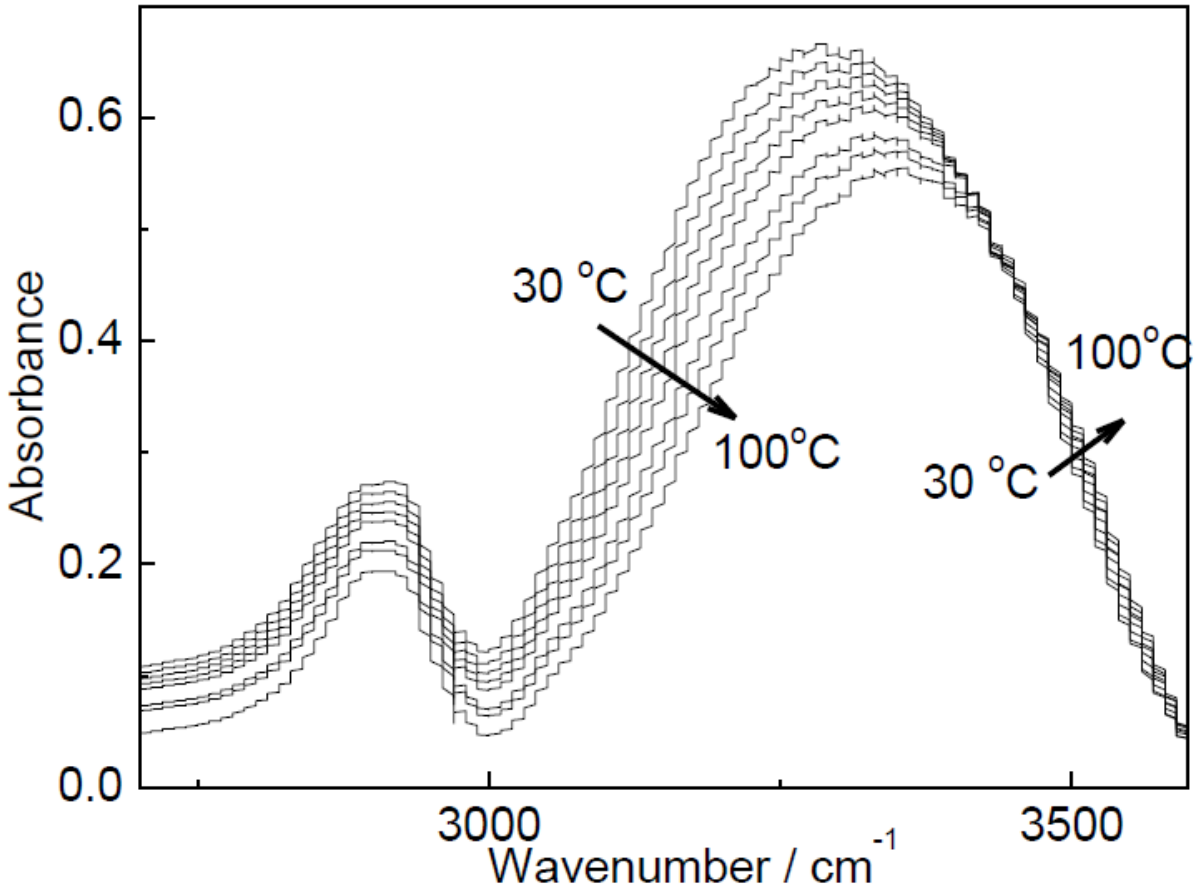

Figure 10. FTIR spectra of pure glucose film as function of temperature. Orientation of arrow indicates the increase of temperature.

Figure 11

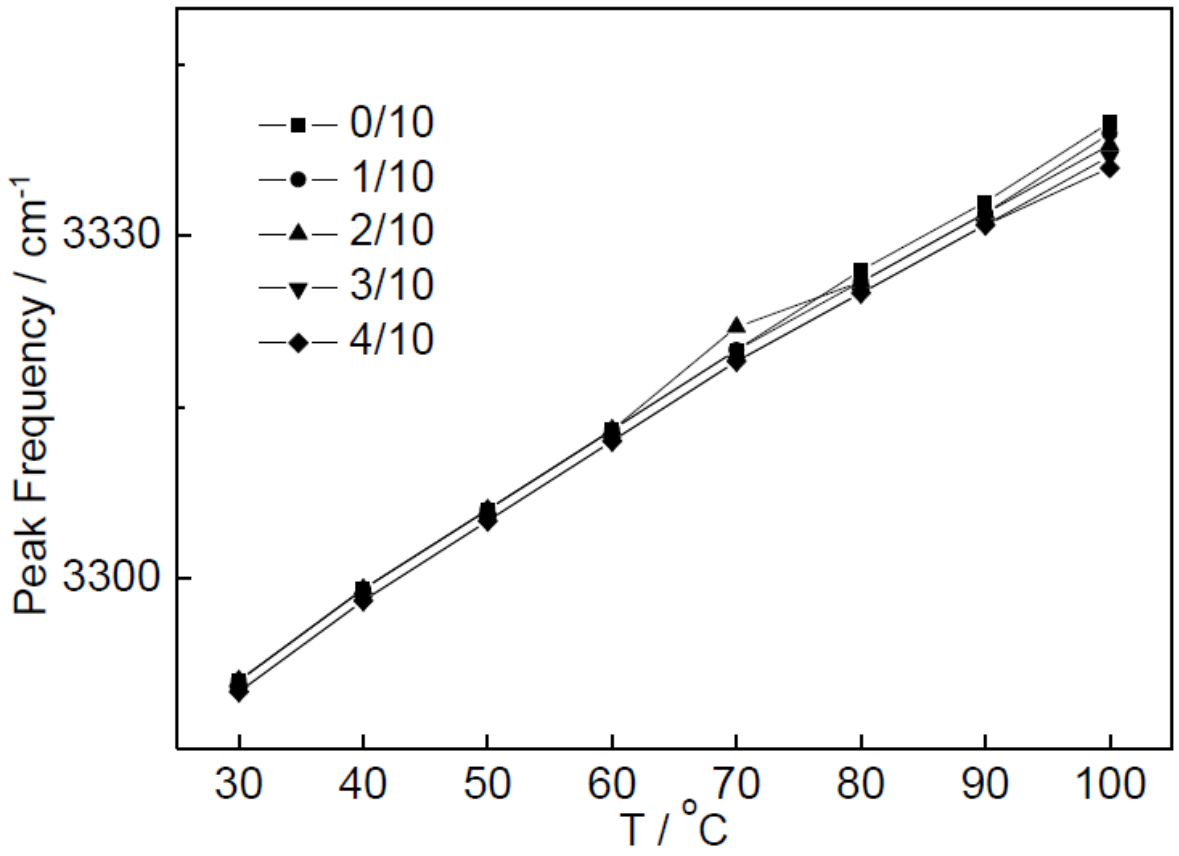

Figure 11. Peak frequency for FTIR spectra above 3000 cm^{-1} as function of temperature in glucose films containing varying content of glycerol.

Figure 12

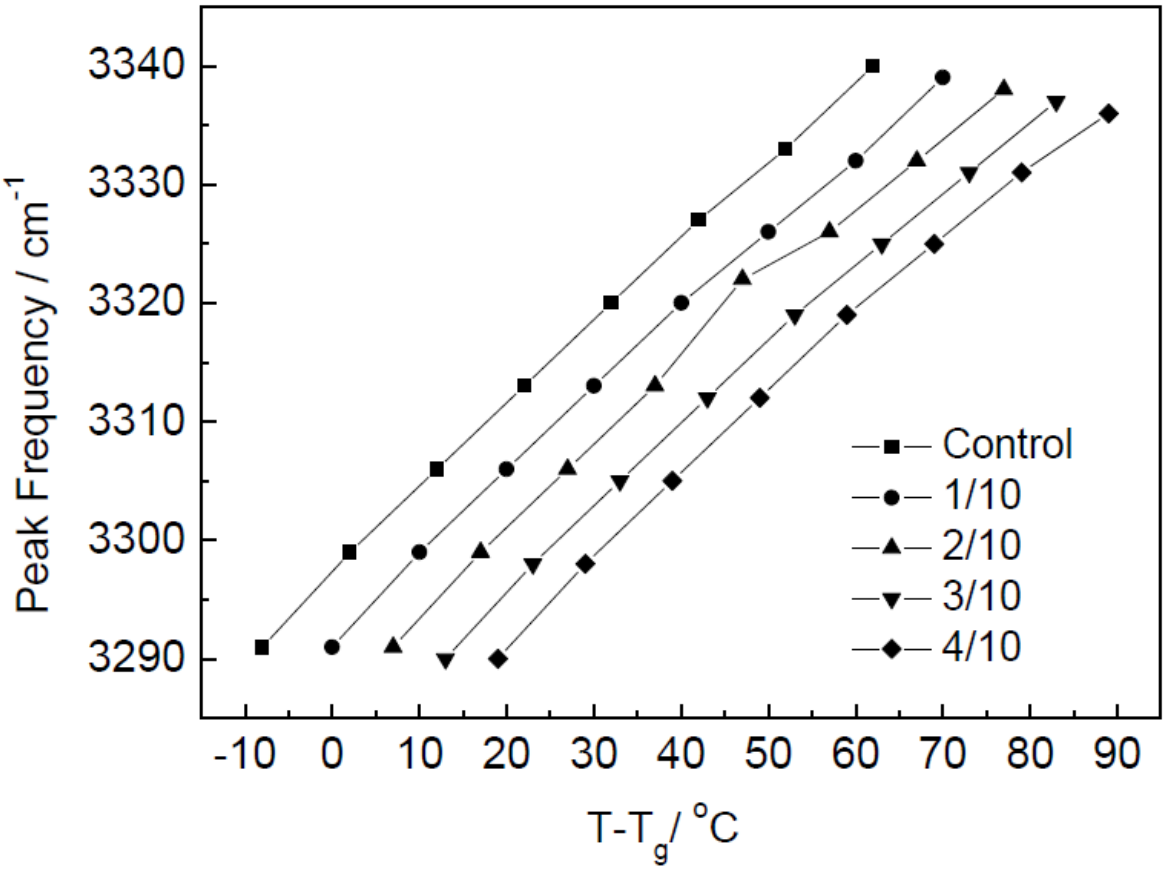

Figure 12. Normalized IR absorbance above 2990 cm^{-1} at 30 ℃ for glucose films containing varying content of glycerol. Orientation of arrow indicates the increase of glycerol content.

Figure 13

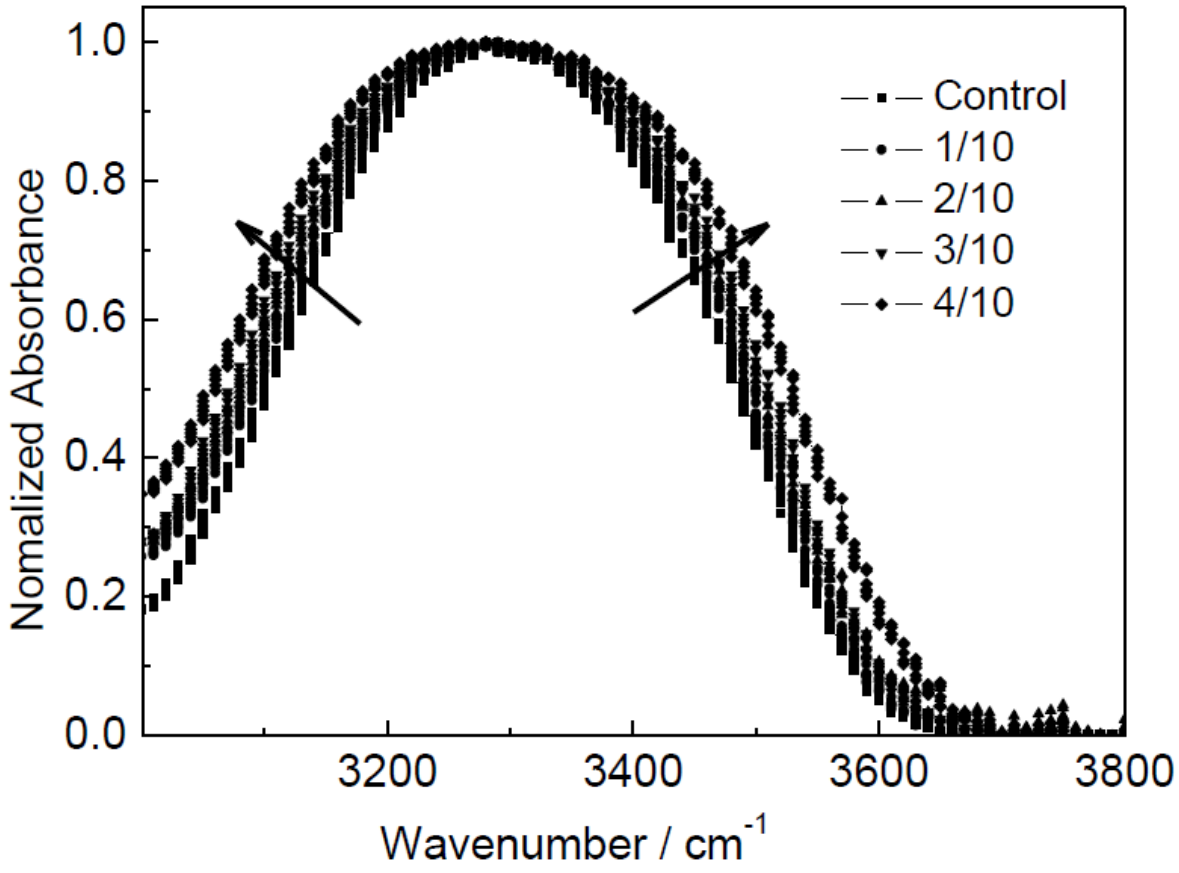

Figure 13. Effect of temperature on the half bandwidth for FTIR spectra above 3000 cm^{-1} in glucose films containing varying content of glycerol.

3.3 Infrared spectroscopy

Hydrogen bonds are the primary intermolecular forces that maintain the state of the amorphous sugar matrix. Changes in molecular mobility thus inevitably reflect changes in the hydrogen bond network. Hydroxyl groups in a carbohydrate solid can be either associated, hydrogen bonded to other hydroxyl groups, or free, not involved in hydrogen bonds. The vibrational frequency of both types of hydroxyls are distributed in the frequency range 3000-3600 cm^{-1}, while the frequency of free hydroxyls extends primarily into the higher frequency region (Kondo, 1997). Thus, when associated hydroxyls change to free hydroxyls, the hydroxyl absorbance in this region will shift to higher frequency.

The FTIR absorbance above 3000 cm^{-1} shifted to higher frequency with increase in temperature in all samples; representative data for pure glucose are plotted in Figure 10. An increase in thermal energy thus causes a shift in the distribution from associated to free hydroxyl groups, that is, breaks some hydrogen bonds. Although the absorbance in the region 3000-3300 cm^{-1}, assigned to both associated and free hydroxyls, weakened significantly with increase in temperature, the increase in the higher frequency region, assigned primarily to free hydroxyls, was marginal. We speculate that this is because the extinction coefficient of associated hydroxyls is much larger than that of free hydroxyls. The absorbance over the region from 2700-3000 cm^{-1} is attributed to the signal from stretch hydrogen of hydrocarbon structure. It weakened as well, consistent with that concurrently the effect of neighboring signal from hydroxyl was lost.

The peak frequency (in the region above 3000 cm^{-1}) of samples containing different glycerol contents increased linearly with temperature (Figure 11) with no significant difference

found between samples with different glycerol content. Thus, glycerol did not induce any significant change in the balance of associated versus free hydroxyl groups at any temperature.

The effect of glycerol on the hydroxyl absorbance from 3000-3600 cm^{-1} is illustrated in Figure 12 with data at 30 ℃. Although glycerol had no effect on the peak frequency it did cause a significant increase in the bandwidth. The half bandwidth of the hydroxyl absorbance is plotted as a function of temperature for each glycerol concentration in Figure 13. The half bandwidth reflects the hydrogen bond energy distribution for both associated and free hydroxyls. One possible interpretation of these data is that active mobility of hydroxyl results in broadened distribution of stretching orientation from hydroxyl and furthermore broadened half-band width of characteristic peak. Glycerol acted as plasticizer in glucose and activated the mobility of matrix. Hence, the half bandwidth increased with increase of glycerol content.

4. Conclusion

The mobility of amorphous solids is strongly influenced by composition and temperature, with the latter altering the molecular motions and the strength of intermolecular force, mainly hydrogen bond force modulating the state of matrix. Temperature and glycerol exerted the effects by different ways in this study. Temperature increase activated the molecular motions and caused the associated hydroxyl to dissociate to free hydroxyl, loosening the intermolecular interactions within the matrix as indicated by our results, glycerol could act as an effective plasticizer in glucose. The increase in molecular mobility by addition of glycerol caused broadened distribution of stretching orientation from hydroxyl. Thus, both the increase in temperature and the addition of glycerol could lead to the increase in molecule mobility of the matrix, whereas their effects on the hydrogen bond network were different.

Glucose is the simplest saccharide with a molecule volume closest to that of glycerol. Therefore, they can tightly interact with each other in a matrix with perfect compatibility, which can be reflected that the dipolar relaxation and molecular mobility of glucose matrix relative to the physical states based on T_g detect by Ery B were not much influenced by adding of glycerol. This renders a unique role to glycerol in glucose different from that in other matrixes: glycerol did not act as antiplasticizer in low content as it did in other matrixes.

References

Andronis, V., Zografi, G. (1997) Molecular mobility of supercooled amorphous indomethacin, determined by dynamic mechanical analysis. *Pharmaceutical Research*, 14, 410-414.

Anopchenko, A., Psurek, T., VanderHart, D., Douglas, J. F., Obrzut, J. (2006) Dielectric study of the antiplasticization of trehalose by glycerol. *Physical Review E*, 74, 031501-1-031501-10.

Couchman, P. R., Karasz, F. E. (1978) A classical thermodynamic discussion of the effect of composition on class-transition temperature. *Macromolecules*, 11, 117-119.

Cuq, B., Gontard, N., Cuq, J. L., Guilbert, S. (1997) Selected functional properties of fish myofibrillar protein-based films as affected by hydrophilic plasticizers. *Journal of Agricultural and Food Chemistry*, 45, 622-626.

Duchowicz, R., Ferrer, M. L., Acuña, A. U. (1998) Kinetic spectroscopy of erythrosine phosphorescence and delayed fluorescence in aqueous solution at room temperature. *Photochemistry and Photobiology*, 68, 494-501.

Fairley, P., Monahan, F. J., German, J. B., Krochta, J. M. (1996) Mechanical properties and water vapor permeability of edible films from whey protein isolated and sodium dodecyl sulfate. *Journal of Agricultural and Food Chemistry*, 44, 438-443.

Gao, C., Stading, M., Wellner, N., Parker, M. L., Noel, T. R., Clare Mills, E. N., Belton, P. S.(2006) Plasticization of a protein-based film by glycerol: a spectroscopic, mechanical, and thermal study. *Journal of Agricultural and Food Chemistry,* 54, 4611-4616.

Kim, Y. S., Hochstrasser, R. M. (2005) Chemical exchange 2D IR of hydrogen-bond making and breaking. *Proceedings of the National Academy of Sciences*, 102, 11185-11190.

Kondo, T. (1997) The assignment of IR absorption bands due to free hydroxyl groups in cellulose. *Cellulose*, 4, 281-292.

Lettinga, M. P., Zuihof, H., van Zandvoort, M. A. M. J. (2000) Phosphorescence and fluorescence characterization of fluorescein derivatives immobilized in various polymer matrices. *Physical Chemistry Chemical Physics*, *2*, 3697-3707.

Liang, J., Tian, Y. X., Fu, L. M., Wang, T. H., Li, H. J., Wang, P., Han, R. M., Zhang, J. P., Skibsted, L. H. (2008) Daidzein as an antioxidant of lipid: effects of the microenvironment in relation to chemical structure. *Journal of Agricultural and Food Chemistry*, 56, 10376-10383.

Liang, J., Tian, Y. X., Yang, Fan., Zhang, J. P., Skibsted, L. H. (2009) Antioxidant synergism between carotenoids in membranes. Astaxanthin as a radical transfer bridge. *Food Chemistry*, 115, 1437-1442.

Lourdin, D., Bizot, H., Colonna, P. (1997) ‘‘Antiplasticization’’ in starch-glycerol films? *Journal of Applied Polymer Science*, 63, 1047-1053.

Lukasik, K. V., Ludescher, R. D. (2006) Molecular mobility in water and glycerol plasticized cold- and hot-cast gelatin films. *Food Hydrocolloids*, 20, 96-105.

Nelson, E. W.; Newton, R. F. (1941) The heat capacity of glucose class. *Journal of the American Chemical Society*, 63, 2178-2182.

Pivonka, N. L. (2003) Probing a strong hydrogen bond with infrared spectroscopy: vibrational predissociation of $BrHbr^{-} \cdot Ar$. *The Journal of Chemical Physics*, 118, 5275-5278.

Pravinata, L. C., You, Y. M., Ludescher, R. D. (2005) Erythrosin B phosphorescence monitors molecular mobility and dynamic site heyerogeneity in amorphous sucrose. *Biophysics Journal*, 88, 3551-3561.

Roussenova, M., Murith, M., Alam, A., Ubbink, J. (2010) Plasticization, antiplasticization, and molecular packing in amorphous carbohydrate-glycerol matrices. *Biomacromolecules* 11, 3237-3247.

Romero-Bastida, C. A., Flores-Huicochea, E., Martin-Polo, M. O., Velazquez, G., Torres, J. A. (2004) Compositional and moisture content effects on the biodegradability of zein/ethylcellulose films. *Journal of Agricultural and Food Chemistry*, 52, 2230-2235.

Rozenberg, M. S. (1996) IR spectra and hydrogen bond energies of crystalline acid salts of carboxylic acids. *Spectrochimica Acta Part A*, 52, 1559-1563.

Shirke, S., Ludescher, R. D. (2005) Dynamic site heterogeneity in amorphous maltose and maltitol from spectral heterogeneity in Erythrosin B phosphorescence. *Carbohydrate Research,* 240, 2661-2669.

Shirke, S., Ludescher, R. D. (2005) Molecular mobility and the glass transition in amorphous glucose, maltose, and maltotriose. *Carbohydrate Research,* 240, 2654-2660.

Simon-Lukasik, K. V., Ludescher, R. D. (2004) Erythrosin B phosphorescence as a probe of oxygen diffusion in amorphous gelatin films. *Food Hydrocolloids*, 18, 621-630.

Simperler, A., Kornherr, A., Chopra, R., Bonnet, P. A., Jones, W., Motherwell, W. D. S., Zifferer, G. (2006) *The Journal of Physical Chemistry B*, 110, 19678-19684.

Sonar, P., Singh, S. P., Sudhakar, S., Dodabalapur, A., Sellinger, A. (2008) High-mobility organic thin film transistors based on benzothiadiazole-sandwiched dihexylquaterthiophenes. *Chemistry of Materials*, 20, 3184-3190.

Sun, W. Q. (1997) Glassy state and seed storage stability: the WLF kinetics of seed viability loss at T > T_g and the plasticization effect of water on storage stability. *Annals of Botany*, 79, 291-297.

Sundaresan, K. V., Ludescher, R. D. (2008) Molecular mobility and oxygen permeability in amorphous β-lactoglobulin films. *Food Hydrocolloids*, 22, 403-413.

Suyatma, N. E., Tighzert, L., Copinet, A. (2005) Effects of hydrophilic plasticizers on mechanical, thermal, and surface properties of Chitosan films. *Journal of Agricultural and Food Chemistry*, 53, 3950-3957.

Teixeira, E. M., Da RÓZ, A. L., Carvalho, A. J. F., Curvelo, A. A. S. (2007)The effect of glycerol/sugar/water and sugar/water mixtures on the plasticization of thermoplastic cassava starch. *Carbohydrate Polym*ers, 69, 619-624.

Vittadini, E., Dickinson, L. C., Lavoie, J. P., Pham, V., Chinachotti, P. (2003) Water mobility in multicomponent model media as studied by ^{2}H and ^{17}O NMR. *Journal of Agricultural and Food Chemistry*, 51, 1647-1652.

You, Y. M., Ludescher, R. D. (2007) The effect of glycerol on molecular mobility in amorphous sucrose detected by phosphorescence of erythrosine B. *Food Biophysics*, 2, 133-145.

You, Y. M., Ludescher, R. D. (2008) The effect of salts on molecular mobility in amorphous sucrose monitored by erythrosin B phosphorescence. *Carbohydrate Research*, 343, 2641-2649.

You, Y. M., Ludescher, R. D. (2009) Effect of xanthan on the molecular mobility of amorphous sucrose detected by erythrosin B phosphorescence. *Journal of Agricultural and Food Chemistry*, 57, 709-716.

Chapter III: Influence of Glycerol on the Molecular Mobility, Oxygen Permeability and Microstructure of Amorphous Zein Films

A manuscript accepted by *Food hydrocolloids*

Jun Liang, Qiuyang Xia, Simon Wang, Ji Li, Qingrong Huang, Richard. D. Ludescher

1. Introduction

Environmental concerns about the use of nondegradable plastics for packaging and disposable consumer goods have led to intensified research on the development of biodegradable packaging materials (Zhao, Torley & Halley, 2008). Edible, biodegradable films and coatings, by acting as barriers to control the transfer of moisture, oxygen, carbon dioxide, lipids, and flavor components, can prevent quality deterioration and increase the shelf-life of food products (Naushad Emmambux & Stading, 2007; Ghanbarzadeh & Oromiehi, 2009). In addition, edible films or coatings may provide mechanical integrity and improve the handling characteristics of the food. They can be effective carriers of many functional ingredients, such as antimicrobial agents to improve safety and stability of foods (Byun, Kim & Scott, 2010), antioxidants to prevent lipid oxidation (Liang & Ludescher, 2010), and flavorings and pigments to improve quality of foods (Soares and Hotchkiss, 1998).

Zein, the prolamine from maize seeds, has been extensively investigated as a commercial material for edible packaging because of its thermoplastic properties and excellent film-forming behavior (Lawton, 2002; Subramanian & Sampath, 2007; Tihminlioglu, Atik & Özen, 2011; Sanchez-Grarcia, Hilliou & Lagaron, 2010*).* Zein is used in the formulation of coatings for nuts, confectioneries, and pharmaceutical tablets. Preparation of zein films generally involves casting its alcohol or acetone solutions on inert and flat surfaces. The formed films can be peeled off after the solvent is evaporated (Lai &Padua, 1997). Zein films are brittle, and thus, plasticizers

are usually needed to improve their flexibility. Glycerol is one of the most important plasticizers and is widely used in zein films.

The effects of glycerol on the physical properties of polymer matrices have also been extensively studied. Low-molecular weight compounds or diluents, acting as external plasticizers, are an integral part of polymeric systems. They serve to increase the flexibility and workability of the otherwise rigid neat polymers. However, they may serve as mechanical antiplasticizers when present at low concentrations, resulting instead in stiffer polymer– diluent blends than the neat polymer. The phenomena that glycerol can act as both a plasticizer and an antiplasticizer are well-known and have received increasing attention from food scientists and technologists in recent years (Chang, Karim & Seow, 2005). It has been reported that glycerol can exert different effects depending on its concentration. Lourdin and colleagues reported that glycerol at a content below 12% could increase the ductility of potato starch film. However, the ductility decreased when the amount of glycerol exceeded 12% (Lourdin, Bizot & Colonna, 1997). A similar antiplasticizing effect of glycerol was also found in the matrices of trehalose and maltodextrin (Anopchenko, Psurek, VanderHart, Douglas & Obrzut, 2006; Roussenova, Murith, Alam & Ubbink, 2010). In most cases, there exists a critical glycerol content that marks the onset of a change in functionality from antiplasticizer to plasticizer. Those conclusions, however, were typically obtained from macroscopic methods like DSC and film stress analysis, while rarely depending upon molecular techniques such as positron annihilation lifetime spectroscopy. In the microscale point of view, data concerning how glycerol can affect the molecular mobility that underlies matrix functionality, as far as we know, are rare.

Gas permeability is an important property of edible biopolymeric film systems. The ease with which mass transfer can occur across a film ultimately determines its value as a gas barrier.

Oxygen is responsible for many of the degradative processes that limit the shelf life of foods, and its exclusion or reduction in a food's internal environment is critical. Oxygen permeability (*P*) can be related to its diffusion coefficient (*D*) and solubility (*S*) in a particular material by the equation $P = DS$ (Crank &Park, 1968). Glycerol can affect the oxygen permeability in the zein matrix in two distinct ways: (1) modulate the oxygen diffusion coefficient (D) by changing the matrix mobility as a plasticizer/ antiplasticizer, and (2) lower the oxygen solubility (S) in the zein matrix (Liang & Ludescher, 2012).

Phosphorescence probe techniques have been shown to provide detailed information about correlations among local molecular mobility, dynamic heterogeneity, and oxygen permeability in amorphous solid biomaterials (Nack &Ludescher, 2006; Subramanian & Sampath, 2007; Sundaresan & Ludescher, 2008). In this study we have used phosphorescence of Erythrosin B (Ery B), a triplet state molecular probe, to monitor the local molecular properties and mobility of amorphous zein/glycerol films cast from 70% ethanol aqueous solution. Measurements of the Ery B emission energy and excited-state lifetime provide information about how glycerol influences the mobility of the matrix. Comparison of the phosphorescence lifetime in the presence or absence of air was used to monitor the oxygen permeability. Microstructural changes in the zein film were also determined by atomic force microscopy (AFM). This research provides insight into the molecular mechanism by which glycerol modulates the physical and functional properties of edible polymer barriers which can help improve our ability to engineer edible food films with appropriate functionalities.

2. Materials and Methods

2.1 Sample Preparation.

Amorphous zein films were prepared by using our published method with slight modification (Liang & Ludescher, 2011). α-Zein (Biochemical-grade, Wako Pure Chemical Industries, Ltd., Tokyo, Japan) was added to 70% (v/v) ethanol in water solution to reach a final concentration of 0.5% (w/v). Glycerol (99% GC pure; Sigma Chemical, St. Louis, MO) was added to zein solution to obtain the final contents of 0, 5, 10, 20 and 30 percent in dry zein-glycerol films. Ery B (sodium salt, Sigma Chemical, St. Louis, MO) was dissolved in deionized water to prepare 10 mM probe stock solution; aliquots from this solution were added to the zein solution to make sample solutions with probe/zein mole ratio of about 3:20 (assuming a molecular weight 2×10^4 g/mol for zein).

To prepare zein films for luminescence measurements, 15 μl of protein/probe/glycerol solution at room temperature was spread on approximately one third of a quartz slide (30 × 13.5 × 0.6 mm, custom made by NSG Precision Cells, Farmingdale, NY). Before usage, the slides were soaked in Terg-A-Zyme (Alconox, Inc., NY) soap solution for > 24 h to remove surface impurities, washed with deionized water, rinsed with ethanol and dried with acetone. The sample slides were stored at room temperature against the desiccants DrieRite and P_2O_5, in order to maintain 0% RH, for at least one week and protected from light to prevent any photobleaching of Ery B. The desiccants were refreshed as necessary.

For AFM experiments, films were prepared using the same method used to prepare slides for luminescence except that the sample solutions were spread on mica chips (around 0.5 cm × 0.5 cm).

2.2 Phosphorescence Measurements and Analysis.

All measurements were conducted on a Cary Eclipse spectrophotometer (Varian Instruments, Walnut Creek, CA) equipped with a temperature controller and multicell holder. All measurements were made at least in triplicate and the slides were first heated and cooled and then data were collected from 0 to 100°C in all experiments.

High purity nitrogen (minus O_2) or dry air (plus O_2) was flowed directly into capped quartz fluorescence cuvettes holding the slides. The cuvette was flushed for at least 30 min at 50°C before each set of measurements. The cuvette was capped with a lid having inlet and outlet ports for the gas line, so all experiments were performed at constant pressure. Each phosphorescence intensity decay was an average of 50 cycles. For each cycle, data were collected from a single lamp flash with a delay of 0.04 ms, a 0.05 ms gate, and 10.0 ms total decay time. Phosphorescence and delayed fluorescence emission scans were collected over the range from 540 to 800 nm with an excitation wavelength of 520 nm. The excitation and emission monochromators were both set at 20 nm band pass. For phosphorescence emission scans, each data point (collected at 1 nm intervals with a 0.1 s averaging time) was collected from a single flash with 0.2 ms delay and 5 ms gate time.

For lifetime measurements, because intensity decays were non-exponential, a stretched exponential function was selected to analyze the intensity decays:

$$I(t) = I(0) \exp\left[-(t/\tau)^{\beta}\right] + \text{constant} \qquad (1)$$

where $I(0)$ is the initial intensity, τ is the stretched exponential lifetime, and β is an exponent varying from 0 to 1 that characterizes the lifetime distribution. The use of a stretched exponential model provides an analysis in terms of a continuous distribution of lifetimes, which

is appropriate for describing a complex glass possessing a distribution of relaxation times for dynamic molecular processes. The smaller the β value, the more non-exponential the intensity decays and the broader the distribution of lifetimes (You & Ludescher, 2009).

The energy of the emission maximum (ν_p) and the full-width-at-half maximum (FWHM) of the emission band were determined by using a log-normal line shape function,

$$I(\nu) = I_0 \exp\left\{-\ln(2)\left(\frac{\ln[1 + 2b\,(\nu-\nu_p)/\Delta]}{b}\right)^2\right\} \qquad (2)$$

where I_0 is the maximum emission intensity, ν_p is the peak frequency (cm^{-1}), Δ is a linewidth parameter, and b is an asymmetry parameter. The bandwidth Γ (FWHM) is calculated according to the following equation:

$$\Gamma = \Delta\left[\frac{\sinh(b)}{b}\right. \qquad (3)$$

For delayed luminescence spectra collected from 540-750 nm, a sum of two log-normal functions with independent parameters was used to separately fit the delayed fluorescence ($I_{DF}(\nu)$) and phosphorescence ($I_P(\nu)$) bands.

The phosphorescence lifetimes were used to calculate the rate constants associated with the various processes that depopulate the triplet state. Our analysis of the delayed emission is similar to the photophysical scheme for Ery B outlined by Duchowicz and coworkers using slightly different nomenclature (Duchowicz, Ferrer & Acuña, 1998). The measured phosphorescence lifetime (τ) is the inverse sum of all possible de-excitation rates for the triplet state T_1:

$$1/\tau = k_P = k_{RP} + k_{TS1} + k_{TS0} + k_Q[O_2] \qquad (4)$$

Here k_{RP} is the rate of radiative decay to the ground state, k_{TS1} is the rate of reverse intersystem crossing to S_1, k_{TS0} is the rate of intersystem crossing to the singlet manifold followed by vibrational relaxation to S_0, and $k_Q[O_2]$ is rate of oxygen quenching (assumed negligible in the absence of oxygen). The radiative decay rate has a value of 41 s^{-1} for Ery B (Lukasik & Ludescher, 2006).

Reverse intersystem crossing is a thermally activated process that has an exponential dependence on the energy gap ΔE_{TS} between T_1 and S_1 (Pravinata, You &Ludescher, 2005):

$$k_{TS1}(T) = k^{o}_{TS1}\exp(-\Delta E_{TS}/RT) \qquad (5)$$

The ratio of intensity of delay fluorescence (I_{DF}) to phosphorescence (I_P), where I_{DF} and I_P are determined from analysis of emission spectra using the log-normal function (Eq. (2)), is proportional to the rate of reverse intersystem crossing. A plot of $\ln(I_{DF}/I_P)$ versus 1/T thus has slope of $-\Delta E_{TS}/R$. Values of k^{o}_{TS1} for Ery B reported in the literature vary from 0.3×10^7 s^{-1} in ethanol and 6.5×10^7 s^{-1} in water (Duchowicz, Ferrer & Acuña, 1998) to 111×10^7 s^{-1} in solid polyvinyl alcohol (Lettinga, Zuihof &van Zandvoort, 2000). We estimated the maximum possible value for k^{o}_{TS1} in zein with 20% glycerol by assuming that $k_{TS1}(T)$ cannot result in values for k_{TS0} that decrease with temperature (You & Ludescher, 2010). This procedure thus estimated the minimum possible values of $k_{TS0}(T)$. We used a value of $k^{o}_{TS1} = 0.3 \times 10^7$ s^{-1} in this research and the measured value of ΔE_{TS} to calculate $k_{TS1}(T)$.

In the presence of oxygen, the quenching rate $k_Q[Q]$ is the product of the rate constant k_Q and the oxygen concentration $[O_2]$. For measurements done while flushing nitrogen over the slides, we assume that no oxygen quenching occurred ($[O_2] = 0$). The value of $k_Q[Q]$ can thus be calculated directly using Eq. 4 by taking the difference between the inverse lifetimes in the

presence (air) and absence (N_2) of oxygen. A major non-radiative decay route is through intersystem crossing to the ground S_0. The decay rate is expressed by k_{TS0}, which reflects the rate of quenching of the probe due to coupling of the excited T_1 state to a highly excited vibration of the ground S_0 state followed by dissipation of vibrational energy from the probe into the matrix. This value of k_{TS0} is thus a measure of matrix molecular mobility (You & Ludescher, 2010). The temperature–dependence of k_{TSO} can be calculated from measurements of the Ery B lifetime under nitrogen using Eq. 4 because k_{RP} is known and $k_{TS1}(T)$ can be calculated as described above (Eq. 5).

2.3 Atomic Force Microscopy (AFM).

Tapping mode AFM images were collected using a NanoScope IIIA Multimode AFM (Veeco Instruments Inc., Santa Barbara, CA) equipped with a silicon-etched RTESP7 cantilever (Veeco Nanoprobe, Camarillo, CA) under ambient conditions. Before tip engagement, the drive frequency of the silicon tip was tuned with the aid of Nanoscope 5.30 software and fixed at 200-250 kHz for further scanning. All of the collected images were flattened before further analysis.

Figure 14

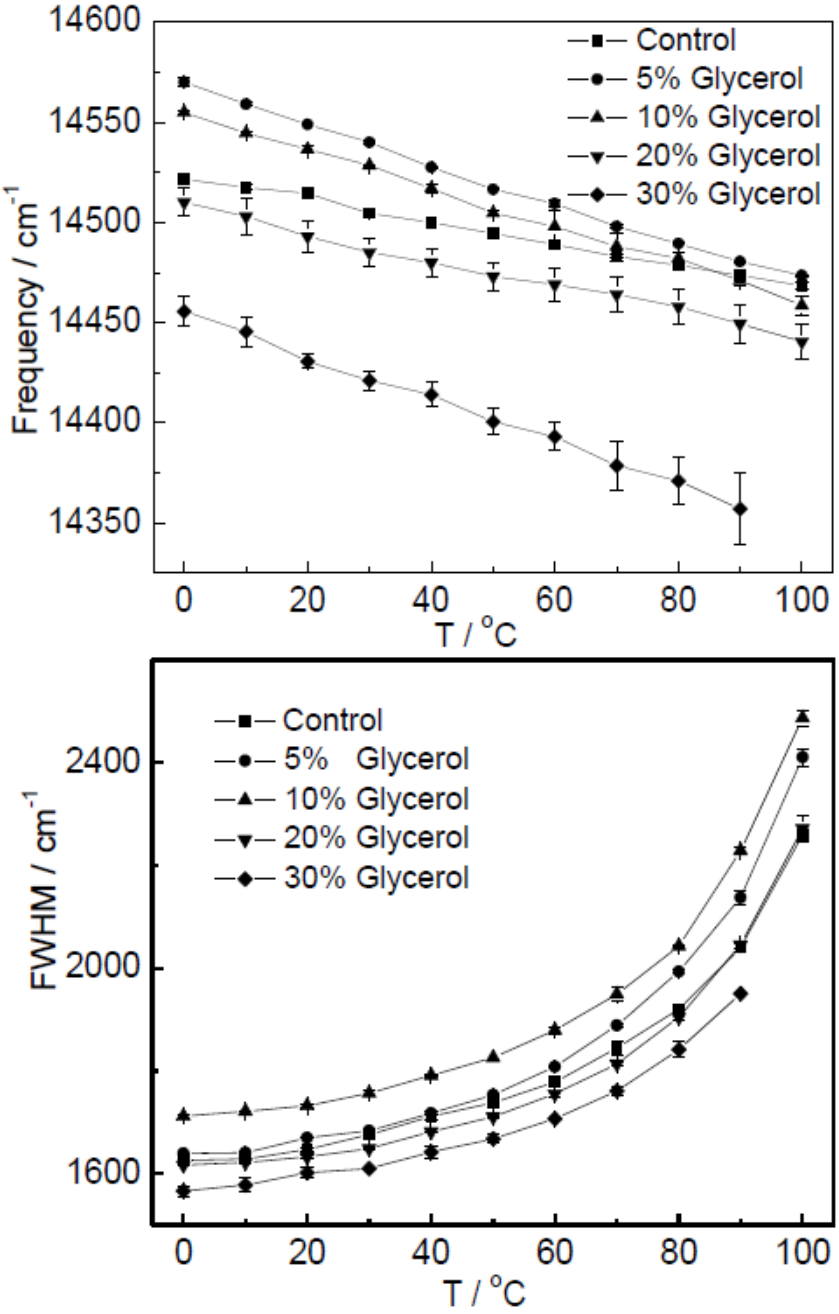

Figure 14: Effect of temperature on the peak frequency and bandwidth (FWHM) for phosphorescence emission from Ery B dispersed in zein and zein/glycerol films.

3. Results and Discussion

3.1 Delayed emission spectra.

The delayed emission spectra of Ery B in amorphous zein/glycerol films displayed the typical longer wavelength phosphorescence band (maximum ~690 nm) due to emission from the triplet T_1 state and a shorter wavelength delayed fluorescence band (maximum ~555 nm) due to emission from the singlet S_1 state repopulated by thermally stimulated reverse intersystem crossing from T_1. Delayed emission spectra from zein films with different glycerol content showed the expected decrease in phosphorescence (I_P) and increase in delayed fluorescence (I_{DF}) intensity with increasing temperature (data not shown). The intensity ratio was analyzed as a van't Hoff plot of $\ln(I_{DF}/I_P)$ versus 1/T and the linear slope was used to estimate the energy gap (ΔE_{TS}) between the triplet and singlet states. These plots were linear with $R^2 \geq 0.995$; the slopes from zein samples containing various glycerol contents showed negligible differences (data not shown), indicating that the energy gap, and thus $k_{TS1}(T)$, was not greatly affected by addition of glycerol.

The peak emission frequency (ν_P) and bandwidth (Γ) for both delayed fluorescence and phosphorescence emission were determined by fitting emission spectra to a log-normal line shape function (Eqs. 2 and 3). The values of ν_P for phosphorescence emission from films containing various glycerol contents are plotted in Fig. 14a. All ν_P curves showed an approximately linear decrease with temperature. Since the phosphorescence peak frequency provides a measure of the average energy of emission, this decrease in emission energy reflects an increase in the average extent of matrix dipolar relaxation around the excited molecule prior to emission (Pravinata, You & Ludescher, 2005), indicating a gradual yet consistent temperature-dependent change in the properties of the matrix around the probe. This structural reorganization

decreased the energy of the Ery B emission either by increasing the local matrix polarity and/or hydrogen bonding ability around the probe or, more probably, by increasing the rate and thus the extent of dipolar relaxation during the probe's excited state lifetime.

At low and intermediate temperature, the presence of glycerol increased the average emission energy at low weight ratios (≤ 10 %) and decreased the energy at higher weight ratios. These changes are consistent with a decrease in the average extent (and perhaps rate) of dipolar relaxation around the excited state probe at low and an increase in the extent (and rate) of dipolar relaxation at high glycerol content. This is the expected response of this probe to antiplasticization at low and plasticization at high glycerol content (You & Ludescher, 2007).

The phosphorescence bandwidth increased gradually at low and more steeply at high temperature in all films (Fig. 14b). The addition of glycerol in high content (20% and 30%) decreased in bandwidth over the whole temperature range while the films with low content of glycerol (5% and 10%) increased in bandwidth. The phosphorescence bandwidth reflects the extent of inhomogeneous broadening due to a range of energetic interactions between the matrix and the excited probe (You & Ludescher, 2008); it thus reflects the local molecular structure and interactions of the matrix and not large scale phenomenon such as phase separation. A decrease in bandwidth for films with high content of glycerol thus reflects a corresponding decrease in the width of the distribution of energetically distinct matrix environments. Meanwhile it's interesting to find that the films with low content of glycerol (5% and 10%) presented an increase in bandwidth, indicating that the matrix-probe interactions at low glycerol were more variable than without glycerol or at high glycerol.

Figure 15

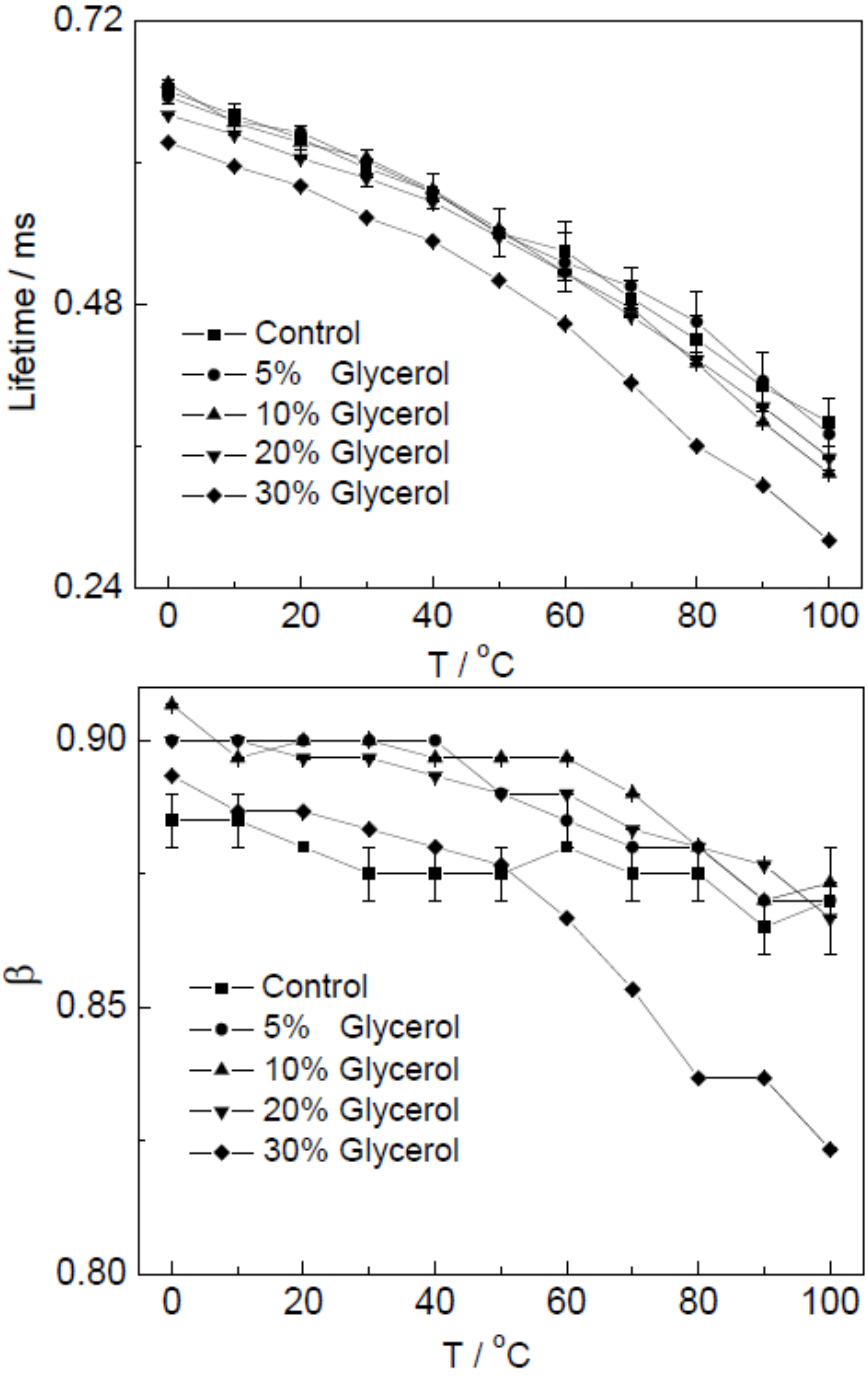

Figure 15: Effect of temperature on the lifetime and stretching exponent (β) obtained from fits to a stretched exponential decay model of the intensity decay of Ery B dispersed in zein and zein/glycerol films purged with N_2 (minus O_2)

3.2 Phosphorescence emission lifetimes.

The phosphorescence emission intensity decay transients from Ery B in films of zein/glycerol under purging with either nitrogen or dry air were collected as a function of temperature over the range from 0 to 100°C. All intensity decay transients were well fit using a stretched exponential decay model (Eq. 1) in which the lifetime τ and stretching exponent β were the physically relevant fitting parameters; R^2 was ≥ 0.995 for all fits indicating that our model adequately describes the decay kinetics. The stretching exponent β of all samples in nitrogen decreased with temperature (Fig. 15b), indicating that the distribution of lifetimes in the phosphorescence decay broadened with increase in temperature in a manner consistent with the increase in inhomogeneous broadening of the emission spectra.

The phosphorescence lifetime under N_2 (minus O_2) decreased monotonically with increasing temperature (Fig. 15a); the decrease was gradual at low and steeper at higher temperature in all samples indicating that the non-radiative decay rates were thermally activated. There was an obvious decrease in lifetime at all temperatures in films with 30% glycerol and a slight decrease in films with 20%, while the lifetimes were unaffected in films with 5% and 10% glycerol.

To quantify the influence of glycerol on oxygen permeability in zein films, we measured the phosphorescence decay of Ery B under dry air where oxygen collisions can also quench the excited triplet state. Because the oxygen quenching constant $k_Q[O_2]$ is the product of terms proportional to both the rate of oxygen diffusion (k_Q) and the thermodynamics of oxygen solubility ($[O_2]$), it reflects the permeability of the zein/glycerol matrix to oxygen. The lifetimes under dry air in films with varying content of glycerol are plotted as a function of temperature in Fig. 16. The phosphorescence lifetime under air (plus O_2) was significantly increased by the presence of glycerol in a dose-dependent fashion.

The value of $k_Q[O_2]$ as a function of temperature was calculated from the lifetimes in air and in nitrogen using Eq. 4; these data are plotted versus temperature in Fig. 17. The value of $k_Q[O_2]$ decreased with the increase of glycerol content in the zein films while also increasing as a function of temperature in all samples.

Figure 16

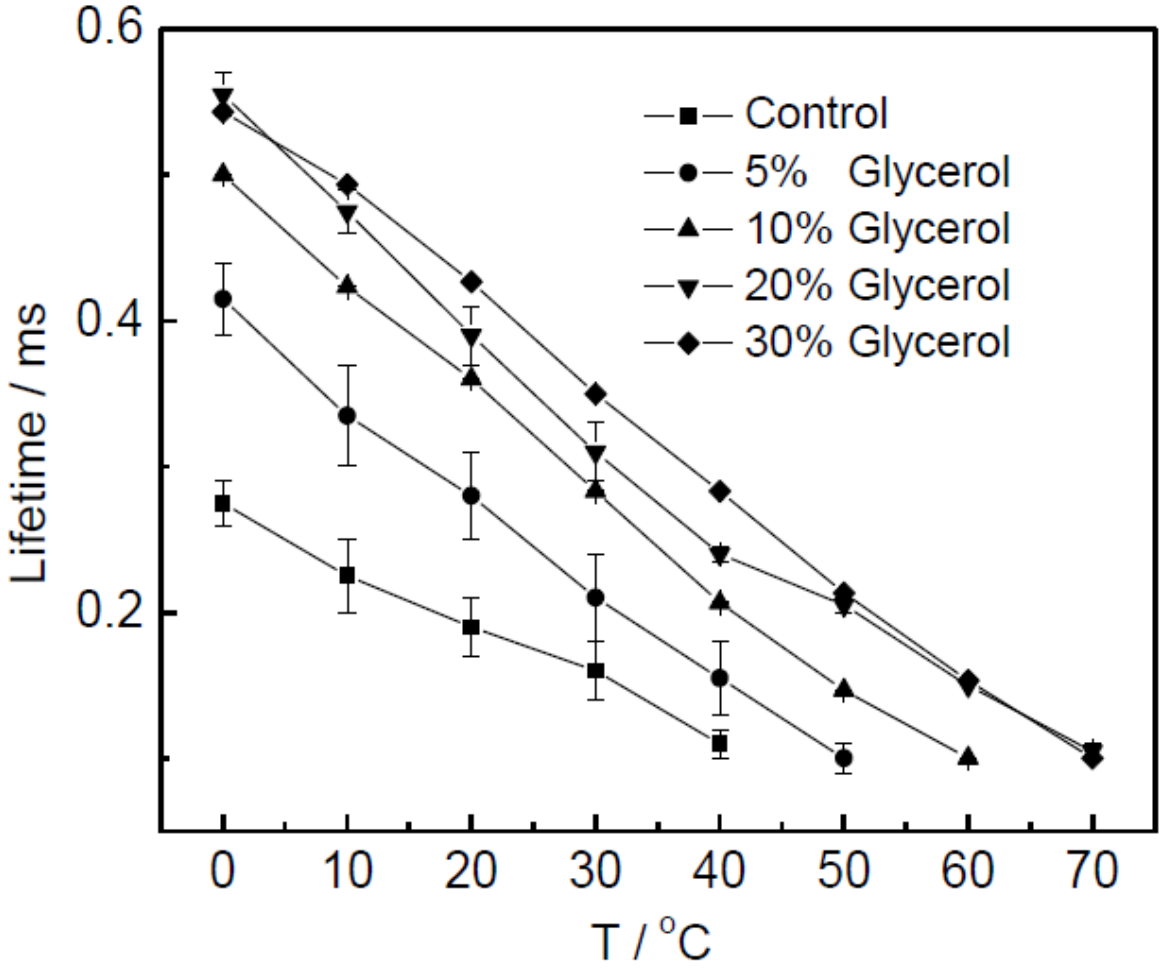

Figure 16: Effect of temperature on the lifetime obtained from fits to a stretched exponential decay model of the intensity decay of Ery B dispersed in zein and zein/glycerol films purged with air (plus O_2).

Figure 17

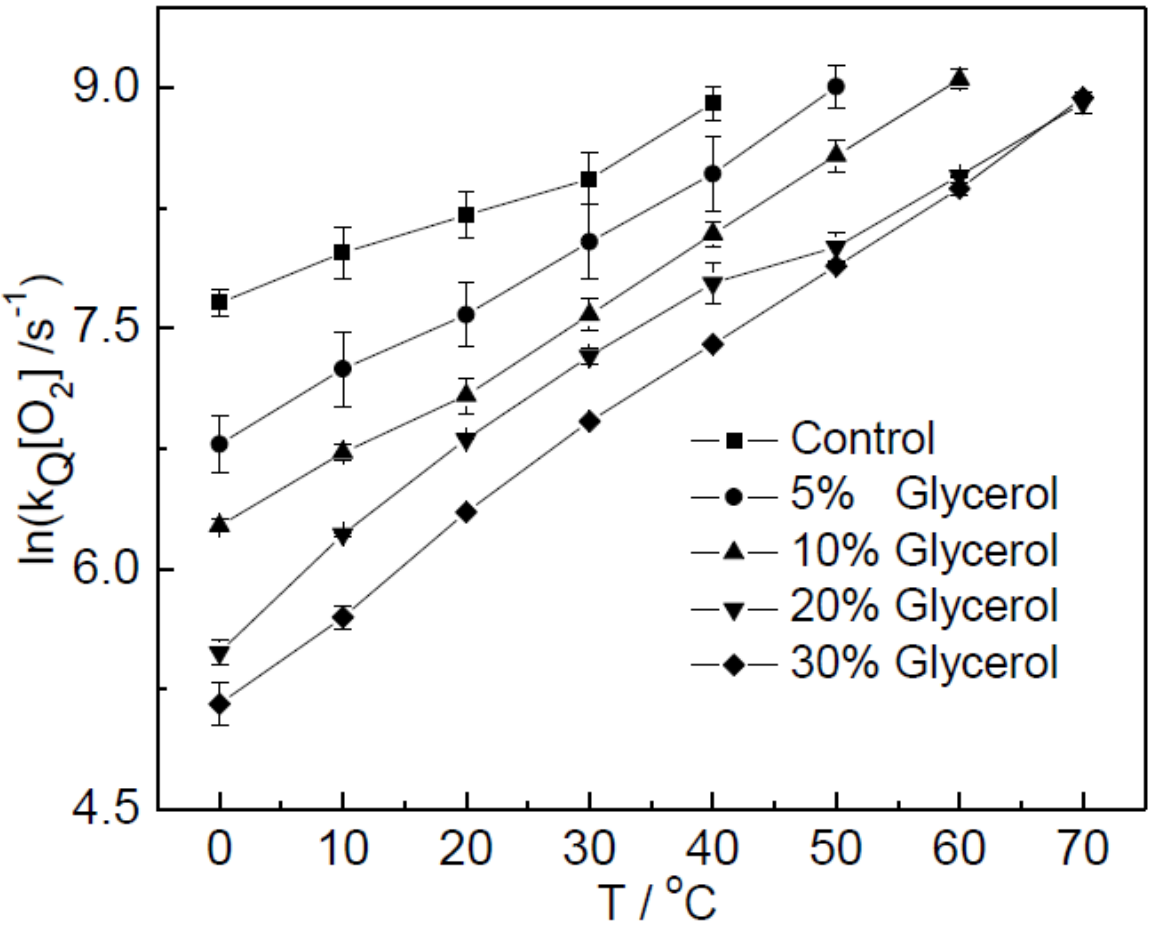

Figure 17: Temperature dependence of oxygen quenching rate $k_Q[O_2]$ for Ery B in zein and zein/glycerol.

Figure 18

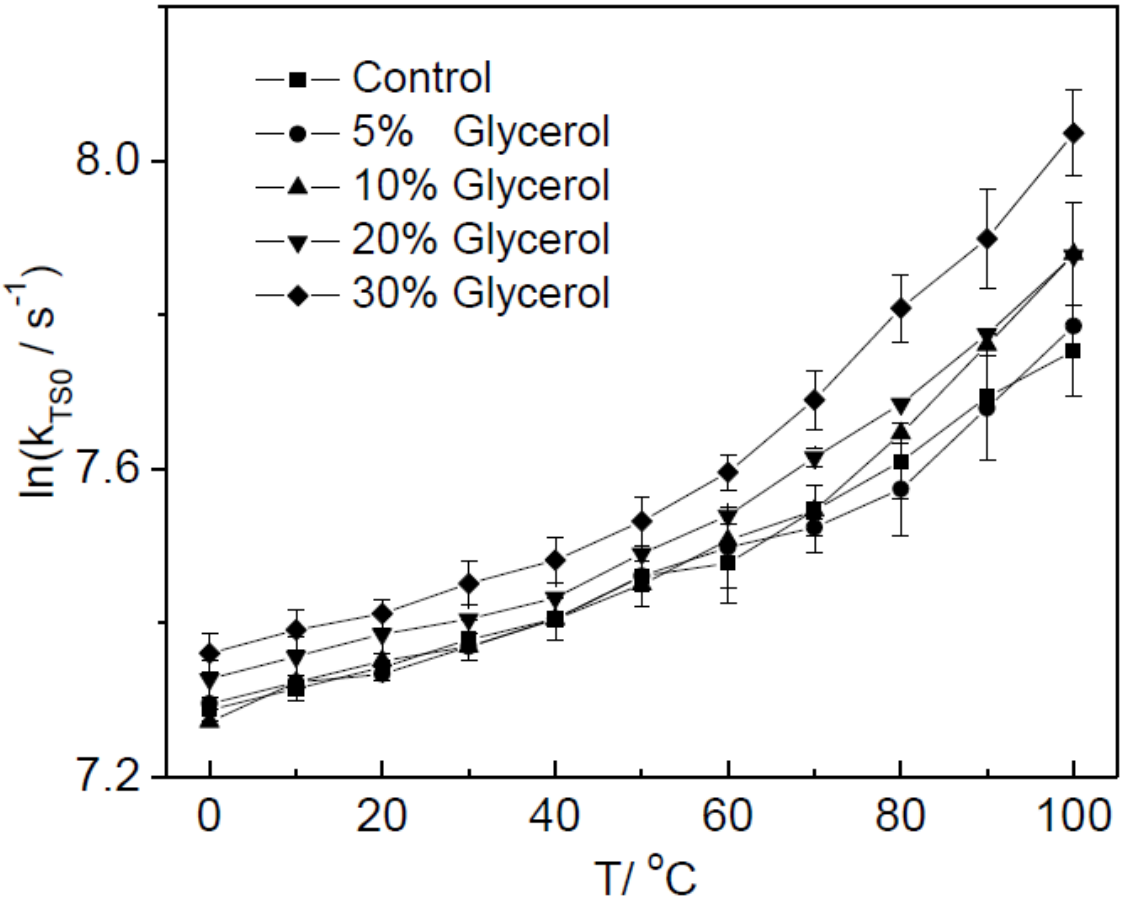

Figure 18: Effect of temperature on the rate constant for non-radiative decay (k_{TS0}) of the triplet T_1 state to the ground S_0 singlet state; data were calculated from the lifetime data of Figure 15.

Figure 19

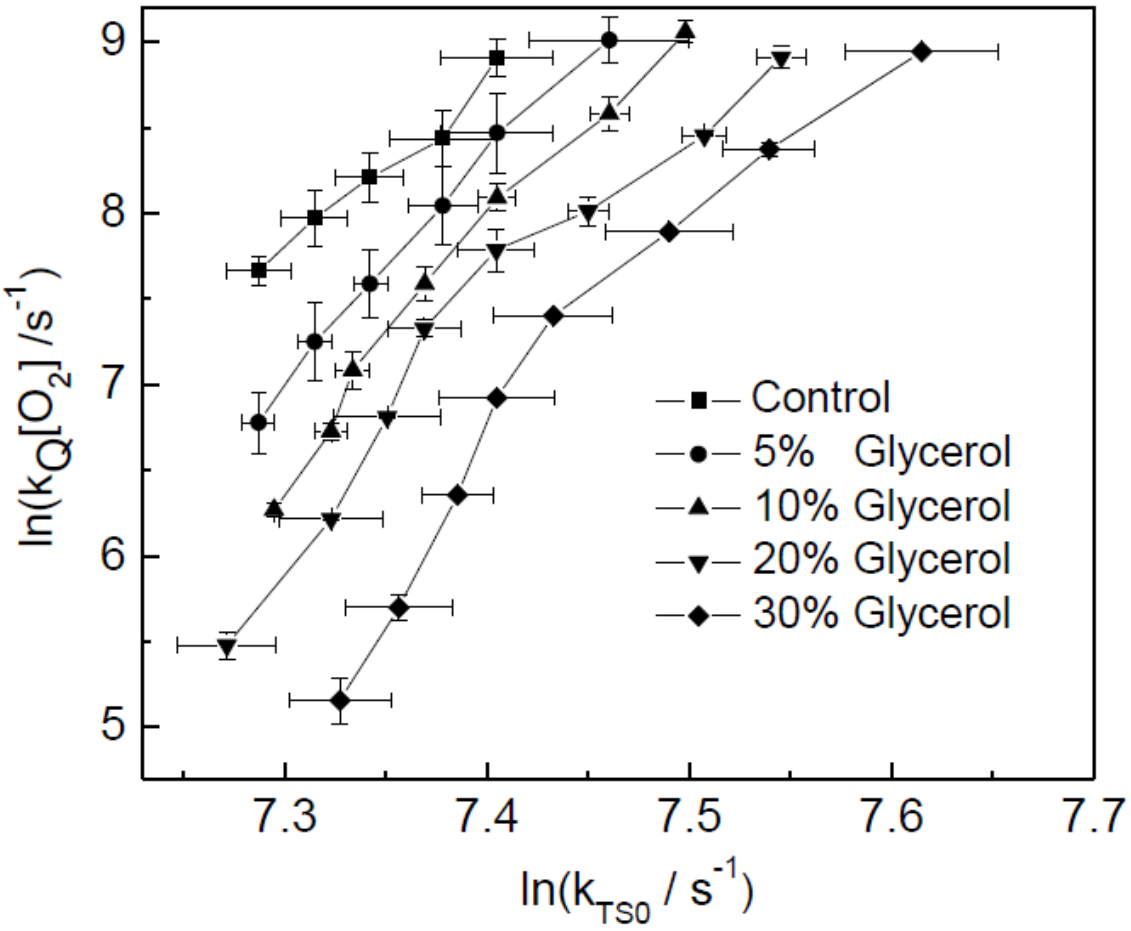

Figure 19: Dependence of $k_Q[O_2]$ on k_{TS0} for pure zein/glycerol films.

In the absence of oxygen, the lifetime of Ery B reflects the rate constants for radiative emission, k_{RP}, reverse intersystem crossing, k_{TS1}, and matrix quenching, k_{TS0} (Eq. 4). The value of k_{RP} is 41 s^{-1} and constant (Duchowicz, Ferrer & Acuña, 1998). Since the magnitude of k_{TS1} can be estimated as described above (see section **Delayed emission spectra)**, it is possible to estimate $k_{TS0}(T)$ from the lifetime data under N_2 using Eq. 4. The calculated values of $k_{TS0}(T)$ for Ery B in zein or zein/glycerol films are plotted as $\ln(k_{TS0})$ versus temperature in Fig. 18. The magnitude of these values indicated that the temperature-dependent increase in k_{TS0} had the largest influence on the Ery B lifetime measured under N_2. In general, the matrix quenching rate increased with an increase in glycerol content. While the addition of 30% glycerol significantly increased k_{TS0}, and thus significantly increased the local mobility of the zein film, the addition of $\leq$ 20% caused little increase in k_{TS0} and thus had little effect on the matrix mobility.

Phosphorescence emission energy and intensity from Ery B is sensitive to two distinct modes of molecular mobility in amorphous biomaterials: matrix dipolar relaxation around the excited T_1 triplet state before emission decreases the energy of triplet state and thus lowers the emission energy; and matrix collisions that promote intersystem crossing from the excited T_1 triplet state to the ground S_0 singlet state increase k_{TS0} and thus lower the lifetime. This study of matrix mobility in amorphous zein using Ery B phosphorescence indicates that both of these modes of molecular mobility are modulated in a complex concentration-dependent manner by glycerol. As suggested by the analysis below, this change in matrix mobility and solubility difference between zein and glycerol directly influenced the oxygen permeability.

As illustrated in Fig. 19, the relationship between the oxygen quenching rate ($k_Q[O_2]$) and the matrix quenching rate (k_{TS0}) showed a clear dependence on the glycerol content of the zein matrix. The oxygen quenching rate, our molecular-level proxy for oxygen permeability,

increased with matrix mobility in all samples as expected for a process that depends in part on the rate of diffusion. The dependence of permeability on mobility was dramatic and monotonic in the pure zein matrix and became both less pronounced and more complex with the addition of glycerol. However, given the pronounced influence of glycerol on the permeability of oxygen, we speculate that permeability was modulated mainly by decreasing oxygen solubility (S) rather than decreasing the oxygen diffusion rate since the overall increase in matrix mobility due to glycerol (Fig. 17) is expected to also increase oxygen diffusion rate and thus increase permeability.

Figure 20

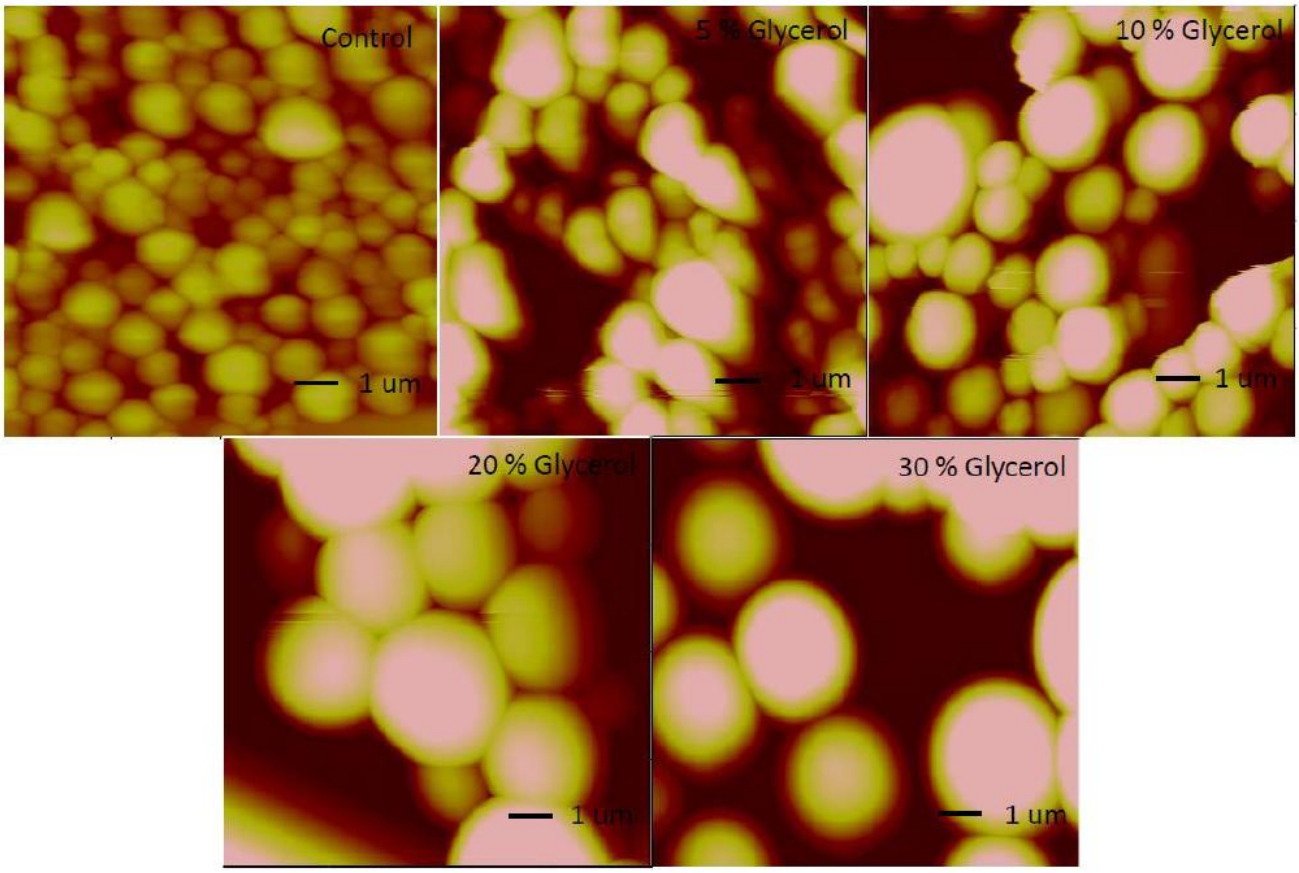

Figure 20: Tapping mode atomic force microscopy (AFM) height images of zein and zein/glycerol films.

3.3 Atomic Force Microscopy (AFM).

Early studies of zein molecular structure estimated an α-helix content between 50 and 60% (Wang & Padua, 2010). These authors have concluded, based on surface plasmon resonance studies, that the zein molecule contains sharply defined hydrophobic and hydrophilic domains on its surface. Interactions of these domains drive zein complex formation. Kim and Xu (2008) proposed that zein could form micelle-like structures in ethanol/water solution with hydrophilic or hydrophobic particles modulated by the content of ethanol. The zein complex is sufficiently stable that only the strong detergent SDS can dissociate it (Moore, Puvvada & Blankschtein, 2003). For this study, films for AFM were cast on a mica slide about 0.5 cm × 0.5 cm. Considering the zein concentration in the ethanol solution used to cast films, and assuming a partial specific volume of 1.37 cm^3/g (Tanford, 1961), the protein thickness on the slides was ~4,000 nm. The films thus included many layers of zein protein.

As AFM only provides very local images of the surface of a film (10 μm square in this study), sample homogeneity is very important. Before measurement, each sample chip was carefully checked under the microscope associated with the AFM to ensure no crystallization or phase separation occurred in the glycerol-plasticized films. Since previous research has shown that zein films containing varying levels of glycerol are homogeneous throughout the cooling and heating cycles over the temperature range from -100 to 150°C (Ghanbarzadeh, Oromiehie, Musavi, Razmi & Milani, 2006), we are confident that the AFM images shown represent the microstructure of the entire films.

AFM images for height of the surface microstructure of zein or zein/glycerol films are shown in Fig. 20. The samples of pure zein and zein with low content of glycerol (≤10%)

showed a relatively flat surface with generally uniform particles and little indication of particle aggregation. However, images of films with high content of glycerol (≥ 20 %) showed a range of zein globules of different size that were in general larger.

The aggregation state of the zein complex thus appears to be modulated by the presence of glycerol. Kim and Xu (2008) proposed that the zein complex in 70% ethanol/water solution exposes a hydrophilic surface and that the complex doesn't change during the evaporation of solvent. Glycerol binding to hydrophilic patches on the surface of zein aggregates can facilitate the aggregation of zein by increasing the viscosity on the surface.

4. Conclusion

This investigation has shown that glycerol can significantly modulate the physical properties of zein films in a dose-dependent manner. At low content (≤10%), glycerol decreased the local dipolar relaxation of the amorphous zein matrix and thus appeared to act as an antiplasticizer on the molecular level while at high content (≥20%), glycerol increased the local dipolar relaxation and acts as a plasticizer. Although the matrix mobility is constant or only slightly increased for films with glycerol concentration at and below 20%, the impact of adding glycerol on a functional property such as oxygen permeability is much more significant and shows a clear dose-dependent response. Although this decrease in oxygen permeability may reflect microstructure changes of the zein matrix and a change in the aggregation state of the zein complex during the process of film forming, additional work is needed to confirm this interpretation. Another uncertainty is what role the microstructure changes play in the role-conversion of glycerol from antiplasticizer to plasticizer (note that this changeover occurs at the same glycerol content at which aggregation behavior changes). Despite those uncertainties, our

results indicate that in addition to acting as both an antiplasticizer and a plasticizer depending on content, that glycerol suppresses oxygen permeability in zein films at all content levels.

References

Zhao, R. X., Torley, P., Halley, P. J. (2008) Emerging biodegradable materials: starch- and protein-based bio-nanocomposites. *Journal of Material. Science,* 43, 3058-3071.

Naushad Emmambux, N., Stading, M. (2007) In situ tensile deformation of zein films with plasticizers and filler materials. *Food Hydrocolloids*, 21, 1245–1255.

Ghanbarzadeh, B., Oromiehi, A. R. (2009) Thermal and mechanical behavior of laminated protein films. *Journal of Food Engineering*, 90, 517-524.

Byun, Y. J., Kim, Y. T., Scott, W. (2010) Characterization of an antioxidant polylactic acid(PLA) film prepared with α-tocopherol, BHT and polyethylene glycol using film cast extruder. *Journal of Food Engineering*, *100*, 239-244.

Liang, J., Ludescher, R. D. (2011) Antioxidant modulate molecular mobility, oxygen permeability, and microstructure in zein films. *Journal of Agriculture and Food Chemistry*, 59, 13173-13180.

Soares, N. F. F., Hotchkiss, J. H. (1998) Naringinase immobilisation in packaging films for reducing naringin concentration in grapefruit juice. *Journal of Food Science*, 63, 61–65.

Lawton, J. W. (2002) Zein: A history of processing and use. *Cereal Chemistry, 79*, 1-18.

Subramanian, S., Sampath, S. (2007) Adsorption of zein on surface with controlled wettability and thermal stability of adsorbed zein films. *Biomacromolecules*, 8, 2120-2128.

Tihminlioglu, F., Atik, Ì D., Özen, B. (2011) Effect of corn-zein coating on the mechanical properties of polypropylene packaging films. *Journal of Applied Polymer Science*, 119, 235-241.

Sanchez-Garcia, M. D., Hilliou, L., Lagaron, J. M. (2010) Nanobiocomposites of carrageenan, zein, and mica of interest in food packaging and coating applications. *Journal of agriculture and Food Chemistry*, 58, 6884-6894.

Lai, H. M., Padua, G. W. (1997) Properties and microstructure of plasticized zein films.

Miscellaneous, 74, 771-776.

Chang, Y. P., Karim, A. A. Seow, C. C. (2006) Interactive plasticizing-antiplasticizing effects of water and glycerol on the tensile properties of tapioca starch films. *Food Hydrocolloids*, 20, 1-8.

Lourdin, D., Bizot, H., Colonna, P. (1997) ‘‘Antiplasticization’’ in starch-glycerol films? *Journal of Applied Polymer Science*, 63, 1047-1053.

Crank, J., Park, G. S. (1968) Diffusion in polymers, Academic Press, New York, 1-39.

Liang, J., Ludescher, R. D. (2012) Influence of Glycerol on the Molecular Mobility and Hydrogen Bond Network in the Glucose-Based Matrix. *Carbohydrate Research*, 361, 120-126.

Nack, T. J., Ludescher, R. D. (2006) Molecular mobility and oxygen permeability in amorphous bovine serum albumin films. *Food Biophysics*, *1*, 151-162.

Subramanian, S., Sampath, S. (2007) Adsorption of zein on surface with controlled wettability and thermal stability of adsorbed zein films. *Biomacromolecules*, 8, 2120-2128.

Sundaresan, K. V., Ludescher, R. D. (2008) Molecular mobility and oxygen permeability in amorphous β-lactoglobulin films. *Food Hydrocolloids*, 22, 403-413.

You, Y. M., Ludescher, R. D. (2009) Effect of xanthan on the molecular mobility of amorphous sucrose detected by erythrosine B phosphorescence. *Journal of Agriculture and Food Chemistry*, 57, 709-716.

Duchowicz, R., Ferrer, M. L., Acuña, A. U. (1998) Kinetic spectroscopy of erythrosine phosphorescence and delayed fluorescence in aqueous solution at room temperature. *Photochemistry and Photobiology*, 68, 494-501.

Lukasik, K. V., Ludescher, R. D. (2006) Molecular mobility in water and glycerol plasticized cold- and hot-cast gelatin films. *Food Hydrocolloids*, 20, 96-105

Pravinata, L. C., You, Y. M., Ludescher, R. D. (2005) Erythrosin B phosphorescence monitors molecular mobility and dynamic site heyerogeneity in amorphous sucrose. *Biophysics Journal*, 88, 3551-3561.

Lettinga, M. P., Zuihof, H., van Zandvoort, M. A. M. J. (2000) Phosphorescence and fluorescence characterization of fluorescein derivatives immobilized in various polymer

matrices. *Physical Chemistry Chemical Physics*, 2, 3697-3707.

You, Y. M., Ludescher, R. D. (2010) The effect of molecular size on molecular mobility in amorphous oligosaccharides. *Food Biophysics,* 5, 82-93.

You, Y. M., Ludescher, R. D. (2008) Effect of gelatin on molecular mobility in amorphous sucrose detected by Erythrosin B phosphorescence. *Carbohydrate Research,* 343, 2657-2666.

Wang, Y., Padua, G. W. (2010) Formation of zein microphases in ethanol-water. *Langmuir,* 26, 12897-12901.

Kim, S., Xu, J. (2008) Aggregate formation of zein and its structural inversion in aqueous ethanol. *Journal of Cereal Science,* 47, 1-5.

Moore, P. N., Puvvada, S., Blankschtein, D. (2003) Role of surfactant polar structure in protein-surfactant complexation: zein protein solubilization by SDS and by SDS/$C_{12}E_n$ surfactant solutions. *Langmuir,* 19, 1009-1016.

Tanford, C. (1961) *Physical Chemistry of Macromolecules*. John Wiley & Sons, New York, NY.

Ghanbarzadeh, B., Oromiehie, A., Musavi, M., Razmi, E., Milani, J. (2006) Effect of polyolic plasticizers on rheological and thermal properties of zein resins. *Iranian Polymer Journal,* 15, 779-787.

Chapter IV: Influence of Antioxidant Structure on Local Molecular Mobility in Amorphous Sucrose

A paper published in *Carbohydrate Research*

Jun Liang, Maria D. Corradini, Richard. D. Ludescher

1. Introduction

The shelf life of a food product depends upon maintaining sensory, nutritional, and safety (microbiological and toxicological) attributes throughout production, storage and commercialization (Debeaufort, Quezada-Gallo & Voilley, 1998). Food products are typically developed to address consumer demand for convenience, appearance, and storage stability. Lipid oxidation, one of the main causes for food deterioration during storage, occurs in oil-containing foods when lipid molecules, activated by a catalyzing agent such as heat, light, the presence of metal ions or other factors (Lehtinen, Kiiliäinen, Lehtomäki & Laakso, 2003; Marsili, 1999; Santos, Anjos & Augusto, 1999), react with molecular oxygen to form a highly reactive species (endoperoxide radical, hydroperoxide, etc.). These peroxides break down to a variety of organic compounds, including alcohols, aldehydes, ketones, and acids, resulting in the off odors and flavors often associated with rancidity (Azhar & Nisa, 2006). Antioxidants are thus commonly added to foods to prevent or delay lipid oxidation.

Lipid oxidation in solid foods normally starts from the surface of the product. The oxygen diffuses into the interior of the food and lipid oxidation subsequently propagates throughout the product. Antioxidants incorporated throughout a food matrix are less efficient in controlling oxidation (Arrua, Strumia, & Nazareno, 2010; Liang et al., 2008; Liang, Tian, Yang, Zhang & Skibsted, 2009). It is possible to limit surface lipid oxidation by selectively applying an antioxidant at food surfaces. However, this possibility presents technological difficulties.

Systems are thus needed that can carry and protect the antioxidant until application and appropriate methodologies need to be tested to adequately and evenly deliver the antioxidant onto the food surface.

Food packaging is a standard requirement for commercialization. Therefore, the development of enhanced packaging that directly incorporates antioxidants or the use of additional layers, such as an edible coating material containing antioxidants, on the product can be used to delay or prevent lipid oxidation effects on food surfaces. Sweetened food products such as cereals, cookies, pastries, snack foods, nuts or roasted nuts and candies often include a thick sugar coating. Not only does this surface contribute sweetening but it may also act as a functional layer that protects the food from physical, chemical, biological and environmental damage resulting from shear, oxygen, moisture, light or microbial contamination (Desai & Park, 2005). Sucrose is one of the most widely used disaccharides in coatings for long-term storage due to its propensity to form an amorphous, non-crystalline solid by rapid drying from aqueous solution or cooling from a melt and its low reactivity with amino acids in Maillard since it is a non-reducing sugar (You & Ludescher, 2007). Thus coatings of sucrose or sucrose derivatives containing antioxidants can provide a promising freshness-retaining tool to the food industry particularly for cereal mixes, nuts and flakes (Bauchot & John, 1995).

The performance of antioxidants in packaging or coating films is highly influenced by the physical properties of the film matrix (Roos, 1993; You & Ludescher, 2010; de Graaf, Karman & Janssen, 2003). The importance of molecular mobility in the stability of foods is widely recognized. Physical processes such as molecular diffusion (Tseng & Durning, 2000) and crystallization (Zhou, Zhang, Law, Grant & Schmitt, 2008) are directly modulated by molecular

mobility. Despite extensive research on the potential usage and performance of antioxidants in edible films, data on the effect of antioxidants on the film's matrix mobility have been reported rarely. In a previous study on the effect of propyl gallate and octyl gallate on zein films (liang & Ludescher, 2011), we have shown that the addition of specific functional ingredients such as antioxidants may significantly modify the physical properties, structure and thus functional properties in a manner that will affect the applicability of the films for commercial use. Since antioxidants have low molecular weight they have the potential of behaving as plasticizers in films. Polar and hydrophobic groups of the antioxidant can affect the formation of the hydrogen bond network, directly influencing the molecular mobility of the matrix and thus the coating's stability and the release rate of the incorporated antioxidants into the food.

Figure 21

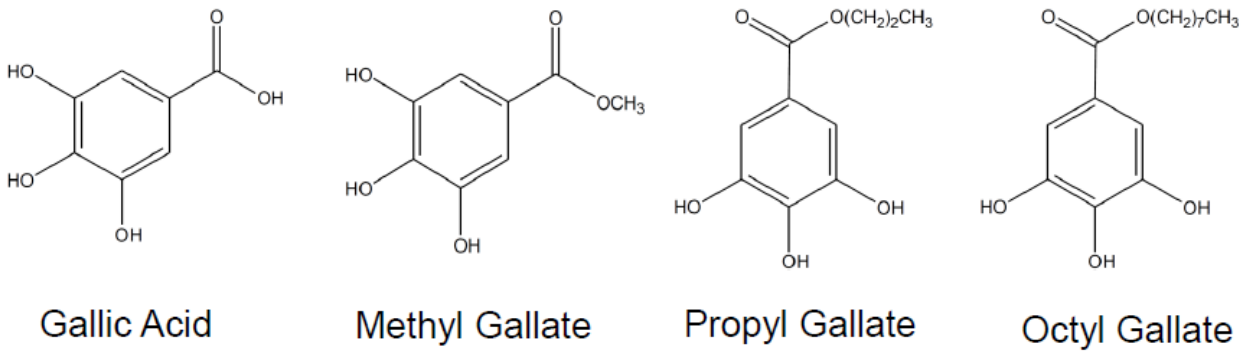

Figure 21: Chemical structure of the gallate antioxidants.

Gallic acid, methyl gallate, propyl gallate and octyl gallate (Fig. 21) are four important antioxidants widely used in keeping food fresh and preventing lipid oxidation. They possess identical hydroxyl benzoyl head groups and differ only in the presence of and length of alkyl groups esterified to the carboxyl group. The hydroxyl benzoyl head group, carboxyl group and the hydrocarbon chain will interact differently with the hydroxyls in the sugar film, although all groups should contribute to the overall plasticizing effect. The hydroxyl benzoyl head and the carboxyl group can form hydrogen bonds with the hydroxyl groups in the sugar matrix and consequently they will become intercalated into the hydrogen bond network, changing its structure and continuity. On the other hand, the alkyl chains can prevent the formation of hydrogen bonds by steric interference. The different number of methylene groups in the methyl, propyl and octyl chains may also contribute to distinctive behavior and mobility of the films. Previous work on zein films indicated that the hydroxyl benzoyl head and the saturated carbon chains act in distinct ways on the film properties. While the presence of the hydroxyl benzoyl head increases zein matrix mobility, the saturated carbon chains affect the aggregation of the zein complex, thus increasing oxygen permeability within the zein films (Liang & Ludescher, 2011).

Phosphorescence techniques have been shown to provide detailed information about interrelations among local molecular mobility, dynamic heterogeneity, and oxygen permeability in amorphous solid biomaterials (Shirke & Ludescher, 2005; Lukasik & Ludescher, 2006; You & Ludescher, 2011; Liang & Ludescher, 2012; Shirke, You & Ludescher, 2006). In this study we have monitored the phosphorescence of tryptophan, a triplet state molecular probe, to assess the local molecular properties and mobility of sucrose films containing gallate–based antioxidants.

Measurements of the tryptophan excited-state lifetime provide information about how the gallate derivatives influence matrix mobility. Samples under the same conditions were also measured by FTIR to monitor hydrogen bonding network integrity. By studying the relation between mobility and hydrogen bond network strength, we can better understand the molecular mechanisms by which antioxidants modulate the physical and functional properties of edible polymer barriers; such insights should improve our ability to engineer edible food films with the desired antioxidant functionality.

2. Materials and Methods

2.1 Sample Preparation

Gallic acid, methyl gallate, propyl gallate and octyl gallate (Sigma Chemical, St. Louis, MO) were dissolved in ethanol (HPLC grade, Sigma Chemical, St. Louis, MO) at a concentration of 1.25 M and were used as stock solutions. Sucrose (Sigma Chemical, St. Louis, MO) was dissolved in mixture of deionized water/ethanol (80/20, v/v) to a final concentration of 2.5 M.

We prepared sucrose - tryptophan (Sigma Chemical) films based on our published method with slight modifications (Shirke, You & Ludescher, 2006). Tryptophan was dissolved in deionized water to prepare a 10 mM stock solution. An aliquot from this solution was added to the sucrose solution to obtain a probe/sucrose molar ratio of around $1:10^3$. Each correspondent antioxidant stock solution was then added to the probe/sucrose mixture to obtain an antioxidant:sucrose mole ratio of 1:5. For the phosphorescence experiments, the mixtures of sucrose/ tryptophan/gallate derivative were intensively shaken on a Fisher Vortex Genie 2 Mixer to ensure that the gallate derivatives and the tryptophan were completely blended with the sucrose. Prior to the film preparation, the slides were soaked in Terg-A-Zyme (Alconox, Inc.,

NY) soap solution for at least 24 h to remove surface impurities, then washed with deionized water. Finally, the slides were rinsed with ethanol and dried with acetone.

To prepare the sucrose-based films, 15 µl of sucrose/gallate derivative solutions at room temperature were spread on approximately one third of a quartz slide (30 × 13.5 × 0.6 mm, custom made by NSG Precision Cells, Farmingdale, NY). Then the slides were placed under a gentle warm air stream using an air gun. Therefore, most of the water and ethanol in the film were evaporated within 5 minutes. In our previous study we have shown that this is an effective way to prevent the crystallization in sugar –based films (Liang & Ludescher, 2012) and the dried amorphous sucrose films were ~20 μm thick. The transparent and homogeneous films formed were stored at room temperature for at least 1 week under air in equilibrium with P_2O_5 and Drierite in order to attain a relative humidity close to 0% inside the desiccators, to protect from light and to prevent photobleaching of tryptophan. The desiccants were refreshed as necessary.

2.2 Luminescence measurements and analysis.

Luminescence measurements were conducted on a Cary Eclipse spectrophotometer (Varian Instruments, Walnut Creek, CA) equipped with a temperature controller and a multicell holder. The sample compartment was purged with dry air to avoid water condensation and the quartz cuvette that held the slide was directly hooked onto a high purity nitrogen line. The cuvette was flushed for at least 30 min at room temperature before beginning the measurements. The cuvette was capped with a lid having inlet and outlet ports for the gas line, so that all experiments were performed at constant pressure. Phosphorescence intensity decay was followed at 450 nm with an excitation of 270 nm. All measurements were performed at least in triplicate and the data were collected at temperatures from 0 to 70 ℃ in all experiments.

Phosphorescence emission scans at 25 ℃ were collected from 390 to 650 nm with an excitation wavelength of 270 nm. The excitation and emission monochromators were both set at 20 nm band pass. Each data point (recorded at 1 nm intervals with a 0.1 s averaging time) was collected from a single flash with 0.2 ms delay and 5 ms gate time.

Since intensity decays were highly heterogeneous, indicative of a wide distribution of lifetime components, a multi-exponential function was selected to characterize the decays recorded during the lifetime measurements (Strambini & Strambini, 2000). The corresponding fits using Eq. 1 were obtained using Origin 7 (OriginLab Corporation, Northampton, MA):

$$I(t) = \sum_{i=1}^{n} \alpha_i \exp(-t / \tau_i) \qquad (1)$$

where τ_i are the decay times, α_i represent the amplitudes of each component at time zero and n is the number of decay times. It should be noticed that in this study all the tryptophan decays were fitted in terms of three discrete components. The number average lifetimes were calculated according to the following equation:

$$\overline{\tau_p} = \frac{\sum_{i=1}^{n} \alpha_i \tau_i}{\sum_{i=1}^{n} \alpha_i} \qquad (2)$$

The calculated phosphorescence lifetime (τ) is the sum of all possible de-excitation rates for the triplet state T_1:

$$\overline{\tau} = (k_{RP} + k_{NR}(T) + k_Q[O_2])^{-1} \qquad (3)$$

where, k_{RP} is the rate of radiative decay to the ground singlet state, and k_{NR} is the rate of non-radiative decay to the ground singlet state and $k_Q[O_2]$ is the rate of oxygen quenching. The radiative decay rate, k_{RP}, is equal to 0.167 s^{-1} for tryptophan (Weinryb & Steiner, 1968).

The rate of non-radiative decay (k_{NR}) to the singlet state reflects the rate of quenching of the probe due to coupling of the excited T_1 state to a highly excited vibration of the ground S_0 state followed by dissipation of vibrational energy from the probe into the matrix. This value of k_{NR} is thus an indication of matrix molecular mobility (Ludescher, Shah, McCaul & Simon, 2001). The effect of temperature on k_{NR} can be estimated by first fitting the tryptophan lifetime decays obtained at several temperatures under anoxic conditions with Eq. 3. Since k_{RP} is known and under the conditions prevalent in this study, i.e., absence of oxygen, $k_Q[O_2]$ can be assumed negligible Eq.3 will allow the estimation of k_{NR} for each temperature . The temperature dependence of k_{NR} can be described by the Arrhenius equation (Eq. 4) which allows for estimation of the activation energy (Ea) for the motions giving rise to non-radiative decay (Hershberger, Maki & Galley, 1980).

$$\ln k_{NR} = \ln k_{NR}^{0} - \frac{\Delta E_a}{R} * \frac{1}{T} \qquad (4)$$

2.3 Attenuated Total Reflectance Fourier Transform Infrared (ATR-FTIR) Spectroscopy

The ATR-FTIR spectra were collected using a Thermal Nicolet Nexus 670 FT-IR spectrometer (Thermo Fisher Scientific Inc., Waltham, MA) equipped with a Smart ARK thermal accessory. The spectra were analyzed using the EZ-OMNIC software. Each spectrum was the average of 512 scans with 4 cm^{-1} resolution in an atmosphere of air equilibrated against P_2O_5 to minimize the interference of moisture under ambient conditions. The samples used in the

luminescence experiment were scraped from slides and spread on the ATR plate for measurement within a temperature range from 30 to 100 ℃.

Figure 22

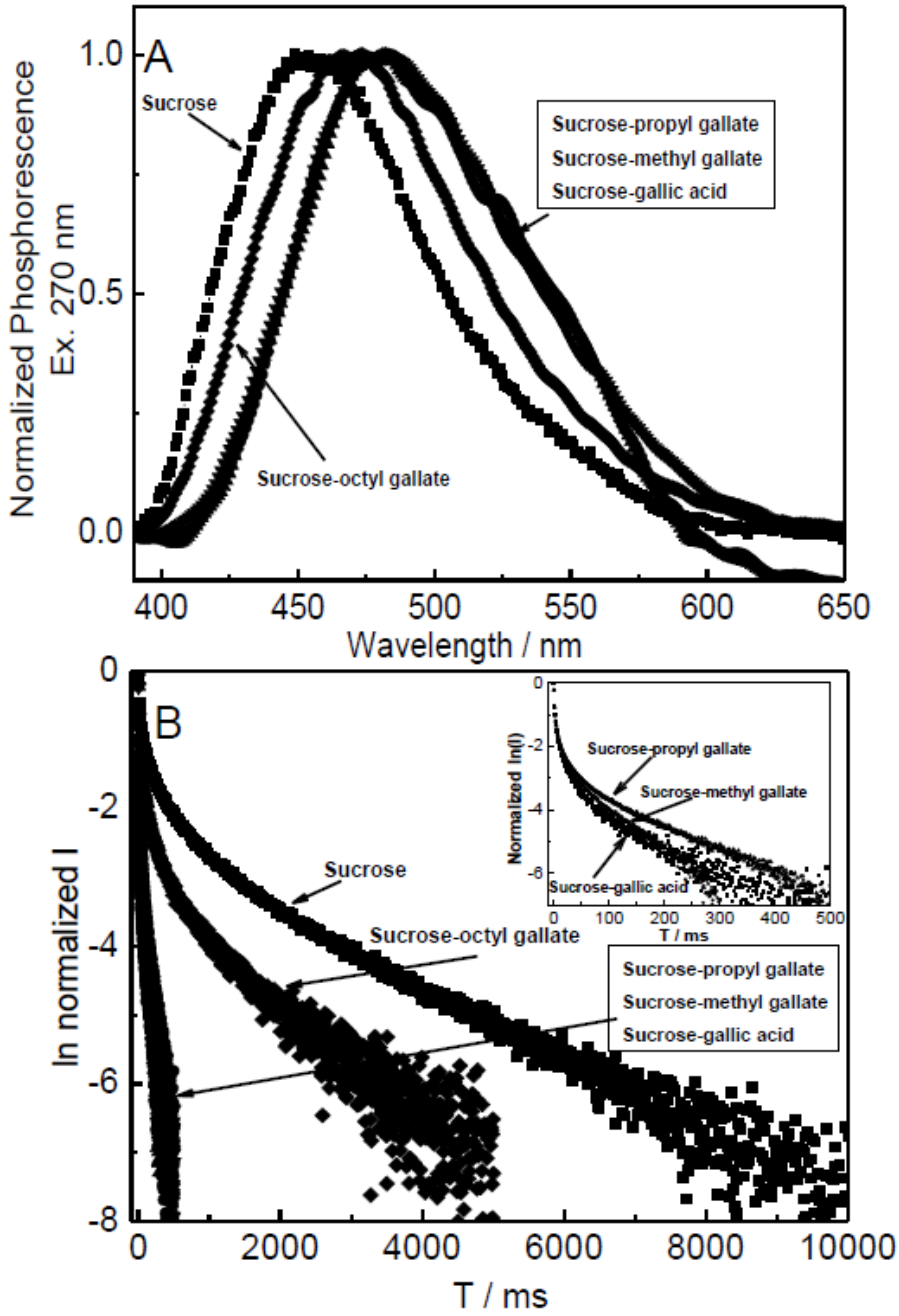

Figure 22: Comparison of the phosphorescence emission spectra (A) and intensity decay kinetics (B) of tryptophan in sucrose and sucrose-antioxidant films.

3. Result and discussion

3.1 Tryptophan phosphorescence in sucrose-based films.

The usefulness of tryptophan phosphorescence in this study depends on the sensitivity of the phosphorescence emission spectrum and decay to the local molecular properties of the sucrose-based films. To show the tryptophan sensitivity to differences in film properties, tryptophan phosphorescence spectra and decay in sucrose and sucrose-gallate derivatives films are compared in Fig. 22.

The phosphorescence spectra of tryptophan in all sucrose-based matrices showed a single peak which shifted as the matrix composition changed. The phosphorescence peak, a measure of average energy of emission, has been related to the polarity (Broos, Gabellieri, van Boxel, Jackson & Strambini, 2003) and flexibility (Gonnelli & Strambini , 1995) of the indole side chain environment in proteins. In the solid sugar films, the matrix mobility in sucrose will be influenced by the additives (gallate derivatives). At 25 ℃, the rank for the phosphorescence peak frequency (Fig. 22A) followed the rank order of sucrose < sucrose-octyl gallate < sucrose-propyl-gallate ≤ sucrose-methyl ≤ sucrose-gallic acid. In protein matrices of comparable albeit more heterogeneous polarity, lower emission energy reflects an increase in the matrix flexibility around Trp (Gonnelli & Strambini , 1995). Thus, the emission data suggest that the mobility in these matrices followed the same rank order.

The tryptophan phosphorescence decay at 20 ℃ was relatively long lived in the dry sucrose films, decaying over a time scale ranging from 4 – 0.5 s depending on matrix composition (Fig. 22B). The tryptophan lifetimes in these samples were unaffected by oxygen (determined from

data, not shown, collected in dry air) indicating that oxygen could not significantly permeate the sucrose based matrix, which was corresponding with our previous results that sucrose could suppress the oxygen diffusion in protein films. Examination of these decay transients indicates that the phosphorescence decay time decreased in the presence of additive and that the decrease varied with additive structure. The phosphorescence decays of tryptophan in samples of sucrose plus gallate derivatives were measured as a function of temperature from 0 to 70 ℃. All intensity decays were well fit with a triple-exponential decay model (Eq. 1), with R^2 values ≥ 0.99 for all fits. The number average lifetime (Eq. 2) for all samples is plotted versus temperature in Fig. 23. The average lifetime decreased monotonically with temperature in all samples; the decrease was gradual at low temperature (0-20 ℃) and became more dramatic at higher temperatures, especially for sucrose and sucrose-octyl gallate films. Below 60 ℃, the average decay time exhibited the following rank order: sucrose >> sucrose-octyl gallate >> sucrose-propyl-gallate ≥ sucrose-methyl gallate ≥ sucrose-gallic acid. Given the sensitivity of the tryptophan phosphorescence lifetime to matrix flexibility/molecular mobility (Gonnelli & Strambin, 1995; Fischer, Gafni, Steel & Schauerte, 2002; Pravinata, You & Ludescher, 2005), such that increasing mobility causes a decrease in lifetime, the addition of antioxidant increased the sucrose matrix mobility in a structure-dependent manner. Gallic acid, containing only hydroxyl benzoyl and carboxyl groups, caused the largest increase in matrix mobility while the presence of a saturated carbon chain counteracted this effect in a length-dependent manner. Above 60 ℃, the decay times were similar in all films except sucrose-gallic acid, indicating that the dynamic effect of additive was weaker in the more mobile matrix at high temperature.

The phosphorescence decays of tryptophan in sucrose and sucrose-gallate films were highly heterogeneous, requiring three distinct exponential terms to adequately fit the data. The individual lifetimes, τ_i, and fractional amplitudes, a_i, for each fit component are plotted as a function of temperature in Fig. 24. In our dynamic analysis, each lifetime component represents a population of tryptophan probe molecules within the amorphous matrix. We do not argue that there are three uniform populations, but rather that the data allow us to identify three classes of molecule: those with fast, intermediate, and slow decays corresponding to environments with high, intermediate, and low molecular mobility, respectively (Gershenson, Schauerte, Giver & Arnold, 2000). The amplitudes reflect the fractional distribution of molecules among these three dynamic environments.

The fit lifetimes ranged from milliseconds to seconds and varied approximately 100-fold in any particular sample at any given temperature. At 0°C, the majority of tryptophan probes (≥ 48%) decayed with a short lifetime (1-20 ms) in all samples; the amplitude of this component increased with temperature. The intermediate (10-250 ms) and long (40-2000 ms) lifetime components contributed less than 35% and 25%, respectively, to the decays at 0 ℃ and the amplitude of both of these components decreased with temperature. The tryptophan probe thus indicated that the amorphous sucrose matrix is dynamically heterogeneous with matrix environments that varied ~100-fold in their local molecular mobility. The specific chemical structure of the antioxidant appeared to increase local dynamics uniformly across all dynamic environments, as each lifetime component followed the same rank order seen in the average lifetime data (sucrose >> sucrose-octyl gallate >> sucrose-propyl gallate ≥ sucrose-methyl gallate ≥ sucrose-gallic acid).

A similar phosphorescence probe study of the effect of antioxidant on molecular mobility in zein films, albeit using a different triplet state probe, also found structure-dependent differences between propyl and octyl-gallate (Liang & Ludescher, 2011). Although the hydroxyl benzoyl head group lowered the local matrix mobility in both sucrose and zein, the saturated carbon chain had a different effect in each matrix. Contrary to the large effect seen in this study, the alkyl chain length did not affect local matrix molecular mobility in amorphous zein films (although it did affect oxygen permeability). The way in which additives modulate molecular mobility is thus dependent on the specific interactions between additive and matrix components.

Figure 23

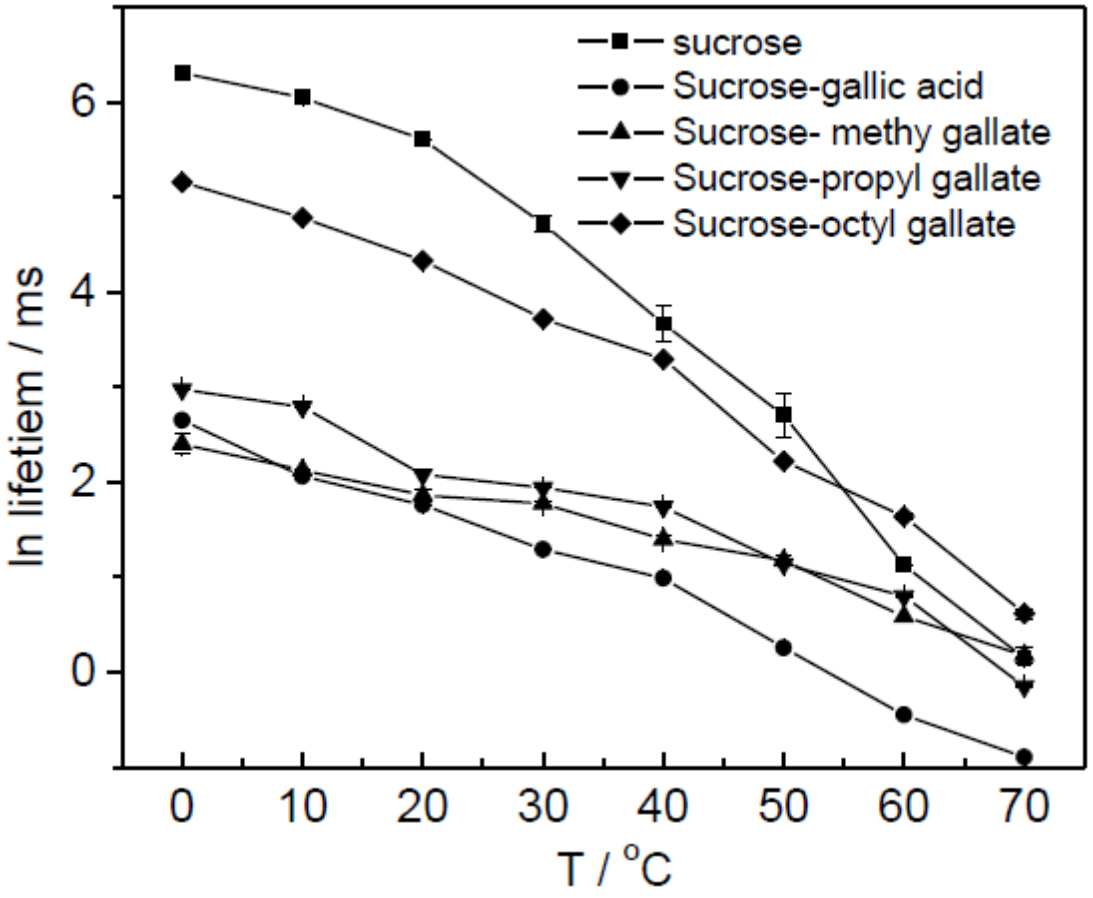

Figure 23: Temperature dependence of the number average phosphorescence lifetime calculated from multi-exponential fits of the intensity decay of tryptophan in sucrose and sucrose-antioxidant films.

Figure 24

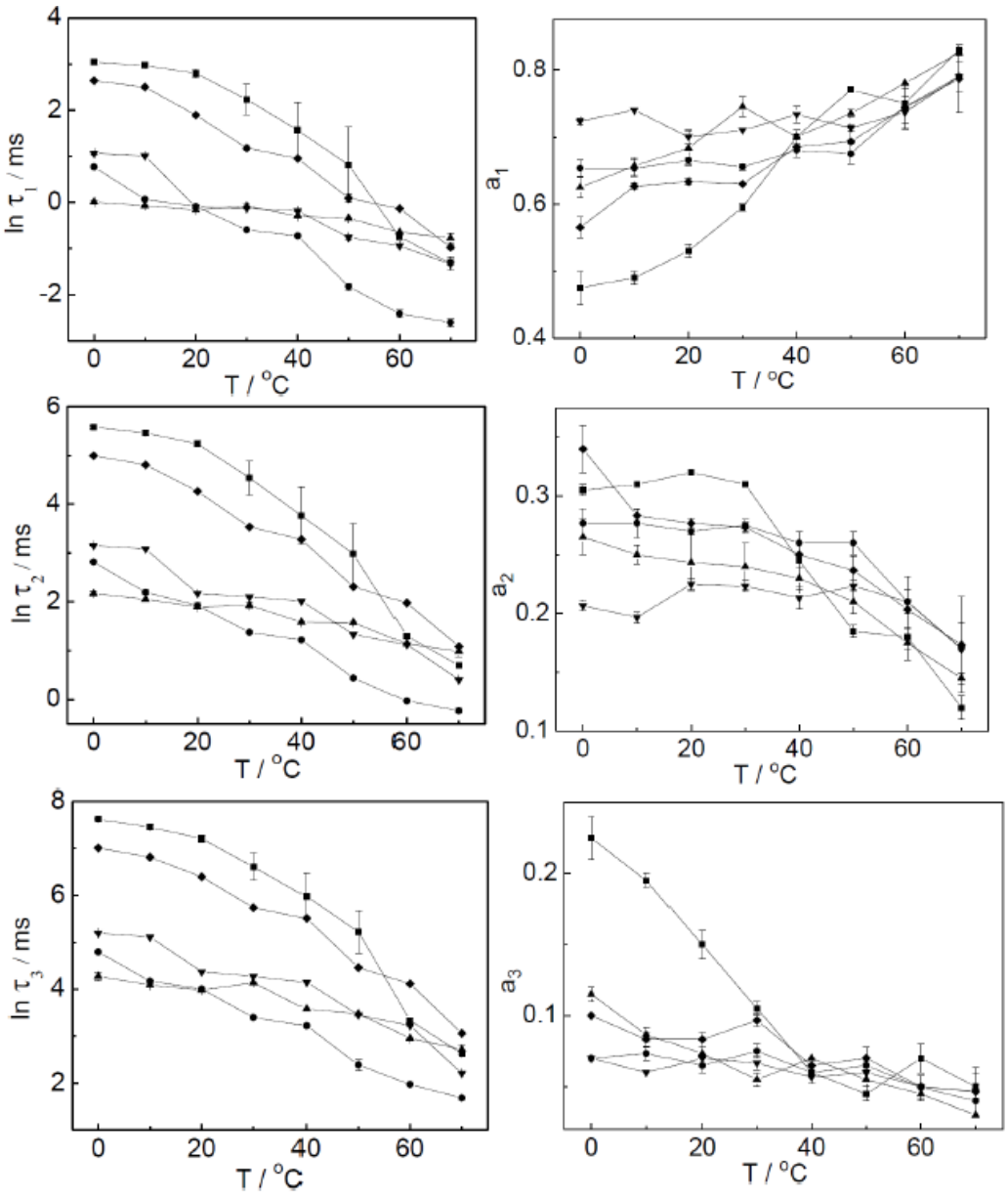

Figure 24: Temperature dependence of the lifetimes (τ_i) and fractional amplitudes (a_i) from multi-exponential fits of tryptophan phosphorescence decay in sucrose (■) and sucrose/gallic acid (●), sucrose/methyl gallate (▲), sucrose/propyl gallate (▼) and sucrose/octyl gallate (◆) films.

Figure 25

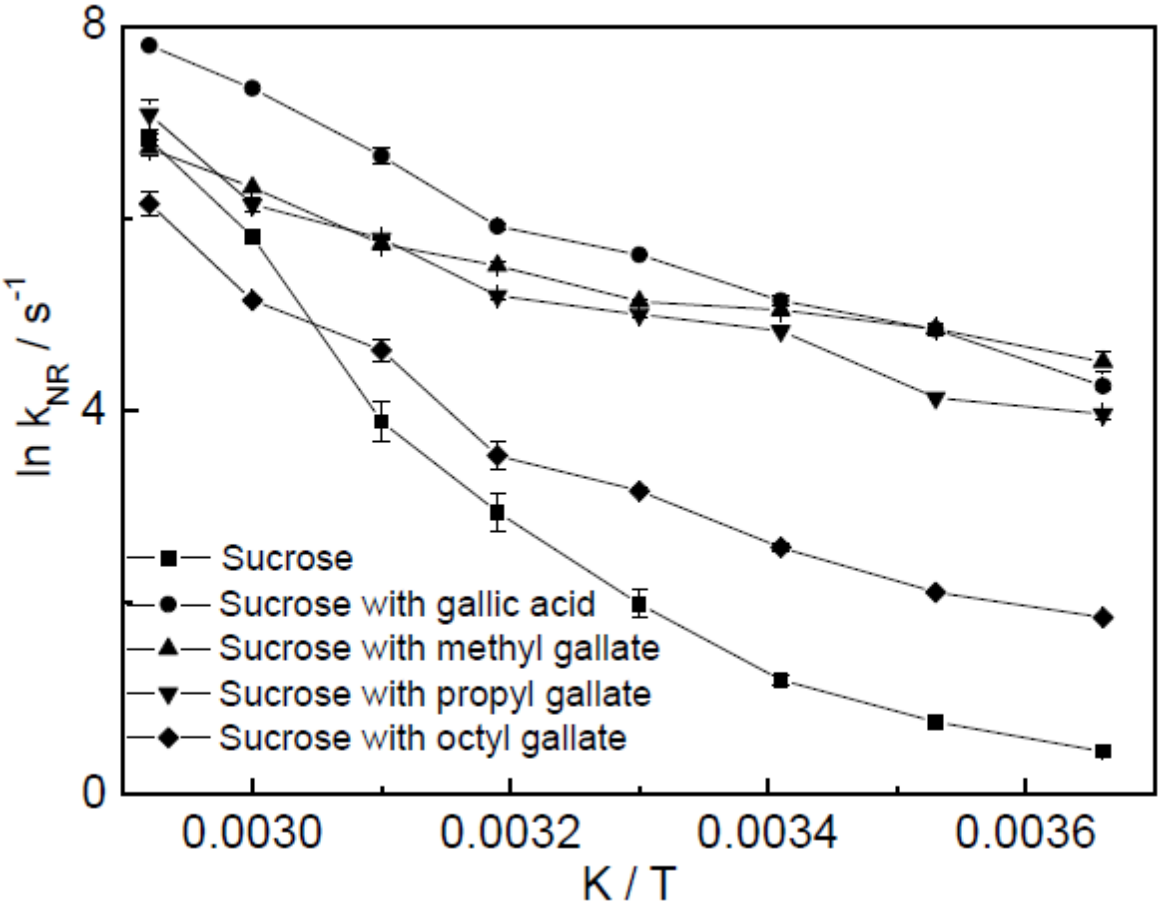

Figure 25: Effect of temperature on the non-radiative decay rate (k_{NR}) of the triplet state of tryptophan in sucrose and sucrose-antioxidant films. Values were calculated from the lifetime data presented in Figure 23.

Figure 26

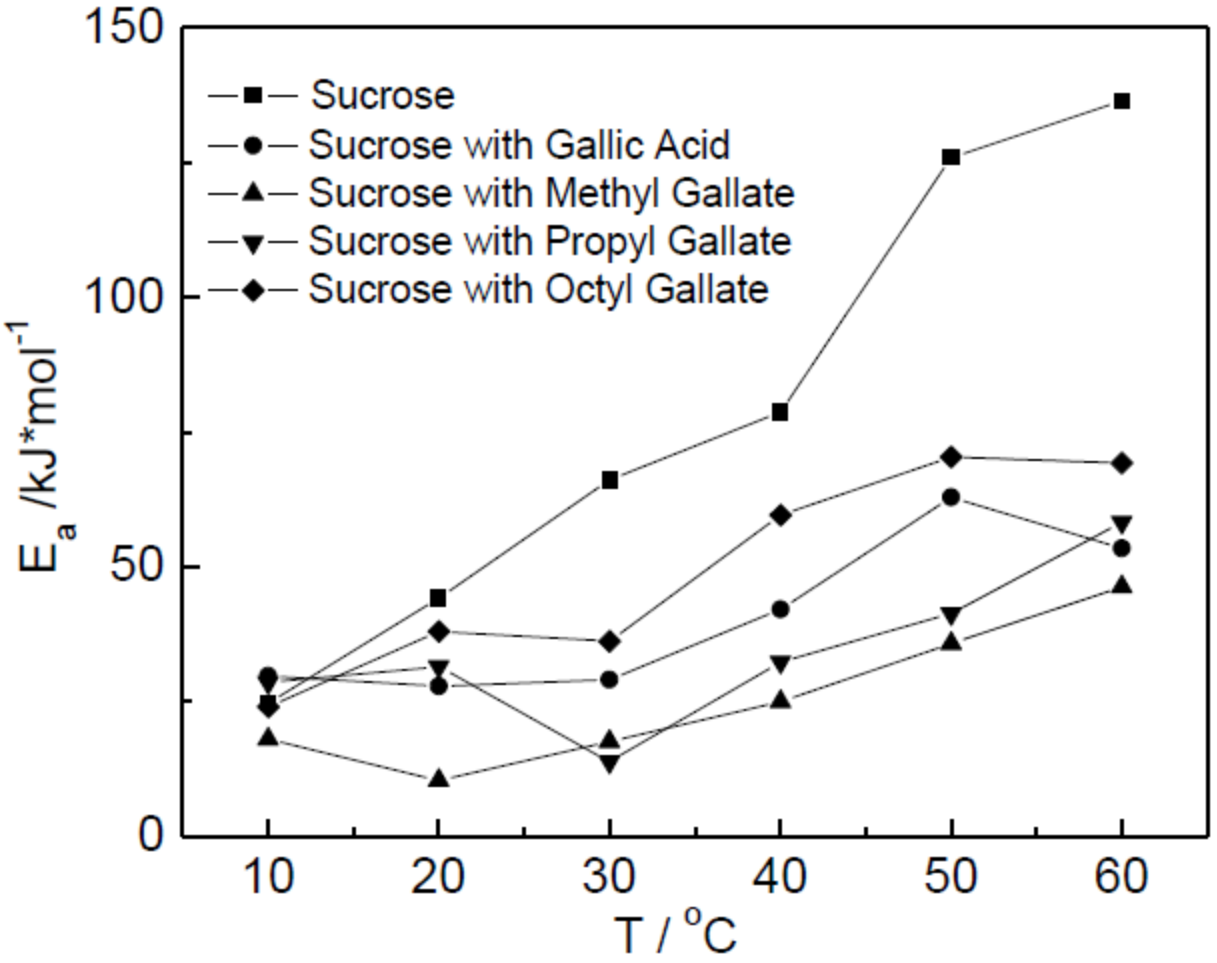

Figure 26: Activation energy for non-radiative decay as a function of temperature for tryptophan in sucrose and sucrose-antioxidant films.

In the absence of influence from oxygen, the phosphorescence lifetime of tryptophan is equal to the inverse of the sum of the rate constants for radiative emission, $k_{RP,}$ and for non-radiative decay of the triplet state, k_{NR}. The value of k_{RP} for tryptophan is 0.167 s^{-1} and constant with temperature (Weinryb & Steiner, 1968). It is thus possible to calculate a number average non-radiative decay rate, $<k_{NR}>$, from the average lifetime data of Fig. 23 (Eq. 3, Materials & Methods). The calculated values of $<k_{NR}>$ for tryptophan in sucrose and sucrose-gallate films are plotted in an Arrhenius fashion in Fig. 25. The $<k_{NR}>$ values, and thus average matrix mobility, show the following rank order at low and intermediate temperatures: sucrose << sucrose-octyl gallate << sucrose-propyl-gallate ≤ sucrose-methyl gallate ≤ sucrose-gallic acid. The curves were decidedly non-linear; $<k_{NR}>$ increased gradually at low and more dramatically at high temperature, indicating that the activation energy for non-radiative quenching in these amorphous sucrose films increased with temperature (Fig. 26). We interpret these calculated energies as the activation energies for those matrix motions that dissipate the triplet state energy of the excited tryptophan into the local matrix as vibration (Lukasik & Ludescher, 2006). In the pure sucrose film, the activation energy ranged from 20 kJ mol^{-1} at 10 ℃ to nearly 130 kJ mol^{-1} at 60 ℃. The energy increased linearly in the glass, to 80 kJ mol^{-1} at 40 ℃, and then jumped to 120 kJ mol^{-1} at 50°C. The energy at low temperature is similar to that seen for the local β-relaxation in sucrose and the increase surely reflects the increasing participation to probe quenching of the more cooperative α-relaxations as the glass transition was approached (Kaminski, *et al*., 2008). Except at 10 ℃, the presence of antioxidant lowered the activation energy for matrix motions in a structure and temperature-dependent manner. In general, the rank order of energy across the measured temperature range was sucrose >> sucrose-octyl gallate > sucrose-gallic acid ≥ sucrose-propyl gallate ≥ sucrose-methyl gallate, and the decrease in energy

compared to sucrose increased with increasing temperature. The decrease in the matrix activation energy is a measure of the plasticizing effect of these antioxidants and can be influenced by factors including free volume around the probe, local structure of the matrix, and hydrogen bond network. In the next section, we discuss how the antioxidant structure modulates the formation and extent of the hydrogen bond network in the sucrose-based films.

Figure 27

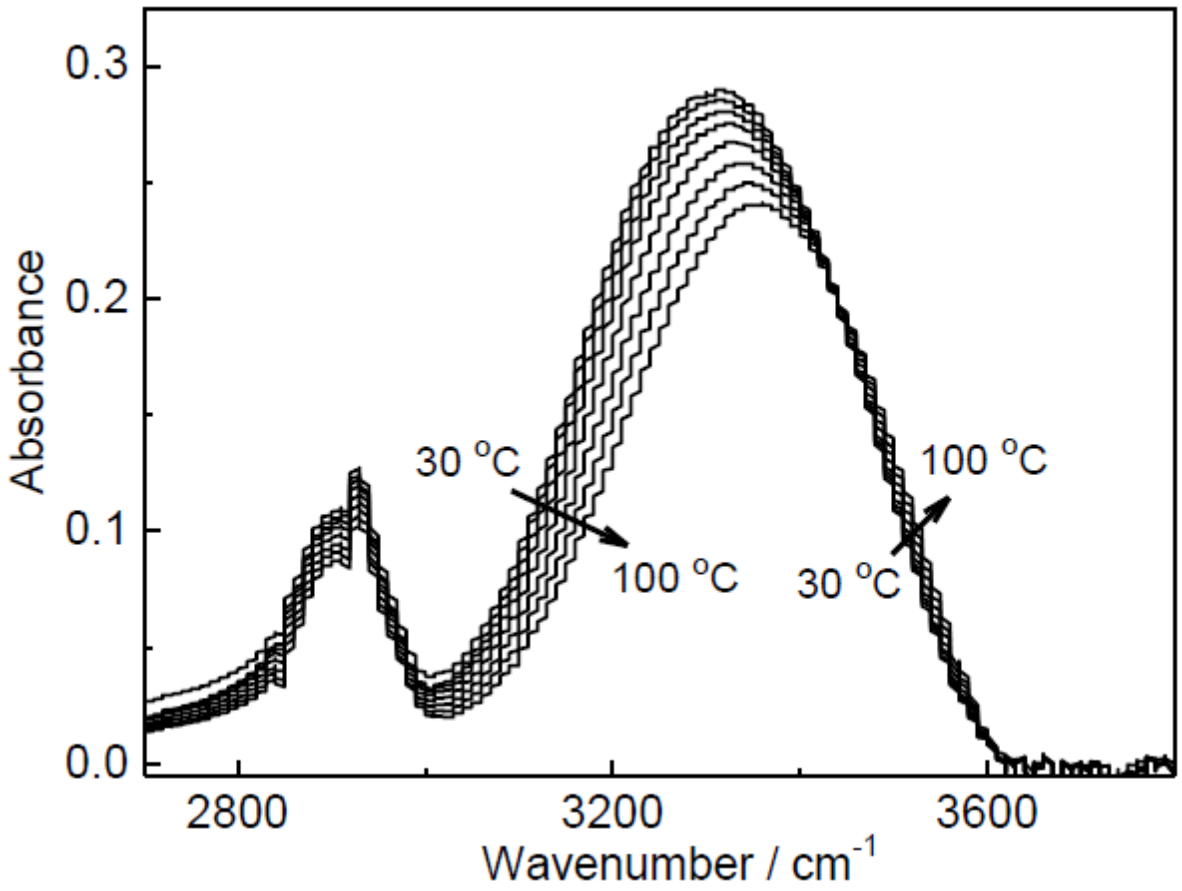

Figure 27: FTIR spectra of sucrose film as a function of temperature from 30 to 100 ℃. Orientation of arrow indicates increasing temperature.

Figure 28

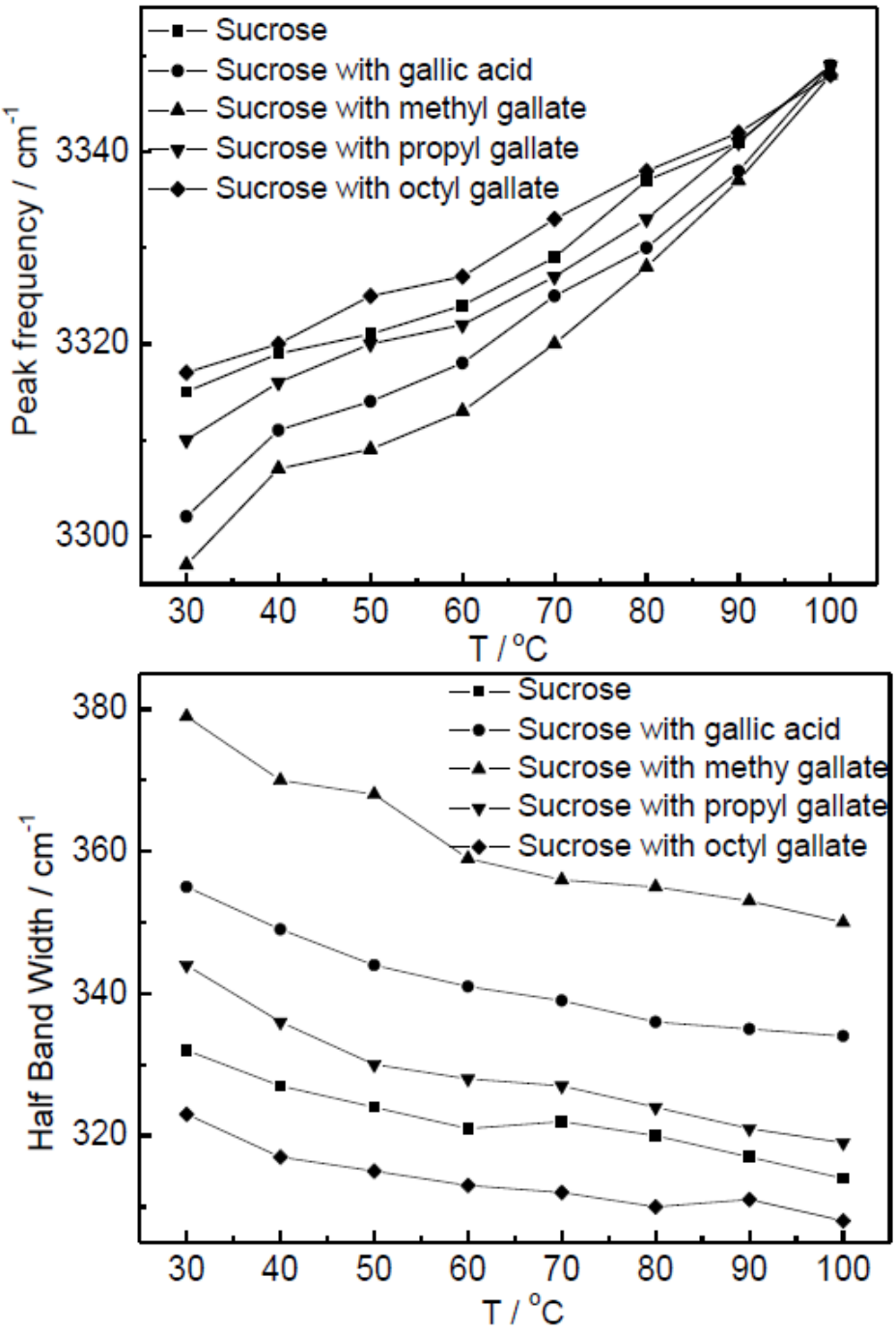

Figure 28: Peak frequency (A) and half bandwidth (B) for FTIR spectra above 3000 cm^{-1} as a function of temperature in sucrose and sucrose-antioxidant films.

3.2 Infrared spectroscopy

Hydrogen bonds provide the primary intermolecular interaction that maintains the physical state of the solid sucrose matrix. Hydroxyl groups in a carbohydrate solid can be either associated, hydrogen bonded to other hydroxyl groups within the matrix, or free, not strongly hydrogen bonded. The vibrational frequency of hydrogen bonded hydroxyls ranges from 3000 to 3600 cm^{-1}, while the frequency of free hydroxyls extends primarily into the higher frequency region (Zecchina, 1992). Thus, a shift in the bonding pattern within the sucrose matrix will be manifest as a shift in hydroxyl absorbance; an increase in hydrogen bonding thus shifts absorbance to lower and a decrease in hydrogen bonding to higher frequencies.

Representative FTIR spectra for pure sucrose over the temperature range from 30 to 100 ℃ are plotted in Fig. 27; the blue shift to higher frequency seen in these spectra reflects thermal disruption of the hydrogen bond network within the matrix. Although the absorbance assigned to both associated and hydrogen-bonded hydroxyls (3000-3300 cm^{-1}) was weakened significantly with temperature, the increase in the higher frequency region, assigned primarily to free/weakly bonded hydroxyls, was marginal; we speculate that this is because the extinction coefficient of associated hydroxyls is much larger than that of free hydroxyls. The absorbance over the region from 2700-3000 cm^{-1} is attributed to C-H stretch vibrations (Snyder, Hsu & Krimm, 1978). Since the baseline in this region reflects the O-H absorbance, this decrease is also consistent with the effect of temperature.

The peak frequency in the region above 3000 cm^{-1} increased linearly with temperature in all sucrose and sucrose-gallate films (Fig. 28A). The peak frequency followed the rank order sucrose-octyl gallate > sucrose > sucrose-propyl gallate > sucrose-gallic acid > sucrose-methyl

gallate at all but the highest temperatures (90-100 ℃). Given the relation between frequency and hydrogen bonding, the network hydrogen bond strength within the sucrose matrix varied in the reverse rank order (sucrose-methyl gallate > sucrose-gallic acid > sucrose-propyl gallate > sucrose > sucrose-octyl gallate). It appears that the gallate hydroxyl benzoyl group increased the hydrogen bond strength in the matrix and that this effect was countered somewhat by a saturated carbon chain esterified to the carboxyl group.

The half bandwidth of the hydroxyl absorbance, plotted as a function of temperature in Fig. 28B, provides a measure of the width of the distribution of hydrogen bond energies within the matrix. The rank order for the half bandwidth was the exact reverse of that seen for the peak frequency indicating that a stronger hydrogen bond network is associated with a narrower distribution of bond strengths. This same correlation was also seen in glucose matrices plasticized with glycerol (Liang & Ludescher, 2011). Actively mobile hydroxyl groups associated with a more weakly bonded matrix network may broaden the distribution of stretch orientations and thus broaden the absorption band.

These data on hydrogen strength suggest that the structural origins of the influence of antioxidant on matrix mobility are complex. Irrespective of structure, each of the antioxidants increased the matrix mobility and decreased the activation energy for this mobility. Except for octyl gallate, however, each of the antioxidants increased the strength of the hydrogen bond network. The antioxidants thus do not appear to modulate molecular mobility by simply modulating the strength of the hydrogen bond network (Hamada, Iijima & Gcgregor, 1987) but also apparently by modulating the matrix free volume in complex ways (Naoki & Katahira, 1991; Murthy, 2006) and perhaps by other specific interactions.

4. Conclusion

This work indicates that interactions among the components in amorphous sucrose films significantly affect the local molecular mobility and the integrity of the hydrogen bond network in a complex, temperature-dependent manner. We have used a homologous series of gallate derivatives containing three common chemical groups, the hydroxy benzoyl group, a carboxyl substituent, and a variable alkyl chain, in an effort to determine how antioxidant structure modulates the matrix molecular mobility. Our results suggest that the hydroxyl benzoyl head and carboxyl groups in the gallate antioxidants increase the local mobility and hydrogen bond network strength while the saturated carbon chains act to decrease mobility and bond strength. This research emphasizes how the specific chemical structure of functional additives such as antioxidants modulates the physical properties of amorphous films in complex ways. Such research improves our ability to engineer edible food films with specific food functionalities while also demonstrating the potential for using tryptophan phosphorescence to monitor local molecular mobility in food matrixes.

References

Debeaufort, F.; Quezada-Gallo, J.; Voilley, A. (1998) Edible films and coatings: tomorrow's packaging: a review. *Critical Reviews in Analytical Chemistry*, 38, 288-313.

Lehtinen, P.; Kiiliäinen, K.; Lehtomäki, I.; Laakso, S. (2003)Effect of heat treatment on lipid stability in processed oats. *Journal of cereal Science*, 37, 215-221.

Marsili, R.T. (1999) Comparison of solid-phase microextraction and dynamic headspace methods for the gas chromatographic-mass spectrometric analysis of light-induced lipid oxidation products in milk. *Journal of Chromatographic Science*, 37, 17-23.

Santos, C. X. C.; Anjos, E. I.; Augusto, O. (1999) Uric acid oxidation by peroxynitrite: multiple

reactions, free radical formation, and amplification of lipid oxidation. *Archives of Biochemistry and Biophysics*, 372, 285-294.

Azhar, K. F.; Nisa, K. (2006) Lipids and their oxidation in seafood. *Journal of the Chemical Society of Pakistan*, 28, 298-305.

Arrua, D.; Strumia, M. C.; Nazareno, M. A. (2010) Immobilization of caffeic acid on a polypropylene film: synthesis and antioxidant properties. *Journal of Agriculture and Food Chemistry*, 58, 9228-9234.

Liang, J.; Tian, Y. X.; Fu, L. M.; Wang, T. H.; Li, H. J.; Wang, P.; Han, R. M.; Zhang, J. P.; Skibsted, L. H. (2008) Daidzein as an antioxidant of lipid: effects of the microenvironment in relation to chemical structure. *Journal of Agriculture and Food Chemistry*, 56, 10376-10383.

Liang, J.; Tian, Y. X.; Yang, Fan.; Zhang, J. P.; Skibsted, L. H. (2009) Antioxidant synergism between carotenoids in membranes. Astaxanthin as a radical transfer bridge. *Food Chemistry*, 115, 1437-1442.

Desai, K. G.H.; Park, H. J. (2005) Recent developments in microencapsulation of food ingredients. *Drying Technology*, 23, 1361-1394.

You, Y. M.; Ludescher, R. D. (2007) The effect of glycerol on molecular mobility in amorphous sucrose detected by phosphorescence of erythrosine B. *Food Biophysics*, 2, 133-145.

Bauchot, A. D.; John, P. (1995)Sucrose ester-based coatings formulated with food-compatible antioxidant in the prevention of superficial scald in stored apples. *Journal of the American Society for Horticultural Science*, 120, 491-496.

Roos, Y. (1993) Melting and glass transitions of low molecular weight carbohydrates. *Carbohydrate Research*, 238, 39-48.

You, Y. M.; Ludescher, R. D. (2010) The effect of molecular size on molecular mobility in amorphous oligosaccharides. *Food Biophysics*, 5, 82-93.

de Graaf, R. A., Karman, A. P., Janssen, L. P. B. (2003) Material properties and glass transition temperatures of different thermoplastic starches after extrusion processing. *Starch*, 55, 80-86.

Tseng, K. C.; Durning, C. J. (2000) Molecular mobility in polymer thin films. *Physical Review E*

, 61, 1800-1811.

Zhou, D.; Zhang, G. G. Z.; Law, D.; Grant, D. J. W.; Schmitt, E. A. (2008)Thermodynamics, molecular mobility and crystallization kinetics of amorphous griseofulvin. *Molecular Pharmaceutics*, 5, 927-936.

Liang, J., Ludescher, R. D. (2011) Antioxidant modulate molecular mobility, oxygen permeability, and microstructure in zein films. *Journal of Agriculture and Food Chemistry*, 59, 13173-13180.

Shirke, S.; Ludescher, R. D. (2005) Molecular mobility and the glass transition in amorphous glucose, maltose, and maltotriose. *Carbohydrate Research*, 240, 2654-2660.

Lukasik, K. V.; Ludescher, R. D. (2006) Molecular mobility in water and glycerol plasticized cold- and hot-cast gelatin films. *Food Hydrocolloids*, 20, 96-105.

You, Y. M., Ludescher, R. D. (2011) Effect of starch on the molecular mobility of amorphous sucrose. *Journal of Agriculture and Food Chemistry*, 7, 3340-3347.

Liang, J.; Ludescher, R. D. (2012) Influence of glycerol on the molecular mobility and hydrogen bond network in the glucose-based matrix. *Carbohydrate Research*, 361, 120-126.

Shirke, S., You, Y.M., Ludescher, R. D. (2006) Molecular mobility and dynamic site heterogeneity in amorphous lactose and lactitol from erythrosin B phosphorescence. *Biological Chemistry*, 123, 122-133.

Broos, J.; Gabellieri, E.; van Boxel, G. I.; Jackson, J. B.; Strambini, G. B. (2003)Tryptophan phosphorescence spectroscopy reveals that a domain in the NAD(H)-binding component (dI) of transhydrogenase from Rhodospirillum rubrum has an extremely rigid and conformationally homogeneous protein core. *The Journal of Biological Chemistry*, 278, 47578-47584.

Gonnelli M. & Strambini G.B. (1995) Phosphorescence Lifetime of Tryptophan in Proteins. *Biochemistry-US* ,34(42),13847-13857.

Fischer C.J., Gafni A., Steel D.G., & Schauerte J.A. (2002) The triplet-state lifetime of indole in aqueous and viscous environments: Significance to the interpretation of room temperature phosphorescence in proteins. *Journal of the American Chemical Society,* 124(35),10359-10366.

Pravinata, L. C.; You, Y. M.; Ludescher, R.D. (2005) Erythrosin B phosphorescence monitors molecular mobility and dynamic site heterogeneity in amorphous sucrose. *Biophysics Journal*, 88, 3551-3561.

Gershenson, A.; Schauerte, J. A.; Giver, L.; Arnold, F.H. (2000) Tryptophan phosphorescence study of enzyme flexibility and unfolding in laboratory-evolved thermostable esterases. *Biochemistry*, 39, 4658-4665.

Weinryb, I.; Steiner, R. F. (1968) The luminescence of tryptophan and phenylalanine derivatives. *Biochemistry*, 7, 2488-2495.

Lukasik, K. V.; Ludescher, R. D. (2006) Molecular mobility in water and glycerol plasticized cold- and hot-cast gelatin films. *Food Hydrocolloids*, 20, 96-105.

Kaminski, K.; Kaminska, E.; Hensel-Bielowka, S.; Chelmecka, E.; Paluch, M.; Ziolo, J.; Wlodarczyk, P.; Ngai, K. L. (2008)Identification of the molecular motions responsible for the slower secondary (β) relaxtion in sucrose. *The Journal of Physical Chemistry B*, 112, 7662-7668.

Zecchina, A.; Bordiga, S.; Spoto, G.; Marchese, L.; Petrini, G.; Padovan, M. (1992) Silicalite characterization. 2. IR spectroscopy of the interaction of carbon monoxide with internal and external hydroxyl groups. *The Journal of Physical Chemistry*, 96, 4991-4997.

Hamada, K.; Iijima, T.; Gcgregor, R. (1987) Effects of hydrogen bonds on the mobility of spin probes in Nylon films. *Polymer Journal*, 19, 709-717.

Naoki, M.; Katahira, S. (1991) Contribution of hydrogen bonds to apparent molecular mobility in supercooled D-sorbitol and some polyols. *The Journal of Physical Chemistry*, 95, 431-437.

Murthy, N. (2006) Hydrogen bonding, Mobility, and structure transitions in aliphatic polyamides. *Journal of Polymer Science Part B: Polymer Physics*, 44, 1763-1782.

Snyder, R. G.; Hsu, S. L.; Krimm, S. (1978) Vibrational spectra in the CH stretching region and the structure of the polymethylene chain. *Spectrochimica Acta Part A*, 34, 395-406.

Strambini, E. G.; Strambini, G. B. (2000) Tryptophan phosphorescence as a monitor of protein conformation in molecular films. *Biosensors and Bioelectronics*, 15, 483-490.

Ludescher, R. D.; Shah, N. K.; McCaul, C. P.; Simon, K. V. (2001) Beyond Tg: optical

luminescence measurements of molecular mobility in amorphous solid foods. *Food Hydrocolloids*, 15, 331-339.

Hershberger, M.W., Maki, A.H., Galley, W.C. (1980) Phosphorescence and ODMR studies of a class of anomalous tryptophan residues in globular proteins, *Biochemistry*, 19, 2204–2209.

Chapter V: Effects of Glycerol on the Molecular Mobility and Hydrogen Bond Network in Starch Matrix

A paper accepted by *Carbohydrate Polymers*

Jun Liang, Richard. D. Ludescher

1. Introduction

Over the last few years, there has been a renewed interest in biodegradable plastics made from annually renewable, natural polymers (Lawton, 1996). An important renewable raw material is starch. Starch is a versatile food ingredient and is widely used as a texturizer, thickener, gelling agent, adhesive, and moisture-retainer. One of the basic properties of starch is its film-forming ability. Starch consists primarily of branched and linear chains of glucose molecules, namely amylopectin and amylose, respectively. The film-forming ability of starch is principally due to hydrogen bonds between the long-chain, unbranched amylose. Although tensile strengths of the starch films are high, they are brittle and exhibit little or no elongation (Lawton & Fanta, 1994). Thus, a plasticizer is always added to increase flexibility. As one of the most commonly used plasticizers, glycerol is compatible with amylose and could interfere with amylose packing (Garcia, Martino & Zaritzky, 1999; Jansson & Thuvander, 2004).

Numerous studies have investigated the physical characteristics of starch-based films and the mechanism underlying film formation (Das, Ray, Bandyopadhyay, Gupta, Sengupta, Sahoo, Mohanty & Misra, 2010; Dufresne & Vignon, 1998; Otey, Westhoff & Doane, 1987; Lee, Armstrong, Thomasson, Sui, Casada & Herrman, 2010). The potential applications of starch films are closely related to the film microstructure (Romera, Moraes, Zoldan, Pasa & Laurindo, 2012), film-forming conditions (Jonhed, Andersson & Järnström, 2008), and interactions among the depositions in the starch films (García, Martino & Zaritzky, 2000). It's proved that the pure

starch amorphous solid could have a high T_g of around 230 ℃ (Orford, Parker, Ring & Smith, 1989). Although foods are considered stable in the glass below T_g due to an absence of large-scale molecular motions, and thus the T_g is a useful index temperature for stability in amorphous foods, various physical and chemical reactions can still occur in the glassy state, indicating that T_g cannot be considered as a threshold temperature for stability and that molecular mobility below T_g cannot be neglected.

The effects of glycerol on the physical properties of amorphous starch have also been studied. It has been reported that glycerol can exert different effects depending on its concentration. Lourdin and colleagues reported that glycerol at a content below 12% could decrease the ductility of potato starch film; when the amount of glycerol exceeded 12%, however, the ductility increased (Lourdin, Bizot & Colonna, 1997). Similar antiplasticizing effects of glycerol were also found in the matrixes of trehalose and maltodextrin (Anopchenko, Psurek, VanderHart, Douglas & Obrzut, 2006; Roussenova, Murith, Alam & Ubbink, 2010). In most cases, there exists a critical glycerol content that marks the onset of a change in functionality from antiplasticizer to plasticizer. These results, however, were all obtained using macroscopic methods like DSC, film stress analysis, and positron annihilation lifetime spectroscopy. Data concerning how glycerol can affect the molecular mobility and interaction forces in the starch and other polymer matrix on the microscopic level are, as far as we know, limited.

Starch films are hydrogen-bonded solids and so the properties of the matrix are modulated by hydrogen bonding interactions among the molecules in the matrix. Wolkers and colleagues established that the OH stretching vibration at ~3300 cm^{-1} increases with the

temperature in seven amorphous sugars and $\nu_{OH}(T)$ displayed a characteristic change in slope at the sugar T_g's (Wolkers, Oldenhof, Alberda & Hoekstra,1998; Wolkers, Oliver, Tablin & Crowe, 2004). This increase in ν_{OH} reflects a change from associated hydroxyl to free hydroxyl following the increase of temperature. Recently, we have used FTIR to evaluate the influence of glycerol on the physical state of amorphous solid glucose. We found that addition of glycerol can broaden the distribution of stretching orientations and thus broaden the absorption band from stretching of OH, consistent with the increase in molecular mobility (Liang & Ludescher, 2012).

Here we report studies of the influence of glycerol on molecular mobility in amorphous potato starch obtained from analysis of the phosphorescence from Ery B embedded in the matrix. Glycerol weight content was varied from 0 to 30 percent by addition of glycerol to the starch solution before film formation. The temperature-dependence of mobility was measured and analyzed at different glycerol contents, generating families of mobility versus temperature curves. Samples in the same conditions were measured by FTIR in the temperature range from 30 to 100 ℃. By studying the relation between mobility and hydrogen bond strength and network, we seek to understand how glycerol can modulate the starch matrix mobility as a function of concentration.

2. Materials and methods

2.1 Sample preparation.

We prepared amorphous starch films containing varying content of glycerol by using a slightly modified version of our published methods for making sugar/glycerol films (Liang & Ludescher, 2012). Potato starch (Sigma Chemical, St. Louis, MO), 2.5 g, was dissolved in 50 ml

deionized water and heated to boiling on a stir plate for at least 10 min to make sure starch was totally denatured. Glycerol (99% GC pure; Sigma Chemical, St. Louis, MO) was added to obtain the final content of 0, 5, 10, 20 or 30 percent of the dry weight of starch. The glycerol-starch solutions were stirred at room temperature for at least half an hour to make sure the glycerol was totally blended with starch. For the luminescence experiments, starch-glycerol mixtures were prepared from solutions containing Ery B at the appropriate concentration. Erythrosin B (Ery B; Sigma Chemical, MO), disodium salt, was dissolved in deionized water to prepare a 10 mM stock solution; an aliquot from this solution was added to the starch solution to obtain a mole ratio of $1:10^4$ for dye/glucose unit in the starch.

The starch solutions were cooled down to room temperature prior to spreading 15 μl on approximately one third of a quartz slide ($30 \times 13.5 \times 0.6$ mm, custom made by NSG Precision Cells, Farmingdale, NY). The slides were placed under a gentle warm air stream using an air gun to rapidly (within 5 min) evaporate the moisture.

Slides were soaked in Terg-A-Zyme (Alconox, Inc., NY) soap solution over 24 h to remove surface impurities, then washed with deionized water, and finally rinsed with ethanol and dried with acetone before using.

For the experiment of IR and X-ray, the films were prepared with the same method as that for luminescence except that the sample solutions were spread on ATR plates for the IR experiment or glass slides for the X-ray experiment. The quartz slides, ATR plates and glass slides with film were stored at room temperature against the desiccant Drierite for at least 1 week and kept in an atmosphere of P_2O_5 in order to maintain 0% RH. The desiccant P_2O_5 was refreshed as necessary.

2.2 X-ray Diffraction.

X-ray diffraction were taken with a Philips (Model 42273) x-ray diffractometer (Philips, Mahwah, NJ), using the following conditions: target, Cu-kα radiation; voltage, 35 kV; current, 20 mA; scanning speed, 2^{o} 2θ/ min; time constant, 1 sec. The intensity was measured at the scanning angle (2θ) from 10 to 35^{o}.

2.3 Phosphorescence Measurements and Analysis.

All luminescence measurements were conducted on a Cary Eclipse spectrophotometer (Varian Instruments, Walnut Creek, CA) equipped with a temperature controller and multicell holder. All measurements were made at least in triplicate and the temperatures were varied from 0 to 100 ℃.

A high purity nitrogen stream was routed into the sample compartment and directly into the quartz fluorescence cuvettes that held the slides. The cuvette was capped with a lid having inlet and outlet ports for the gas line, so all experiments were performed at ambient pressure. Each intensity decay was averaged over 50 cycles. For each cycle, data was collected from a single flash with a decay of 0.04 ms. a 0.05 ms gate, and 10.0 ms total decay time. Phosphorescence and delayed fluorescence emission scans were collected over the range from 540 to 800 nm with an excitation wavelength of 520 nm. The excitation and emission monochromators were both set at 20 nm band pass. Each data point (collected at 1 nm intervals with a 0.1 s averaging time) was collected from a single flash with 0.2 ms delay and 5 ms gate time.

For lifetime measurements, because intensity decays are non-exponential, a stretched exponential function was selected to analyze the intensity decays:

$$I(t) = I(0) \exp\left[-(t/\tau)^{\beta}\right] + \text{constant} \quad (1)$$

where $I(0)$ is the initial intensity, τ is the stretched exponential lifetime, and β is an exponent varying from 0 to 1 that characterizes the lifetime distribution (Pravinata, You & Ludescher, 2005). The use of stretched exponential model provides an analysis in terms of a continuous distribution of lifetimes, which is appropriated for describing a complex solid possessing a distribution of relaxation times for dynamic molecular processes (Richert, 2000; Shirke, Takhistov & Ludescher, 2005).

The energy of the emission maximum (Vp) and bandwidth (FWHM) of the emission band were determined by using a log-normal line shape function to fit both delayed fluorescence and phosphorescence (Pravinata, You & Ludescher, 2005).

$$I(\nu) = I_0 \exp\left\{-\ln(2)\left(\frac{ln\left[1+2b\left(\nu-\nu_p\right)\right]/\Delta}{b}\right)^2\right\} \quad (2)$$

where I_0 is the maximum emission intensity, ν_p is the peak frequency (cm^{-1}), Δ is a linewidth parameter, and b is an asymmetry parameter. The full-width at half maximum (FWHM) bandwidth Γ is calculated according to the following equation:

$$\Gamma' = \Delta\left[\frac{\sinh(b)}{b}\right. \quad (3)$$

For delayed luminescence spectra collected from 540-750 nm, a sum of log-normal functions for delayed fluorescence ($I_{DF}(v)$) and phosphorescence ($I_P(v)$) was used to fit the spectra. Each emission band was analyzed for independent fit parameters using a sum of two functions as described in Eq. 2.

The phosphorescence lifetimes were used to calculate the rate constants associated with the various processes that depopulate the triplet state. Our analysis of the delayed emission is similar to the photophysical scheme for Ery B outlined in an earlier study, only using slightly different nomenclature (Duchowicz, Ferrer & Acuña, 1998). The measured phosphorescence lifetime (τ) is the inverse sum of all possible de-excitation rates for the triplet state T_1.

$$1/\tau = k_P = k_{PR} + k_{TS1} + k_{TS0}. \quad (4)$$

Here, k_{PR} is the rate of radiative decay to the ground state, k_{TS1} is the rate of reverse intersystem crossing to S_1, and k_{TS0} is the rate of intersystem crossing to the singlet manifold followed by vibrational relaxation to S_0; the oxygen quenching term is not included as it is negligible under our experimental conditions. The radiative decay rate has a value of 41 s^{-1} for Ery B (Duchowicz, Ferrer & Acuña, 1998).

Reverse intersystem crossing is a thermally activated process that has an exponential dependence on the energy gap ΔE_{TS} between T_1 and S_1 (Nack & Ludescher, 2006).

$$k_{TS1}(T) = k^{o}_{TS1}\exp(-\Delta E_{TS}/RT) \quad (5)$$

The ratio of intensity of delay fluorescence (I_{DF}) to phosphorescence (I_P), where I_{DF} and I_P are determined from analysis of emission spectra using the log-normal function (Eq. 2), is

proportional to the rate of reverse intersystem crossing. A plot of $\ln(I_{DF}/I_P)$ versus 1/T thus has a slope of $-\Delta E_{TS}/R$. The single-triplet energy gap of Ery B is greatly influenced by the surrounding solvent (matrix) (Lettinga, Zuilhof & van Zandvoort, 2000). The k^o_{TS1} for Ery B varies from 0.3 $\times 10^7$ s^{-1} in ethanol (Lettinga, Zuilhof & van Zandvoort, 2000) and 6.5 $\times 10^7$ s^{-1} in water to 111 $\times$ 10^7 s^{-1} in solid polyvinyl alcohol. We estimated the maximum possible value for k^o_{TS1} in starch/glycerol by assuming that $k_{TS1}(T)$ cannot result in values for k_{TS0} decreasing with temperature. This procedure thus estimated the minimum possible values of $k_{TS0}(T)$. The estimated value of k^o_{TS1} was 3 $\times 10^7$ s^{-1} in this study.

One of the non-radiative decay routes is through intersystem crossing to the ground state S_0. The decay rate is expressed by k_{TS0}, which reflects the rate of collisional quenching of probe due to both internal and external factors (Pravinata, You & Ludescher, 2005). The term k_{TS0} primarily reflects the external environmental factors since the self-collisional quenching among probe molecules can be neglected due to the low concentration and slow diffusion within the extremely viscous amorphous solid. We have used the Ery B probe in numerous studies of amorphous carbohydrate and protein solids and found no evidence of clustering. In particular, as summarized in You & Ludescher (2006): studies of the effect of probe concentration in amorphous sucrose reveal that all measured spectroscopic parameters (lifetime, etc.) are identical over the range from 0.5 to 10 x 10^{-4} probe/sucrose, whereas this study used 1x10^{-4} probe/glucose monomer; the emission spectra in amorphous starch do not exhibit the characteristic features associated with exciton interactions associated with clustering (spectral broadening splitting of emission band, wavelength shifts) seen in other studies. In this study, the temperature–dependent term k_{TS0} can be calculated from measured lifetimes using Eq. 4.

2.4 Atomic Force Microscopy (AFM).

Tapping mode AFM images were collected using a NanoScope IIIA Multimode AFM (Veeco Instruments Inc., Santa Barbara, CA) equipped with a silicon-etched RTESP7 cantilever (Veeco Nanoprobe, Camarillo, CA) under ambient conditions. Before tip engagement, the films were check with affiliated microscopy for possible of phase separation and the drive frequency of the silicon tip was tuned with the aid of Nanoscope 5.30 software and fixed at 200-250 kHz for further scanning. All of the collected images were smoothed before further analysis.

2.5 Attenuated Total Reflectance Fourier Transform Infrared (ATR-FTIR) Spectroscopy.

The ATR-FTIR spectra were collected by using a Thermal Nicolet Nexus 670 FT-IR spectrometer (Thermo FisherScientific Inc., Waltham, MA) equipped with a Smart ARK thermal accessory and analyzed using the associated EZ-OMNIC software. Each spectrum was an average of 102 scans with 4 cm^{-1} resolution in an atmosphere of air-dried over P_2O_5 to minimize the interference of moisture in ambient condition. The measurements were conducted at the temperature from 100 down to 30 ℃.

Figure 29

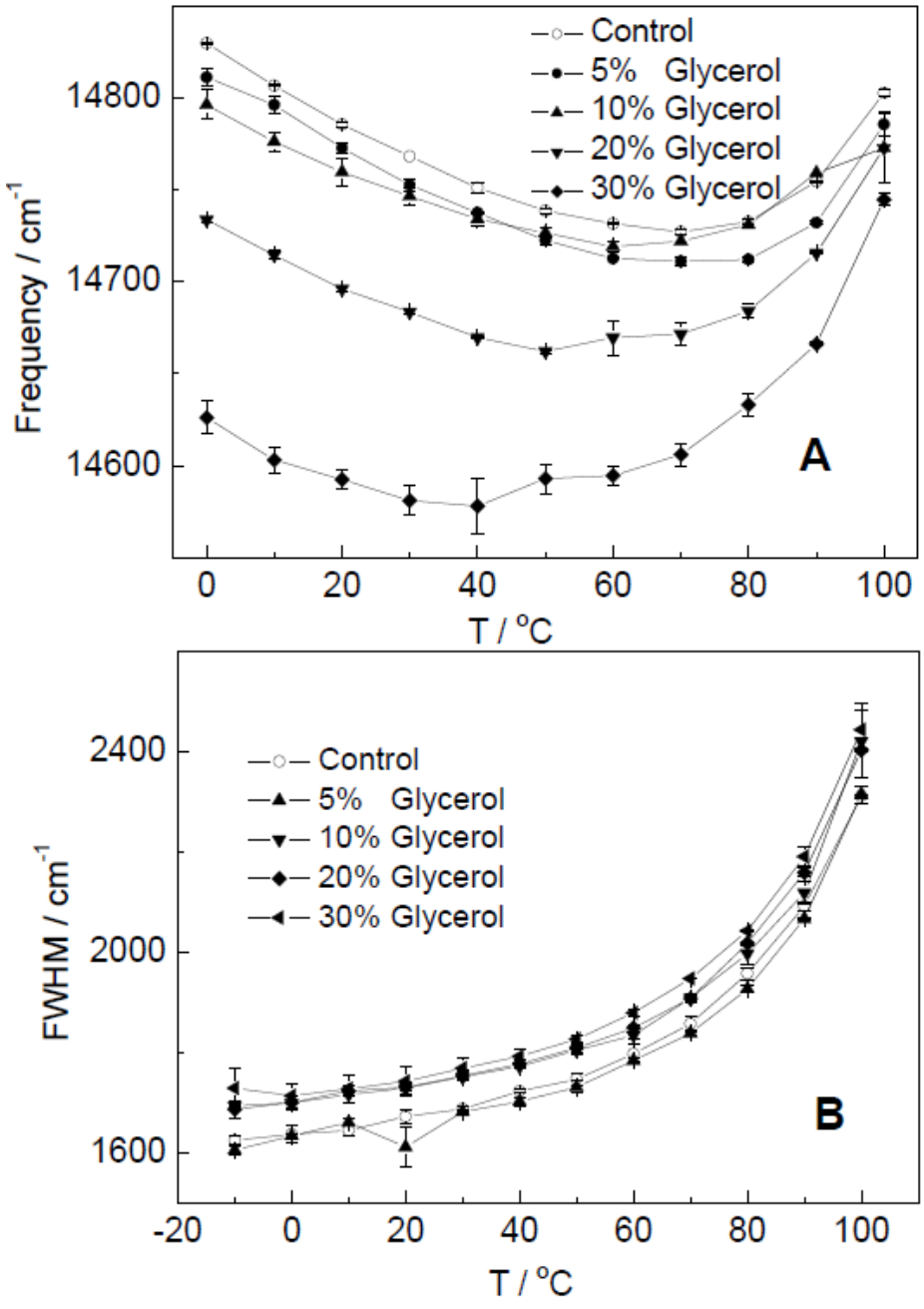

Figure 29: A) Peak frequency for phosphorescence emission from Ery B in amorphous starch-based films with varying weight contents of glycerol. B) Band width (FWHM) for phosphorescence emission from Ery B in amorphous starch-based films with varying weight contents of glycerol.

3. Results and Discussion

3.1 Delayed emission spectra.

During the process of dehydration of the denatured starch solution to form the dried starch films, crystallization competes with the formation of network structure in amylose. When water is rapidly evaporated, amorphous starch films will be formed with little crystallinity (Tajia, 2007) In this study, using X-ray, we confirmed that the starch matrices formed in this way were practically amorphous (data not included).

The delayed emission spectra of Ery B in amorphous starch/glycerol films has a long wavelength emission (maximum ~690 nm) due to phosphorescence from the triplet state T_1 and a short wavelength emission (maximum ~555 nm) due to delayed fluorescence from the singlet state S_1 repopulated by thermally activated reverse intersystem crossing from T_1. Delayed emission spectra in starch with variable glycerol content collected over the temperature range from 0 to 100 ℃ showed a decrease in phosphorescence (I_P) and an increase in delayed fluorescence (I_{DF}) intensity with increasing temperature (data not shown). The intensity ratio was analyzed as $\ln(I_{DF}/I_P)$ versus 1/T and the linear slope was used to estimate the energy gap (ΔE_{TS}) separating the excited triplet and singlet states; the energy gap was used to calculate the rate of reverse intersystem crossing, $k_{TS1}(T)$, according to Eq. 5 (see Materials and Methods for further details). Such plots were linear with $R^2 \geq 0.995$; the slopes from starch samples containing various glycerol contents showed negligible differences (data not shown), indicating that the energy gap, and thus $k_{TS1}(T)$, was not greatly affected by addition of glycerol.

The peak frequency (ν_P) and bandwidth (Γ) for both delayed fluorescence and phosphorescence emission were determined by fitting to a log-normal line shape function (Eq. 2

and 3). The parameters of this fitting process are plotted in Fig. 29 for temperatures from 0-100°C. The values of ν_P decreased gradually and approximately linearly at low temperature and increased at high temperature in all samples. The onset temperature for this reversal was ~70 ℃ in pure starch and decreased with addition of glycerol to ~40 ℃ for starch with 30 wt. % glycerol. The peak frequency decreased with increasing glycerol content at all temperatures; since glycerol also caused a decrease in the Ery B phosphorescence lifetime (discussed below), this decrease in ν_P indicates that the rate of dipolar relaxation around the excited triplet state increased with glycerol content (Pravinata, You & Ludescher, 2005). Glycerol had a much larger effect on the extent and thus the rate of dipolar relaxation at low temperature than at high temperature.

The increase in ν_P at higher temperature, observed for the first time for this probe in amorphous biomaterials, indicates a temperature-dependent change in the matrix structure around the probe. This structural reorganization increased the energy of the Ery B emission either by decreasing the local matrix polarity and/or hydrogen bonding ability around the probe or by decreasing the extent, and perhaps the rate, of dipolar relaxation during the probe's excited state lifetime. Given that the increase in emission energy also occurred to a comparable albeit lesser extent in pure starch, this structural reorganization was facilitated, but not caused, by glycerol.

The phosphorescence bandwidth reflects the range of energetically distinct matrix environments due to interactions between the matrix molecules and the excited probe (Pravinata, You & Ludescher, 2005). The bandwidth increased gradually and approximately linearly at low temperature and increased dramatically at temperatures above 60 ℃ in all films (Fig. 1B). The

bandwidth was unaffected by addition of 5 wt. % glycerol but increased slightly at higher content of glycerol. Since the increase in bandwidth reflects a corresponding increase in the width of the distribution of energetically distinct matrix environments for the EryB probe, glycerol at 10 wt. % and higher caused a small increase in this distribution over the whole temperature range.

Figure 30

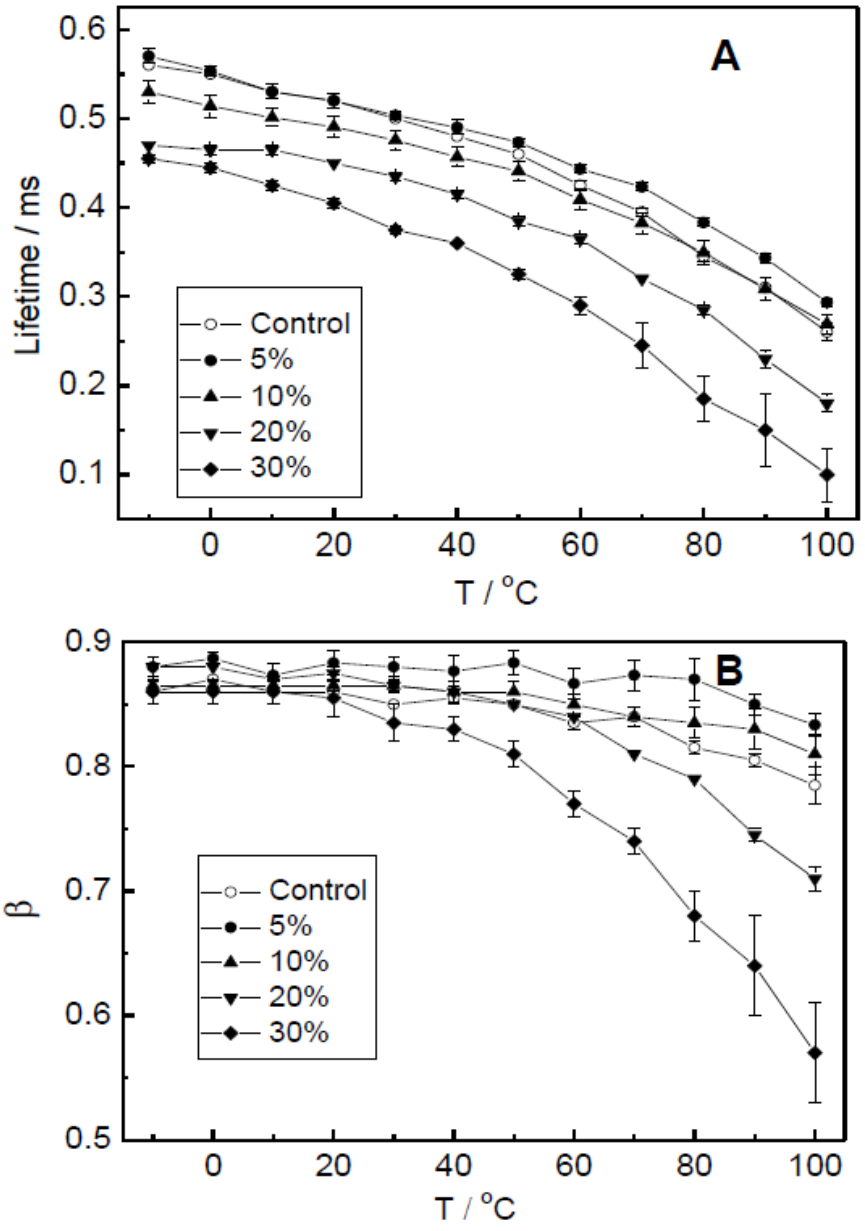

Figure 30: A) Temperature-dependence of lifetime obtained from fits to a stretched exponential decay model of the intensity decay of Ery B in amorphous starch-based matrices with varying weight contents of glycerol. B) Stretching exponent β obtained from fits to a stretched exponential decay model of the intensity decay of Ery B in amorphous starch-based matrices with varying weight contents of glycerol.

3.2 Emission lifetimes.

Glycerol can act both as an antiplasticizer to increase matrix rigidity when present at low content and as a plasticizer to decrease matrix rigidity when present at high content (Lourdin, Coignard, Bizot & Colonna, 1997; Lourdin, Ring & Colonna, 1998). The weight fraction at which glycerol changes from acting as an antiplasticizer to acting as a plasticizer differs based on the physical properties of the matrix. We have indentified this transition point for glycerol at ~6 wt % in amorphous sucrose films using the Ery B phosphorescence probe (You & Ludescher, 2007).

The phosphorescence emission intensity decay transients from Ery B in films of starch/glycerol (under nitrogen) were collected as a function of temperature from 0 to 100 ℃. All intensity decay transients were well-fit using a stretched exponential decay model (eq. 1, Materials and Methods) providing the lifetime τ and stretching exponent β as model fitting parameters; the R^2 was ≥ 0.995 for all fits. For all matrices, the phosphorescence lifetime decreased monotonically with increasing temperature; the decrease was gradual at low and steeper at high temperature indicating that the various non-radiative decay rates were thermally activated (Fig. 30A). The presence of glycerol affected the Ery B lifetime in a dose- and temperature-dependent manner. At 5 wt. % glycerol the lifetime was unaffected at low temperature (≤ 40°C) and increased above that seen in pure starch at higher temperature. At 10 wt. % glycerol the lifetime was decreased below that seen in pure starch at low and intermediate temperature (<80 ℃) but unaffected at higher temperature. At 20%, and even more so at 30% glycerol, the lifetime was significantly below that seen in pure starch over the whole temperature range.

The stretching exponent β provides a measure of the width of the distribution of lifetimes that characterizes the excited state decay kinetics of the Ery B probe; β varies between 1 and 0 with lower values indicating a broader distribution. The magnitude of β thus provides a measure of the extent of dynamic heterogeneity in the matrix (Pravinata, You & Ludescher, 2005; Liang & Ludescher, 2012)). The value of β exhibited biphasic behavior in all films (Fig. 30B), remaining nearly constant at low to intermediate and decreasing at higher temperature. The magnitude of β and the extent and onset temperature of the decrease varied with glycerol content in a biphasic dose-dependent manner. In pure starch, β was ~0.87 and constant up to ~50 ℃ and decreased slightly to ~0.8 at 100 ℃, indicating that the pure starch matrix became slightly more dynamically heterogeneous at high temperature. The addition of small amounts of glycerol, however, increased β across the entire temperature range; the increase was larger at 5 than at 10 wt. %. At higher glycerol content, β decreased in a dose-dependent manner across the entire temperature range. The onset temperature for the decrease in β was also sensitive to the glycerol content, initially increasing from ~50 to ~80 ℃ at low (5-10 wt. %) and then decreasing to ~40 and ~20 ℃ at 20 and 30 wt. % glycerol, respectively. The overall matrix dynamic heterogeneity in these starch films was thus slightly decreased and less temperature-dependent at low (≤ 10 wt. %) and significantly increased and more temperature-dependent at higher glycerol content.

Figure 31

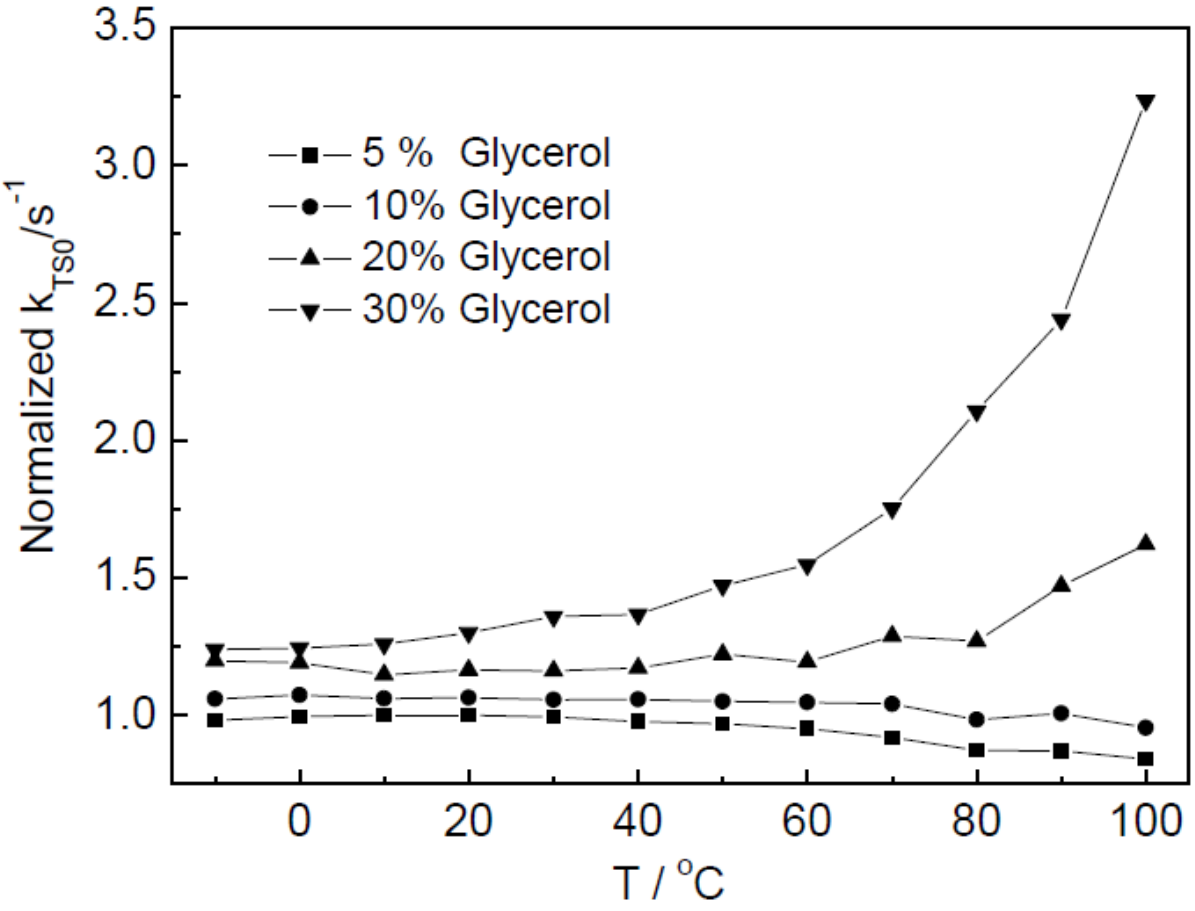

Figure 31: Rate of non-radiative decay of Ery B triplet state in amorphous starch-based matrices with varying weight content of glycerol. Values are plotted normalized to the value in a pure starch matrix at each temperature. Rate data were calculated from the lifetime data of Figure 30 A.

In the absence of oxygen, the lifetime of Ery B reflects values of the rate constants for radiative emission, k_{RP}, reverse intersystem crossing, $k_{TS1,}$ and collisional non-radiative quenching, k_{TS0} (Eq. 4, Materials and Methods). The value of k_{RP} is 41 s^{-1} and constant (Duchowicz, Ferrer & Acuña, 1998; Lettinga, Zuilhof & van Zandvoort, 2000). Since the magnitude of k_{TS1} can be estimated from Eq. 5, it is possible to estimate the lower limit of k_{TS0} as a function of temperature. The calculated values for the collisional quenching constant for Ery B in starch/glycerol films as a function of temperature are plotted in Fig. 31 as the value of k_{TS0} in starch/glycerol divided by the value of k_{TS0} in pure starch at the same temperature in order to highlight the effect of glycerol on the matrix mobility. Glycerol decreased the matrix collisional quenching rate, an indicator of local matrix mobility (Pravinata, You & Ludescher, 2005), at low content fractions (< 10 wt. %) and increased this rate at high content fractions in a temperature-dependent manner.

Using the same probe, we have previously reported that glycerol acts as an antiplasticizer in sucrose at low weight content (~6%) and low temperature (≤ ~45 ℃) (You & Ludescher, 2007) but not in glucose (Liang & Ludescher, 2012). Our data reported here highlight the importance of molecular structure and specific interactions in mediating the antiplasticization phenomenon in hydrogen bonding carbohydrate matrixes.

Figure 32

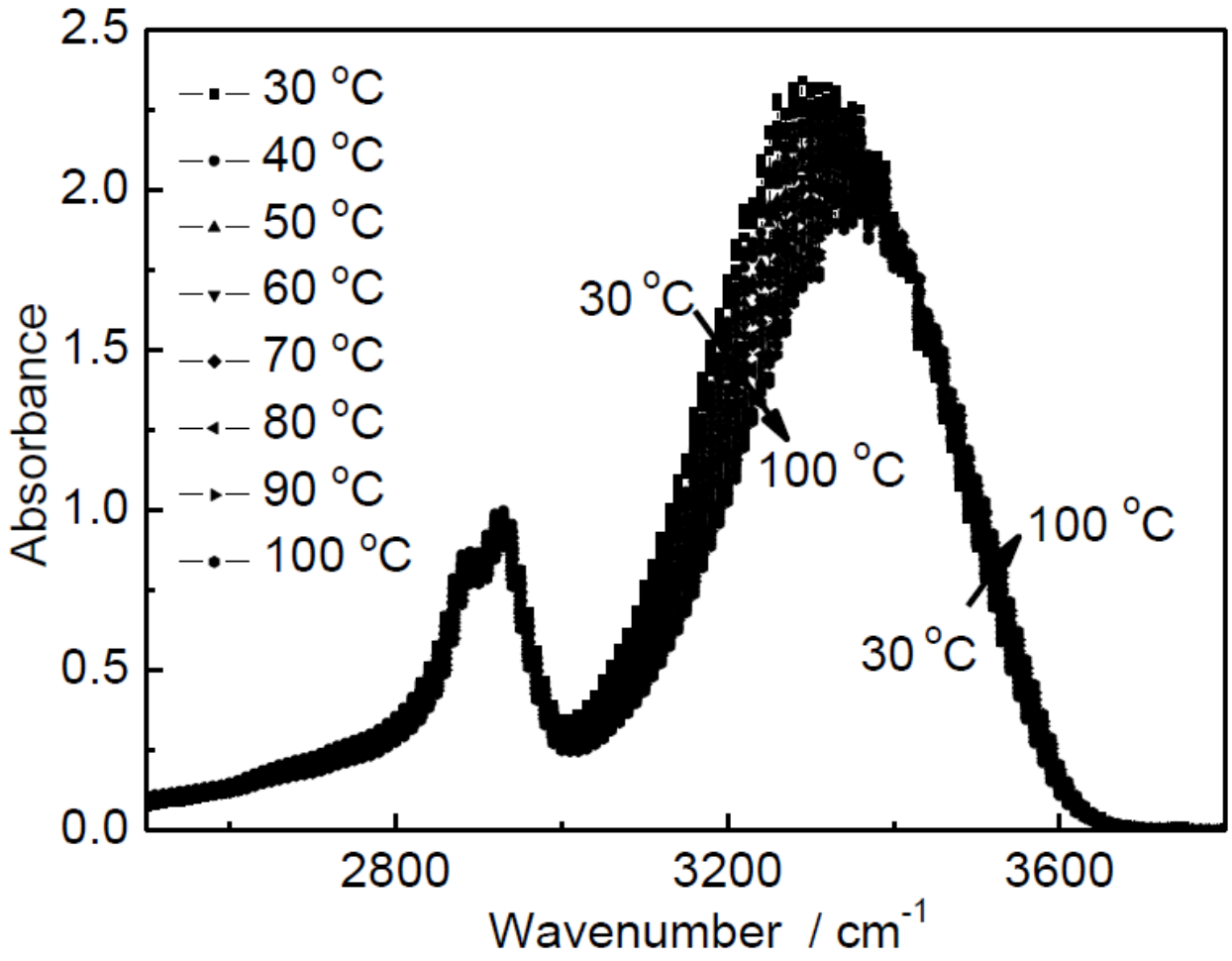

Figure 32: Temperature-dependence of FTIR spectra of starch matrix with glycerol weight content of 20 wt. %. Orientation of arrow indicates increase in temperature.

Figure 33

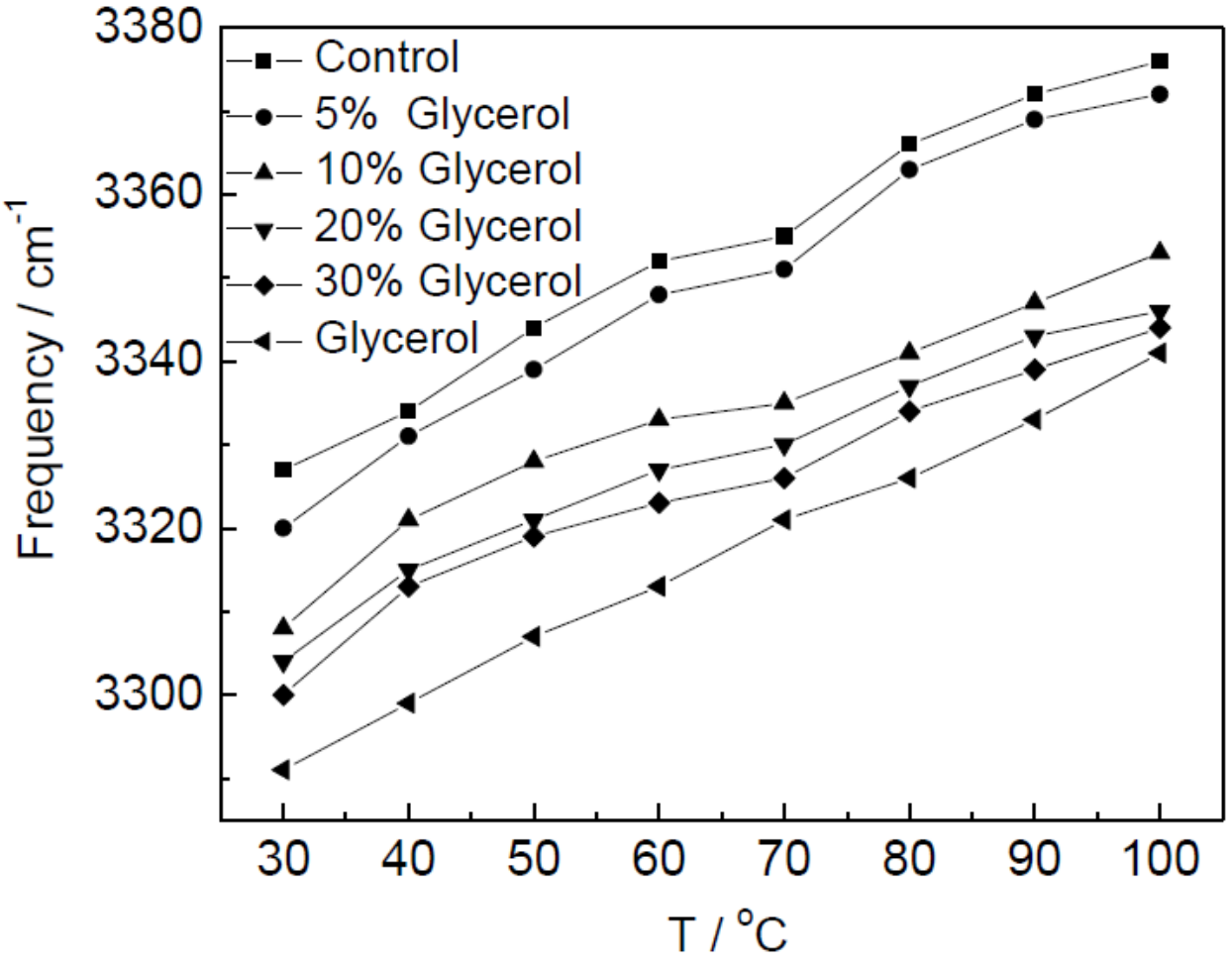

Figure 33: Temperature-dependence of peak frequency for FTIR spectra above 3000 cm^{-1} in amorphous starch-based matrices with varying weight contents of glycerol.

3.3 Attenuated Total Reflectance Fourier Transform Infrared (ATR-FTIR) Spectroscopy.

The hydrogen bond is the most important intermolecular interaction maintaining the status of the starch matrix. Changes in the hydrogen bond network due to changes in matrix composition or temperature will alter this network and thus modulate matrix structure and mobility. The hydroxyls in solid carbohydrates can be present as either associated hydroxyl, connected with other hydroxyls by hydrogen bonds, or free hydroxyls, not specifically associated with other hydroxyls in hydrogen bonds (Dashnau, Sharp & Vanderkooi, 1997). The IR absorbance bands of both hydroxyls are distributed above 3000 cm^{-1}, while that of free hydroxyl spread over the high frequency region (Kondo, 1997). Thus, if associated hydroxyls become free hydroxyls, the signal in the hydroxyl region above 3000 cm^{-1} shifts to higher frequency.

The high frequency region due to the OH stretching vibration (3000-3700 cm^{-1}) of starch films with and without glycerol was measured as a function of temperature. The absorbance band above 3000 cm^{-1} shifted to higher frequency for all samples with an increase of temperature, as illustrated for starch with 20 wt. % glycerol in Fig. 32. These data indicate that the increase in temperature shifted the hydrogen bond distribution from associated toward free hydroxyl groups. The decrease in intensity in the region from 3000-3300 cm^{-1} was more dramatic than the increase in intensity in the region from 3300-3600 cm^{-1}. We speculate that this is because the extinction coefficient of associated hydroxyls is much larger than that of free hydroxyls. The absorbance over the region from 2700-3000 cm^{-1}, attributed to the CH stretch vibration, also decreased with temperature; as the baseline in this region reflects OH absorbance, this decrease is consistent with the effect of temperature on the OH absorbance.

The effect of temperature on the OH absorbance peak frequency of samples containing different content of glycerol is plotted in Fig. 33. The peak frequency, as discussed above, increased with temperature and decreased with glycerol content. The decrease was small at 5 wt. % and considerably larger at 10 wt. % and above. Such a decrease in OH stretching frequency with added glycerol is indicative of a stronger hydrogen bond network.

We have checked the surface structure of starch-based matrices with/without glycerol using AFM and AFM affiliated microscopy and no glycerol/starch phase separation was found in films (data not included). It has been seen clearly in previous studies that amylose and amylopectin are arranged in strands that form the network in both starch gels and more compact starch films (Leloup, Colonna, Ring, Roberts & Wells, 1992). In the rapidly dehydrated films, those strands are further connected with additives and form into amorphous solid (Karmas, Buera & Karel, 1992; Talja, 2007). The polyhydroxyl structure of glycerol provides ideal anchors to adhere to polymers like amylose and amylopectin with polar groups and thus can strongly interact with the amorphous regions of starch matrices (Soest, de Wit, Tournois & Vliegenthart, 1994; Kruiskamp, Smits, Soest & Vliegenthart, 2001). In this study, we believe the decrease of peak frequency from OH mainly indicate an enhanced hydrogen bond network for the whole matrices, though an induction by glycerol which possessing a very low peak frequency from OH cannot be totally excluded.

Amorphous solids are dynamically complex in part because food biomolecules have many modes of molecular mobility, which include all modes of vibrational, rotational, and translational motion that are activated under specified conditions. In rigid solids, many, but certainly not all, of these modes of the molecular mobility are effectively damped by molecular interactions that

may be influenced by matrix composition, temperature, intermolecular forces, etc. For example, at temperatures below T_g, the local mobility within glasses formed by various glucose oligomers (from glucose to maltoheptaose) was systematically dependent upon the structure and mass of the matrix-forming sugar (Tiwari & Ludescher, 2012).

Plasticizers are typically molecules with low molar mass and consequently greater free volume (Chen, Huang, Fang, Yu, Wang, Xiong & Xu, 2010). In high concentration, the addition of plasticizers such as glycerol and other small molecules to starch will lower the glass transition temperature (T_g) and make the material properties more rubber-like (de Graaf, Karman & Janssen, 2003). However, at low concentration in starch, glycerol can act as an antiplasticizer, decreasing elongation at break as well as the moisture and oxygen permeability (Zhang & Han, 2010). These effects may reflect a decrease in the amplitude of localized β-relaxations within the starch matrix (Lourdin, Bizot & Colonna, 1997) due to the formation of hydrogen bond based cross-links between small, mobile plasticizer molecules and polymer side chains (Roussenova, Murith, Alam & Ubbink, 2010). The hydrogen bond network is related to free molecular volume and chemical structure of the matrix molecule (Chen, Huang, Fang, Yu, Wang, Xiong & Xu, 2010) and recent work indicates that molecular mobility is closely related to molecular free volume in carbohydrate/glycerol matrices (Roussenova, Murith, Alam & Ubbink, 2010).

Though hydrogen bonding plays a significant role in modulating molecular mobility, there does not appear to be a rule that can be applied universally. Although it is expected that stronger intermolecular interactions (that is, hydrogen bonds) would decrease mobility, in polymers such as nylons, where β-relaxations can be restricted by hydrogen bonds, the breaking of hydrogen bonds leads to an increase in molecular mobility (Hamada, Iijima & Gcgregor,

1987). However, in small molecule solid matrices and liquids, where the magnitude of van der Waals potential energy per molecule is comparable with that of hydrogen bonds, the size of the molecule is also a significant factor determining molecular mobility (Naoki & Katahira, 1991). In our previous work, we have found that glycerol does not act as an antiplasticizer of amorphous glucose at low concentration (0.1-0.3 mole ratio). This may be because the molecular weight of glucose is similar to glycerol. The glucose matrix also lacks the advanced microstructure found in the potato starch matrix, which makes the interaction of glycerol with starch more complicated than with glucose.

4. Conclusion

Our data indicate that the mobility of the starch matrix increased with temperature and that this increase was influenced in complex ways by the presence of a low molecular weight glycerol plasticizer and by temperature-dependent decreases and glycerol-dependent increases in hydrogen bond strength. For matrices with low glycerol content (<10 wt. %), the decrease in matrix mobility primarily reflected increases in hydrogen bond strength that enhanced intermolecular interaction, increases that damped the effects of an increase in molecular free volume and thus reduced the expected increase of molecular mobility activated by temperature. At high glycerol content, on the other hand, the effects of free volume apparently enabled the thermal activation of modes of vibrational and/or translational motion that increased the matrix molecular mobility, effects that overwhelmed any local increase in hydrogen bond strength. The effect of small molecule additives such as glycerol on the properties of amorphous hydrogen bonded solids is clearly complex and structure specific. The work of elucidating how specific molecular interactions modulate the hydrogen bond network and free volume and consequently

tune the local and global molecular mobility within the matrix will surely be rewarded with increases in the quality and shelf-life of solid foods and pharmaceuticals.

References

Anopchenko, A., Psurek, T., VanderHart, D., Douglas, J. F., Obrzut, J. (2006). Dielectric study of the antiplasticization of trehalose by glycerol. *Physical Review B*, 74, 031501-1-031501-10.

Chen, Z., Huang, W., Fang, P. F., Yu, W., Wang, S. J., Xiong, J., Xu, Y. S. (2010). The hydrogen bond and free volume property of poly (ether-urethane) irradiated by neutron. *Journal of Polymer Science Part B: Polymer Physics*, 48, 381-388.

Das, K., Ray, D., Bandyopadhyay, N. R., Gupta, A., Sengupta, S., Sahoo, S., Mohanty, A., Misra, M. (2010). Preparation and characterization of cross-linked starch/poly(viny alcohol) green films with low moisture absorption. *Industrial & Engineering Chemistry Research*, 49, *2176*-2185.

Dashnau, J. L., Sharp, K. A., Vanderkooi, J. M. (2005). Carbohydrate intramolecular hydrogen bonding cooperativity and its effect on water structure. *Journal of Physical. Chemistry. B*, 109, 24152-24159.

de Graaf, R. A., Karman, A. P., Janssen, L. P. B. (2003). Material properties and glass transition temperatures of different thermoplastic starches after extrusion processing. *Starch*, 55, 80-86.

Duchowicz, R., Ferrer, M. L., Acuña, A. U. (1998). Kinetic spectroscopy of Erythrosin phosphorescence and delayed fluorescence in aqueous solution at room temperature. *Photochemistry and Photobiology*, 68, 494-501.

Dufresne, A., Vignon, M. R. (1998). Improvement of starch film performances using cellulose microfibrils. *Macromolecules*, 31, 2693-2696.

Garcia, M., Martino, M. N., Zaritzky, N. Z. (1999). Edible starch films and coating characterizations: Scanning electron microscopy, water vapor, and gas permeablilites. *Scanning*, 21, 348-353.

Garc á, M. A., Martino, M. N., Zaritzky, N. E. (2000). Lipid addition to improve barrier properties of edible starch-based films and coatings. *Food and Chemical Toxicology*, 65, 941-947.

Hamada, K.; Iijima, T.; Gcgregor, R. (1987). Effects of hydrogen bonds on the mobility of spin probes in nylon films. *Polymer Journal,* 19, 709-717.

Jansson, A., Thuvander, F. (2004). Influence of thickness on the mechanical properties for starch films. *Carbohydrate. Polym*er, 56, 499-503.

Jonhed, A., Andersson, C., J ärnstr öm, L. (2008). Effects of film forming and hydrophobic properties of starches on surface sized packaging paper. *Packaging* Technology Science, 21, 123-135.

Karmas, R., Buera, M. P., Karel, M. (1992). Effect of glass transition on rates of nonenzymatic browning in food systems. *Journal of Agricultural and Food Chemistry***,** 40, 873-879.

Kondo, T. (1997). The assignment of IR absorption bands due to free hydroxyl groups in cellulose. *Cellulose,* 4, 281-292.

Kruiskamp, P. H.; Smits, A. L. M.; Soest, J. J. G.; Vliegenthart, J. F. G. (2001). The influence of plasticizer on molecular organisation in dry amylopection measured by differential scanning calorimetry and solid state nuclear magnetic resonance spectroscopy. *Journal of Industrial Microbiology & Biotechnology*, 26, 90-93.

Lawton, J.W. (1996). Effect of starch type on the properties of starch containing films. *Carbohydrate Polym*er, 29, 203-208.

Lawton, J. W.; Fanta, G. F. (1994). Glycerol-plasticized films prepared from starch-poly (vinyl alcohol) mixtures:Effect of poly(ethylene-co-acrylic acid). *Carbohydrat. Polymer*, 23, 276-280.

Lee, K. M., Armstrong, P. R., Thomasson, J. A., Sui, R., Casada, M., Herrman, T. J. (2010). Development and characterization of food-grade tracers for the global grain tracing and recall system. *Journal of Agriculture and Food Chemistry*, 58, 10945-10957.

Liang, J., Ludescher, R. D. (2012). Influence of Glycerol on the Molecular Mobility and Hydrogen Bond Network in the Glucose-Based Matrix. *Carbohydrate Research*, *361,* 120-126.

Leloup, V. M., Colonna, P., Ring, S. G., Roberts, K., Wells, B. (1992). Microstructure of amylose gels. *Carbohydrate Polymer*, 18, 189-197.

Lettinga, M. P., Zuilhof, H., van Zandvoort, M. A. M. J. (2000). Phosphorescence and fluorescence characterization of fluorescein derivatives immobilized in various polymer matrices. *Physical Chemistry Chemical Physics*, 2, 3697-3707.

Lourdin, D., Bizot, H., Colonna, P. (1997). ‘‘Antiplasticization’’ in starch-glycerol films? *Journal of Applied Polymer Science*, 63, 1047-1053.

Lourdin, D., Coignard, L., Bizot, H., Colonna, P. (1997). Influence of equilibrium relative humidity and plasticizer concentrayion on water content and glass transition of starch materials. *Polymer*, 38, 5401-5406.

Lourdin, D., Ring, S. G., Colonna, P. (1998). Study of plasticizer-oligomer and plasticizer-polymer interactions by dielectric analysis: maltose-glycerol and amylose-glycerol-water systems. *Carbohydrate. Research*, 306, 551-558.

Nack, T. N., Ludescher, R. D. (2006). Molecular mobility and oxygen permeability in amorphous bovine serum albumin films. *Food Biophysics*, 1, 151-162.

Naoki, M.; Katahira, S. (1991). Contribution of hydrogen bonds to apparent molecular mobility in supercooled D-sorbitol and some polyols. *Journal of Physical chemistry*, 95, 431-437.

Orford, P. D., Parker, R., Ring, S. G., Smith, A. C. (1989). Effect of water as a diluent on the glass transition behaviour of malto-oligosaccharides, amylose and amylopectin. *International Journal of Biological Macromolecules*, 11, 91-96.

Otey, F. H., Westhoff, R. W., Doane, W. M. (1987). Starch-Based blown films. 2. *Industrial & Engineering Chemistry Research*, 26, 1659-1663.

Pravinata, L. C., You, Y. M., Ludescher, R. D. (2005). Erythrosin B phosphorescence monitors molecular mobility and dynamic site heyerogeneity in amorphous sucrose. *Biophysical Journal*, 88, 3551-3561.

Richert, R. (2000). Triplet state salvation dynamics: basics and applications. *Journal of Chemical Physics*, 113, 8404-8429.

Romera, C. O., Moraes, J. O., Zoldan, V. C., Pasa, A. A., Laurindo, J. B. (2012). Use of transient and steady-state methods and AFM technique for investigating the water transfer through starch-based films. *Journal of Food Engine*ering, 109, 62-68.

Roussenova, M., Murith, M., Alam, A., Ubbink, J. (2010). Plasticization, antiplasticization, and molecular packing in amorphous carbohydrate-glycerol matrices. *Biomacromolecules*, 11, 3237-3247.

Shirke, S., Takhistov, P., Ludescher, R. D. (2005). Molecular mobility in amorphous maltose and maltitol from phosphorescence of Erythrosin B. *Journal of Physical Chemistry B*, 109, 16119-16126.

Soest, J. J. G.; de Wit, D.; Tournois, H.; Vliegenthart, J. F. G. (1994).The influence of glycerol on structural changes in waxy maize starch as studied by Fourier transform infr-red spectroscopy. *Polymer*, 35, 4722-4727.

Talja, R. A. (2007). Preparation and characterization of potato starch films plasticized with polyols. *Ph.D. dissertation*. Department of Food Technology, University of Helsinki.

Tiwari, R., Ludescher, R. D. (2012), Molecular Mobility in a Homologous Series of Amorphous Glucose Oligomers. *Food Chemistry*, 132, 1814-1821.

Wolkers, W. F., Oldenhof, H., Alberda, M., Hoekstra, F. A. (1998). A Fourier transform infrared microspectroscopy study of sugar glasses: application to anhydrobiotic higher plant cells. *Biochimica et Biophysica Acta*, 1379, 83-96.

Wolkers, W. F., Oliver, A. E., Tablin, F., Crowe, J. H. (2004). A fourier-transform infrared spectroscopy study of sugar glasses. *Carbohydrate Research*, 339, 1077-1085.

You, Y. M., Ludescher, R. D. (2006). Phosphorescence of Erythrosin B as a Robust Probe of Molecular Mobility in Amorphous Solid Sucrose. *Applied Spectroscopy*, 60, 813-819.

You, Y. M., Ludescher, R. D. (2007). The effect of glycerol on molecular mobility in amorphous sucrose detected by phosphorescence of erythrosine B. *Food Biophysics*, 2, 133-145.

Zhang, Y., Han, J. H. (2010). Crystallization of high-amylose starch by the addition of plasticizers at low and intermediate concentrations. *Journal of Food Science*, 75, N8-N16.

Chapter VI: Effect of Additives on Physicochemical Properties in Amorphous starch Matrices

A paper accepted by *Food Chemistry*

Jun Liang, Simon Wang, Richard. D. Ludescher

1. Introduction

The stability and shelf-life of solid foods are often influenced by the physical properties and rates of and chemical reactions in amorphous solid phases. There is a considerable literature on the physico-chemical changes occurring in the primary food ingredients (mainly starches and proteins) during food processing (Burin, Buera, Hough & Chirife, 2002). However, there is a need to understand how minor ingredients (plasticizers, sugars, emulsifiers, antioxidants, etc.) interact with these biopolymers during processing and thus to understand their impact on final product quality.

Starch is both a macronutrient important for nutrition and a versatile food ingredient that is widely used as a texturizer, thickener, gelling agent, adhesive, and moisture-retainer. Much attention has been focused on the influence of small molecules on the properties of starch, including the plasticizing effect of water (Bencz édi, Tomka & Escher, 1998), glycerol (Partanen, Marie, MacNaughtan, Forssell & Farhat, 2004), and sorbitol (Gaudin, Lourdin, Le Botlan, Ilari & Colonna, 1999), and other small molecules (Lourdin, Bizot & Colonna, 1997).

Molecular mobility within amorphous solids is usually manifested by a variety of relaxation processes. Amorphous solids exhibit a primary α or glass transition at T_g which reflects the activation of large-scale molecular motions (α-relations) that underlie the onset of translational motion within the matrix. Relaxations activated at lower temperatures, designated β, γ, etc. from

high to low temperatures and activated at corresponding transition temperatures of T_β, T_γ, etc., correspond to more localized motions within the molecule or progressively smaller segmental motions within polymers. Literature characterizing the glass transition and its corresponding α, as well as β and other relaxations, in amorphous carbohydrates is extensive (Noel, Parker & Ring, 2000; Liang & Ludescher, 2011). However, there have been few studies on the influence of molecular mobility and other physical property changes induced by addition of food additives on the rates of chemical reactions, particularly non-enzymatic browning reaction (NBR) (Karmas, Buera & Karel, 1992; Kawai, Hagiwara, Rikuo & Suzuki, 2005).

NBR is one of the most important chemical reactions affecting food quality during processing and in storage. NBR is an amino-carbonyl reaction whose mechanism and kinetics in real foods, and in models containing reducing sugars and amino compounds as reactants, have been studied extensively (Ajandouz & Puigserver, 1999). The physical state of foods may determine rates of NBR. Solids in foods can exist in a crystalline or amorphous state depending on composition, temperature, and manner of processing. Rapidly frozen or dehydrated food typically contains appreciable amorphous solid (Karmas, Buera & Karel, 1992). The physical stability of amorphous foods is often related to their glass transition temperature (T_g). The glass transition can affect rates of reaction by modulating the diffusion rate of the chemical components; diffusion rate is modulated by the matrix molecular mobility, which is likely to be extremely slow below the glass transition (Lievonen, Laaksonen & Roos, 1998). In an early study correlating the non-enzymatic browning reaction with matrix properties, Karmas and coworkers (Karmas, Buera & Karel, 1992) found that browning rates in different food models were strongly dependent on moisture, temperature, and on the glass transition. Roos and Himberg (Roos &

Himberg, 1994) came to similar conclusions from measurements of non-enzyme browning as a function of water content, water activity, and glass transition at chilling temperatures. However, several studies have stressed the effects of other physical characteristics of the matrix should also be considered. Kawai and coauthors (Kawai, Hagiwara, Rikuo & Suzuki, 2005), for example, have reported faster rates of NBR in amorphous polyvinylpyrrolidone (PVP) than in amorphous trehalose or maltose, despite the much higher T_g value of PVP ; they proposed that hydrogen bonding plays an important role in modulating the browning reaction in glassy matrixes. It is thus important to systemically identify those matrix properties that influence NBR in solid food systems.

In the present study, we have made food models consisting of starch mixtures with either a non-reducing sugar (maltitol, sucrose or trehalose) or methylcellulose (MC) and also containing a reaction system composed of glucose and starch plus lysine. The sugars used are widely applied as sweeteners in food industry and methylcellulose was generally used to improve bread quality by increasing gas retention and preventing loafs from collapsing (Elke & Fabio, 2011). Phosphorescence of Ery B was used to measure the molecular mobility change, while IR was used to detect the hydrogen bond network change induced by adding of food additives in the starch-based amorphous matrix. The rates of NBR were followed by fluorescence in the starch matrix. The influence of food additives on the physical properties and browning reaction in starch matrix was then systemically investigated.

2. Materials and Methods

2.1. Chemicals

Potato starch, maltitol, sucrose, trehalose, methylcellulose (MC), glucose, lysine and Ery B were purchased from Sigma-Aldrich (St. Louis, MO). The labeling extent of methycellulose is around 1.6-1.9 mole methoxy per mole cellulose. Ethanol and acetone were purchased from Fisher Scientific (Pittsburgh, PA). Terg-A-Zyme was purchased from Alconox, Inc. (NY). P2O5 was purchased from Drierite (Xenia, OH).

2.2. Sample Preparation

Two and one-half g of potato starch were dissolved in 50 ml deionized water. The starch solution was boiled on a stir plate (Nuova, Cologna Veneta, Italy) for at least 10 min to ensure that the starch was dissolved and denatured. The solution was then cooled to room temperature while being stirred. Maltitol, sucrose, trehalose or methylcellulose (MC) were added to the starch solution from a 1% stock solution to a final weight ratio to starch of 7/93 or 7 wt. %.

Rapid dehydrating of gelatinized potato starch solution can avoid crystallization (Karmas, Buera & Karel, 1992; Talja, 2007), we prepared starch Ery B films using method of Talja (Talja, 2007) with slight modifications. Ery B in a disodium salt form was dissolved in deionized water to prepare a 10 mM stock solution. An aliquot from this solution was added to starch solution to obtain a molar ratio of around $1:10^4$ of the dye/glucose unit in the starch. For luminescence experiments, starch-sugar or starch-MC mixture was prepared from a solution containing Ery B while being stirred on a stir plate for at least half hour to ensure that sugar or MC was totally blended with starch. To prepare starch-based films, 15 µl of starch/sugar or starch/MC solution at

room temperature was spread on approximately one third of a quartz slide (30 × 13.5 × 0.6 mm, custom made by NSG Precision Cells, Farmingdale, NY). Then the slides were placed under a gentle warm air stream generated by an air gun (Model 201 A, Master Appliance Corp., Racine, WI), and the samples were put at a distance of around 30 cm from the muzzle to avoid being overheated. Therefore, most of the water in the films was evaporated within 5 minutes. The transparent and homogeneous films on slides were stored at room temperature for at least 1 week under air in equilibrium with P_2O_5 in order to maintain 0% RH and protected from light to prevent any photobleaching of Ery B. The desiccants were refreshed as necessary. Before use, the slides were soaked in Terg-A-Zyme soap solution over 24 h to remove surface impurities, then washed with deionized water. Finally, the slides were rinsed with ethanol and dried with acetone.

For studying the rate of non-enzymatic browning, starch-sugar or starch-MC system was prepared using the same method used to prepare slides for luminescence except that Ery B was replaced by glucose and lysine added from a stock solution of 10% w/w to the film forming solution, both at a final concentration of 1% w/w in the dry films.

2.3. Phosphorescence Measurements and Analysis

All measurements were conducted at least in triplicate. Data were collected from 100 to −10 ℃ in all experiments. High purity nitrogen was routed into the sample compartment and directly into the quartz fluorescence cuvette that held the slide. The cuvette was flushed for at least 30 min before measurement. The cuvette was capped with a lid having inlet and outlet ports for the gas line, so that all experiments were performed at constant pressure. Each reported intensity decay observation was the average of 50 cycles. For each cycle, data were collected

from a single flash with a delay of 0.04 ms, a 0.05 ms gate time, and a total decay time of 10.0 ms. Phosphorescence and delayed fluorescence emission scans were collected over a range from 540 to 800 nm with an excitation wavelength of 520 nm. The excitation and emission monochromators were both set at 20 nm band pass. Each data point (collected at 1 nm intervals with a 0.1 s average time) was collected from a single flash with 0.2 ms delay and 5 ms gate time.

For lifetime measurement, because intensity decays were non-exponential, a stretched exponential function was selected to analyze the intensity decays:

$$I\,(t) = I\,(0)\,\exp\,[-(t/\tau)^{\beta}] + \text{constant} \qquad (1)$$

where $I(0)$ is the initial intensity; τ is the stretched exponential lifetime; and β is an exponent varying from 0 to 1 that characterizes the lifetime distribution. The use of a stretched exponential model provides analysis of a continuous distribution of lifetime, which is appropriate for describing a complex glass possessing a distribution of relaxation time for dynamic molecular processes. The smaller the β value, the more non-exponential are the intensity decays and the broader the distribution of lifetimes (Duchowicz, Ferrer & Acuña, 1998).

The energy of the emission maximum and bandwidth of the emission band were determined by using a log-normal line shape function to fit both the delayed fluorescence and phosphorescence.

$$I(\nu) = I_0\,\exp\left\{-\ln(2)\left(\frac{ln\left[1+2b\left(\nu-\nu_p\right)\right]/\Delta}{b}\right)^2\right\} \qquad (2)$$

where I_0 is the maximum emission intensity; ν_p is the peak frequency (in cm^{-1}); Δ is a linewidth parameter; and b is an asymmetry parameter. The bandwidth Γ (full width at half maximum) was calculated according to the following equation:

$$\Gamma = \Delta\left[\frac{\sinh(b)}{b}\right] \quad (3)$$

Delayed luminescence spectra collected at 540-750 nm were fit using a sum of log-normal functions for delayed fluorescence ($I_{DF}(\nu)$) and phosphorescence ($I_P(\nu)$). Each emission band was analyzed for independent fitting parameters using Eq. 3.

The phosphorescence lifetimes were used to calculate the rate constants associated with the various processes that depopulate the triplet state. Our analysis of the delayed emission was similar to the photophysical scheme for Ery B outlined by Duchowicz and coworkers (Duchowicz, Ferrer, & Acuña, 1998). using a slightly different nomenclature. The measured phosphorescence lifetime (τ) is the inverse sum of all possible de-excitation rates ($k_{P)}$ for the triplet state T_1

$$1/\tau = k_P = k_{RP} + k_{TS1} + k_{TS0} + k_Q[O_2] \quad (4)$$

where k_P is the total decay rate; k_{RP} is the rate of radiative decay to the ground state; k_{TS1} is the rate of reverse intersystem crossing to S_1; k_{TS0} is the rate of intersystem crossing to the singlet manifold followed by vibrational relaxation to S_0; $k_Q[O_2]$ is the rate of oxygen quenching (assumed negligible in the absence of oxygen). The radiative decay rate has a value of 41 s^{-1} for Ery B (Shirke & Ludescher, 2005).

Reverse intersystem crossing is a thermally activated process with a rate that is exponentially dependent on the energy gap ΔE_{TS} between T_1 and S_1 (Shirke & Ludescher, 2005):

$$k_{TS1}(T) = k^{o}_{TS1}\exp(-\Delta E_{TS}/RT) \quad (5)$$

The log of the ratio of intensity of delay fluorescence (I_{DF}) to phosphorescence (I_P), where I_{DF} and I_P are determined from analysis of emission spectra using the log-normal function (Eq. 3), is proportional to the rate of reverse intersystem crossing (Shirke & Ludescher, 2005). A plot of $\ln(I_{DF}/I_P)$ versus 1/T has a slope of $-\Delta E_{TS}/R$. Although the value of ΔE_{TS} for Ery B is influenced by the surrounding solvent (matrix), the values measured in the different samples were not different. The rate $k_{TS1}(T)$ can be estimated using an estimated value for k°_{TS1} and the value of ΔE_{TS} determined from such thermal analysis. We estimated the maximum possible value for k^{o}_{TS1} in glucose/glycerol by assuming that $k^{o}_{TS1}(T)$ can not result in values for k_{TS0} decreasing with temperature, thus obtaining the minimum possible values of $k^{o}_{TS0}(T)$. The value of k^{o}_{TS1} used in this study was 1.5×10^{7} s^{-1}.

One of the non-radiative decay routes is through intersystem crossing to the ground state S_0. The decay rate k_{TS0} reflects the rate of collisional quenching of probe due to both internal and external factors. We assume that the term k_{TS0} primarily reflects the external environmental factors since the self-collisional quenching among probe molecules can be neglected within the extremely viscous amorphous solid. The temperature–dependent term k_{TS0} can be calculated from the measured lifetime using Eq 5 using the known value of k_{RP} and the estimated values of $k_{TS1}(T)$.

2.4. Attenuated Total Reflectance Fourier Transform Infrared (ATR-FTIR) Spectroscopy

The ATR-FTIR spectra were collected by using a Thermal Nicolet Nexus 670 FT-IR spectrometer (Thermo Fisher Scientific Inc., Waltham, MA) equipped with a Smart ARK thermal accessory and analyzed using the associated EZ-OMNIC software. Each spectrum was the average of 512 scans with 4 cm^{-1} resolution in an atmosphere of air equilibrate against P_2O_5 to minimize the interference of moisture under ambient condition. Dry starch films mixed with sugar or MC were spread on the heating plate and then the measurements were conducted in a temperature range from 100 down to 30 ℃.

2.5. Non-enzymatic Browning Reaction

All luminescence measurements were made on a Cary Eclipse spectrophotometer (Varian Instruments, Walnut Creek, CA) equipped with a temperature controller and multicell holder. For studying the rate of the browning reaction, samples on slides were heated to either 80 or 100 ℃. The extent of browning was determined spectrophotometrically from the rate of increase in fluorescence intensity at 440 nm with excitation at 350 nm (Matiacevich, Santagapita & Buera, 2005), using a band pass of 20 nm for both excitation and emission. The initial 150/80 minutes of the curves for fluorescence intensity increase in 80 /100 ^{o}C, normalized to the intensity upon completion of the reaction to account for differences between slides, were fit to a zero-order kinetic model using Origin 7.0 software.

Figure 34

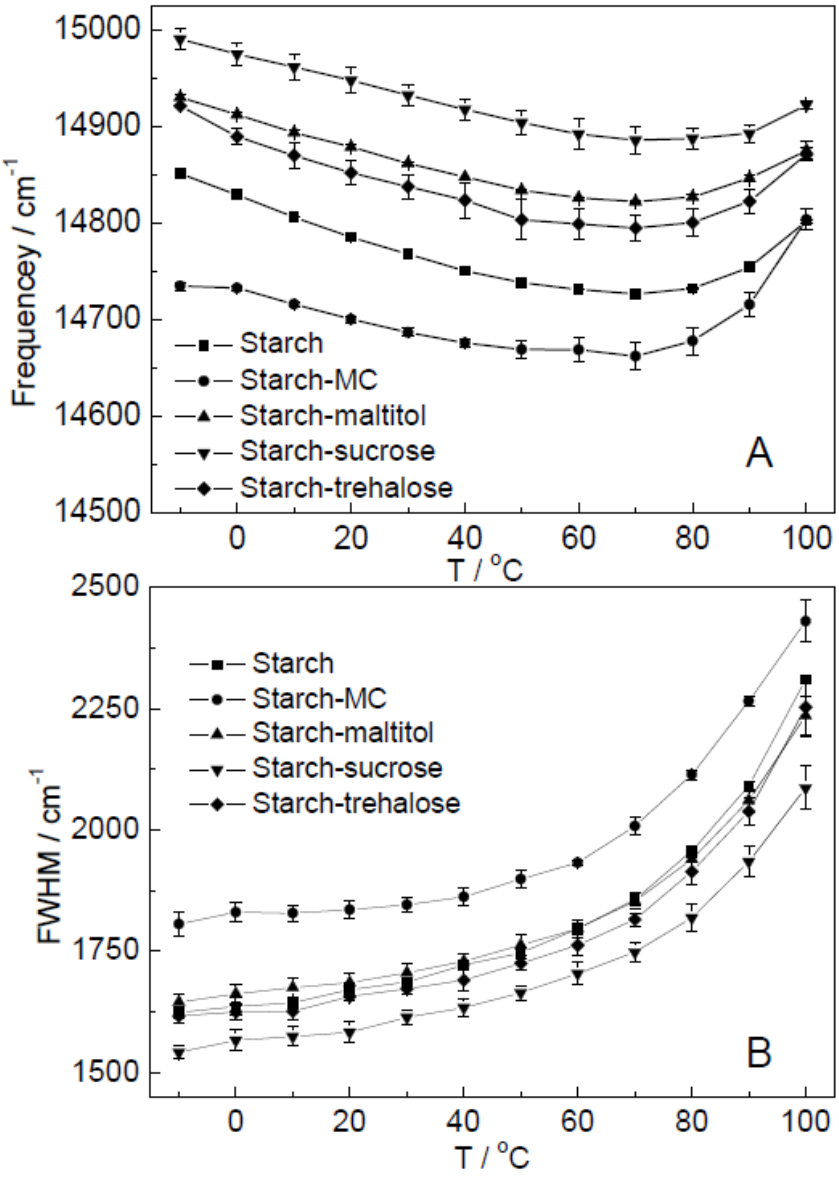

Figure 34: A: Peak frequency for phosphorescence emission from Ery B in amorphous starch-based films with sugars or methylcellulose plotted as a function of Temperature; B: Band width (FWHM) for phosphorescence emission from Ery B plotted as a function of temperature.

3. Results and Discussion

3.1. Delayed emission spectra

It has been seen clearly in previous studies that amylose and amylopectin are arranged in strands that form the network in both starch gels and more compact starch films (Leloup, Colonna, Ring, Roberts & Wells, 1992). In the rapidly dehydrated films, those strands are further connected with additives and form into amorphous solid (Karmas, Buera & Karel, 1992; Talja, 2007). Phosphorescence emission from the triplet probe Ery B provides a sensitive indicator of local matrix mobility in amorphous biomaterials (Shirke & Ludescher, 2005; Liang & Ludescher, 2011). The delayed emission spectra of Ery B in amorphous starch-based films displayed a longer wavelength phosphorescence band (maximum ~690 nm) and a shorter wavelength delayed fluorescence band (maximum ~555 nm). Spectra in all starch-based matrices collected over a temperature range from −10 to 100°C showed a decrease in phosphorescence (I_P) and an increase in delayed fluorescence (I_{DF}) intensity with increasing temperature as expected for this probe (data not shown). The peak frequency (ν_P) and bandwidth (Γ) for phosphorescence emission, determined by fitting emission spectra to a log-normal line shape function (Eq. 3), are plotted in Figure 34A and 34B, respectively.

The peak frequency of the phosphorescence, a measure of the average energy of emission, is modulated by the extent of dipolar relaxation around the probe during the lifetime of the triplet state (Liang & Ludescher, 2011). In these matrixes, this dipolar relaxation must involve OH groups on starch (glucose monomers), or on additive (sugar or MC). In matrixes of comparable polarity, a lower emission energy reflects an increase in the average extent of dipolar relaxation during the lifetime of the excited state; it thus reflects an increase in the rate of dipolar relaxation

compared to the rate of emission. At all temperatures monitored, the peak frequencies followed the rank order starch-MC << starch < starch-trehalose ≤ starch-maltitol < starch-sucrose. Since the rank order of phosphorescence lifetimes (Figure 2A) followed the same progression, these emission frequency data indicate that the dipolar relaxation rates in these matrixes followed the rank order starch-MC >> starch > starch-trehalose ≥ starch-maltitol > starch-sucrose. Given the small amount of additive (7 wt. %) compared to starch (93 wt. %) and the likelihood that the probe is randomly distributed throughout the matrix, the relaxation rates probably reflect the behavior of the starch molecules in the matrix and thus are indicative of the dynamic effect of the additives on the starch matrix.

In all matrices studied the emission frequency decreased with increasing temperature below 70 ℃ and increased with temperature above. The average extent of dipolar relaxation around the excited state thus increased with temperature below and decreased with temperature above 70 ℃. Such an increase with temperature is not typically seen in similar studies using this probe in either sugar or protein solid matrixes or in mixtures. Given that the lifetime trend is unchanged at 70 ℃ (see Fig. 34A below), the decrease in extent of relaxation probably reflects a decrease in the rate of dipolar relaxation above 70 ℃, perhaps due to a change in the local structure of the starch matrix.

The phosphorescence bandwidth provides a measure of the range of energetically distinct environments that the probe samples within the amorphous matrix (Liang & Ludescher, 2011). The rank order of bandwidths is starch-MC >> starch > starch-maltitol ≥ starch-trehalose > starch-sucrose indicating a comparable ranking of energetic heterogeneity within these matrixes (Fig. 34B). Since dipolar interactions are the primary determinate of probe energy within the

hydrogen bonding starch matrix, this ordering indicates a greater distribution of hydrogen bonding interactions in starch-MC than in the starch or starch-sugar matrixes. Given that the rank ordering of energetic heterogeneity reflects the rank ordering of dipolar relaxation rates, it is likely that the energetic heterogeneity reflects (at least in part) the heterogeneity in dipolar relaxation rates. The bandwidths increased for all samples over the entire temperature range. This increase was gradual at low and intermediate temperatures and more dramatic at high temperature.

Figure 35

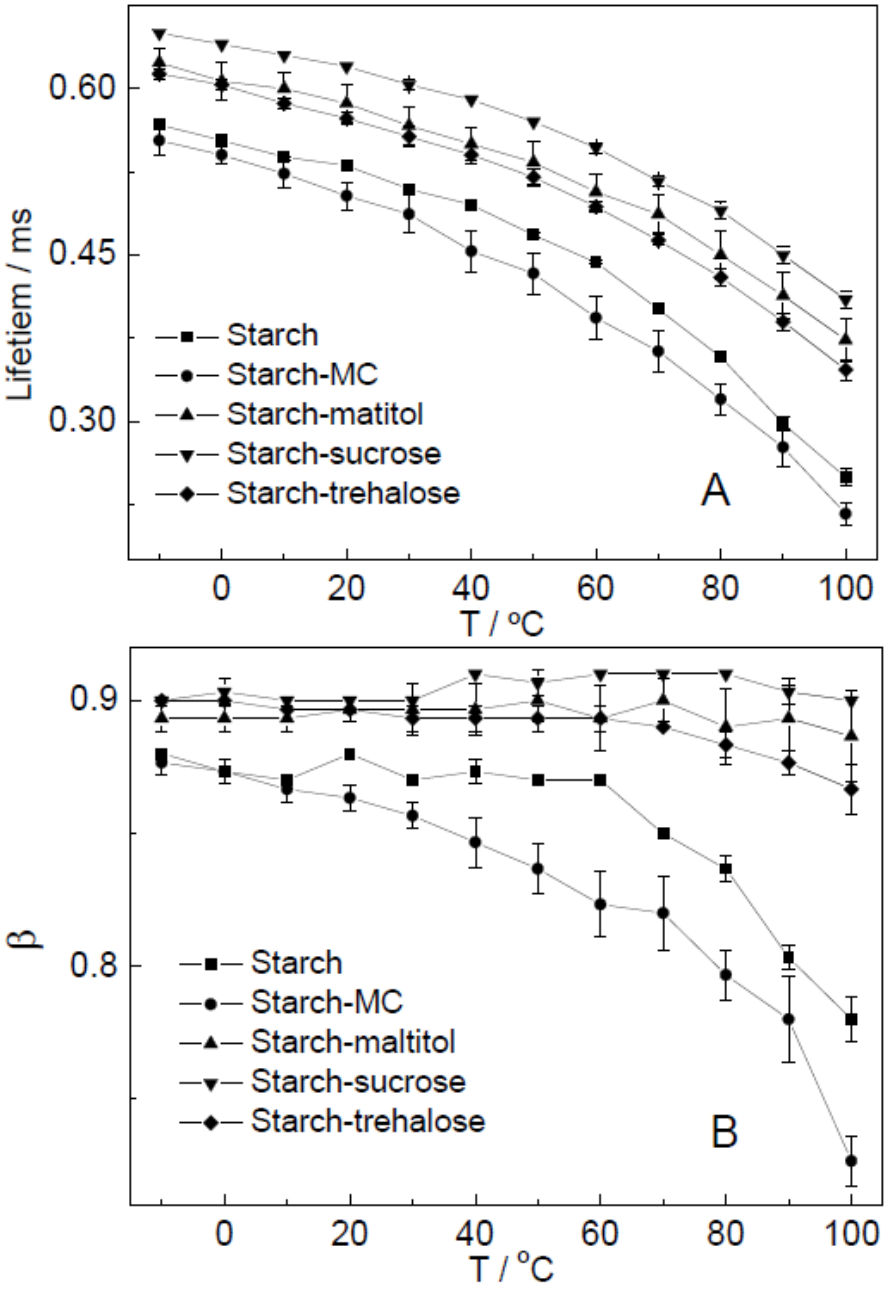

Figure 35: A: Temperature dependence of lifetime obtained from fits to a stretched exponential decay model of the intensity decay of Ery B in amorphous starch-based matrices with sugars or methylcellulose; B: Stretching exponent β obtained from fits to a stretched exponential decay model of the intensity decay of Ery B.

3.2. Emission lifetimes

The phosphorescence emission intensity decays from Ery B in films under N_2 were collected from −10 to 100°C (data not shown). All intensity decay transients were well fit using a stretched exponential decay model (Eq. 1) in which the lifetime τ and stretching exponent β were the fit parameters; R^2 was ≥ 0.995 for all fits. The lifetimes and stretching exponents are plotted as a function of temperature in Fig 35A & 35B, respectively. The lifetimes displayed a similar thermal response in all matrixes—a systematic and monotonic decrease with temperature—indicating that the non-radiative decay rates were thermally activated. The lifetimes for the starch-MC matrix were much shorter than for the starch and starch-sugar matrices at all temperatures; the rank order of lifetimes for all matrixes was starch-MC < starch < starch-trehalose ≤ starch-maltitol < starch-sucrose.

The stretching exponent β is a measure of the width of the distribution of lifetimes required to adequately fit the phosphorescence intensity decays; it is thus an indicator of the dynamic heterogeneity of the matrix. A value of 1.0 indicates an infinitely narrow distribution (a single exponential intensity decay) and lower values indicate progressively wider distributions (Obrzut, Anopchenko, Douglas & Rust, 2010). The value of β decreased significantly with temperature in pure starch and in starch-MC but not in starch-sugar matrixes. It thus appeared that the extent of dynamic heterogeneity of starch and starch-MC increased with temperature. The addition of sugars not only decreased the dynamic heterogeneity of the starch matrix, but also removed any effect of temperature on this dynamic heterogeneity.

Figure 36

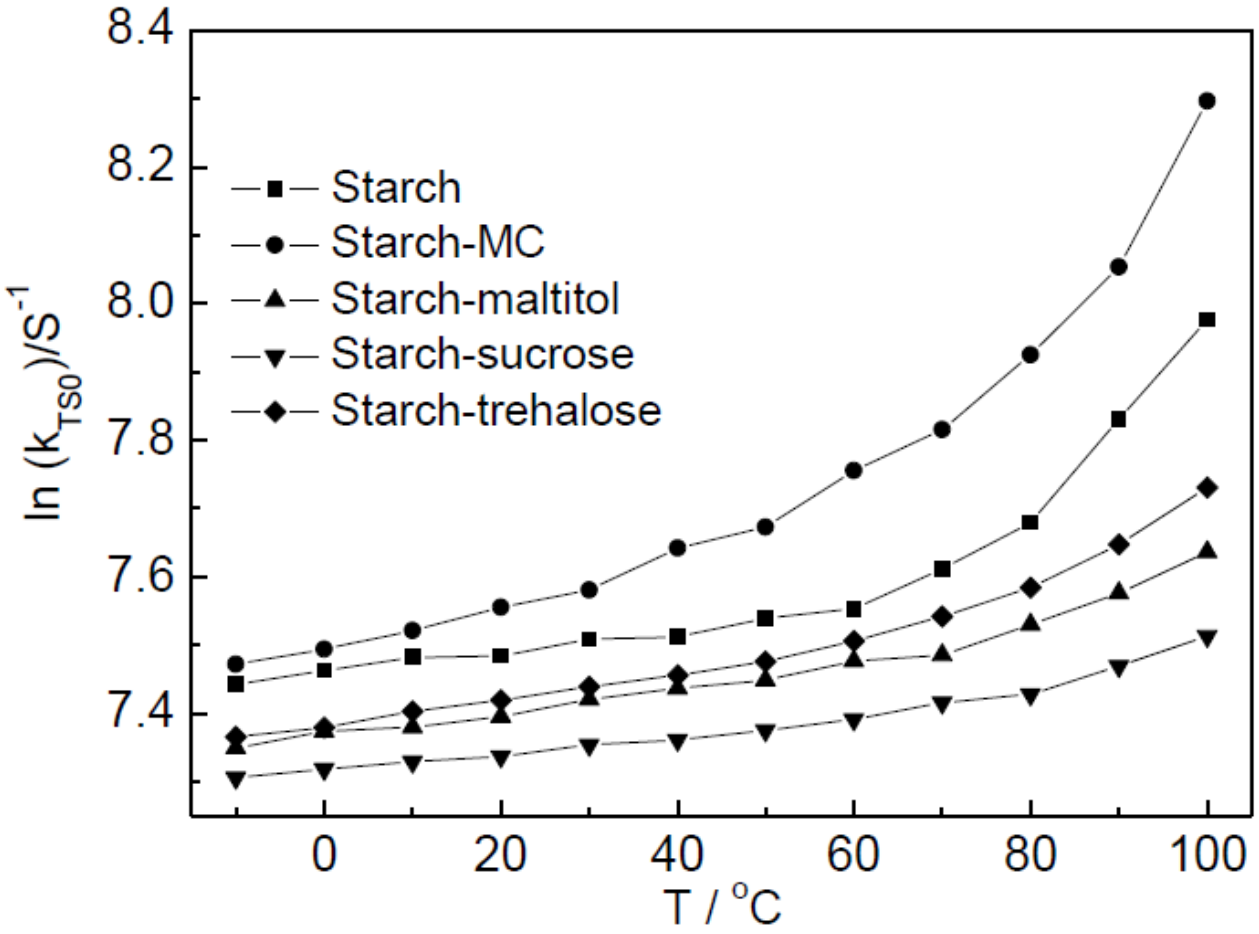

Figure 36: Arrhenius plot of the effect of temperature on the rate constant for nonradioactive decay of triplet T_1 state to S_0 (k_{TS0}). Data were calculated from the lifetime data of Figure 35 A.

In the absence of oxygen, the phosphorescence emission rate k_p (= 1/τ) is the sum of rates for radiative emission (k_{RP}), reverse intersystem crossing $k_{TS1,}$ and collisional quenching k_{TS0}. Since k_{RP} is constant at 41 s^{-1} (Duchowicz, Ferrer & Acuña, 1998), the increase in k_p (decrease in lifetime) with temperature reflects increases in k_{TS1} and k_{TS0}. As described in Materials and Methods, k_{TS1} follows Arrhenius kinetics while k_{TS0} monitors the complex effect of temperature on the mobility of the amorphous matrix (Shirke & Ludescher, 2005; Liang & Ludescher, 2011). We calculated the variation of k_{TS0} with temperature using Eq. 5, the measured value of k_{RP}, and estimates of k_{TS1}; these values are plotted as $\ln(k_{TS0})$ versus 1/T for all samples in Figure 36.

The calculated collisional quenching constants varied systematically with matrix composition; the rank order for k_{TS0} at all temperatures was starch-MC >> starch > starch-trehalose ≥ starch-maltitol > starch-sucrose. The values of $\ln(k_{TS0})$ for all matrixes increased gradually, linearly, and in parallel at low temperature (from −10 to ~40°C) and displayed upward curvature at higher temperature; this curvature began above ~40 ℃ in starch-MC, above ~60 ℃ in starch, and at higher temperatures in the starch-sugar matrixes. In the context of an Arrhenius analysis, the magnitude of the collisional quenching constant is related to the frequency of matrix motions that dissipate the excited triplet state energy and its temperature-dependence proportional to the activation energy for these matrix motions. The activation energy for starch matrix motions was thus constant at low temperature and unaffected by the presence of MC or sugar. At higher temperature, however, the matrix activation energy increased in an additive-dependent manner. The rank order of activation energies at high temperature was also starch-MC >> starch > starch-trehalose ≥ starch-maltitol > starch-sucrose; this was also the rank order of frequency factors.

The temperature-dependence of ln(k_{TS0}) in starch and starch mixtures was similar to that seen in other complex carbohydrates such as malto-oligosaccharides (You & Ludescher, 2010), where upward curvature was seen at temperatures far below T_g, but not to that seen in simple sugars such as glucose or sucrose (Pravinata, You & Ludescher, 2005). In oligosaccharides, there is appreciable mobility within the glass due to local relaxations that reflect the many possible internal modes of segmental motion. It thus appears that the polymer MC enhances while the sugars trehalose, maltitol, and sucrose suppress these local relaxations within the starch matrix. We have observed similar dynamic effects of additives in amorphous solid sugars: polymers such as gelatin, amylose or xanthan gum enhance local matrix mobility of sucrose (You & Ludescher, 2008;You & Ludescher, 2009; You & Ludescher, 2011) while small polyols such as glycerol, maltitol and lactitol suppress local mobility in sucrose, maltose or lactose, respectively (Shirke, Takhistov & Ludescher, 2005). Suppression of local β-type relaxations is thought to be involved in the mechanism of anti-plasticization (Lourdin, Bizot & Colonna, 1997; Obrzut, Anopchenko, Douglas & Rust, 2010). The T_g's of maltitol, sucrose, trehalose and methylcellulose are 39 ^oC (Roos, 1993), 64 ^oC (Gabarra & Hartel, 2008), 120 ^oC (Sussich & Cesàro, 2008) and 184-197 ^oC (Gómez-Carracedo, Alvarez-Lorenzo, Gómez-Amoza & Concheiro, 2003) respectively. In this study, it is shown that for the starch mixed with sugars, k_{TS0} for starch with sucrose is lower than that for starch with matitol, in accord with the principle that the solid with a higher T_g possess a more rigid matrix. For starch-trehalose matrix, it is interesting to find that its k_{TS0} is the highest among the matrices with sugar, though the T_g of trehalose is highest among the sugar additives. We will explain this in the following section.

Figure 37

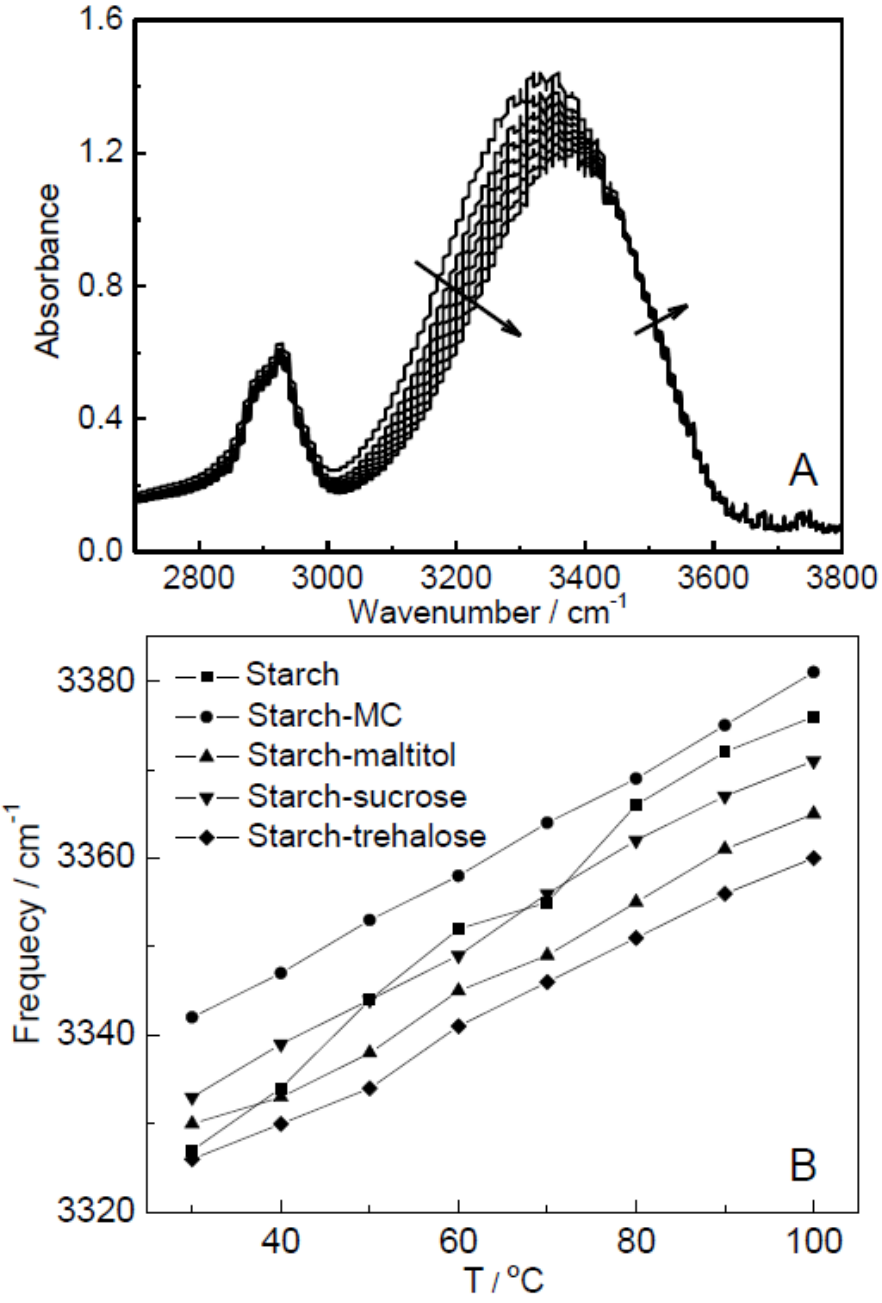

Figure 37: A: FTIR spectra of starch-sucrose matrix as a function of temperature. Orientation of arrow indicates an increase in temperature from 30 to 100 ℃. B: Peak frequency for FTIR spectra above 3000 cm^{-1} as a function of temperature in starch/sucrose matrices.

3.3. Attenuated Total Reflectance Fourier Transform Infrared (ATR-FTIR) Spectroscopy

Hydrogen bonds are the dominant intermolecular interaction among amorphous carbohydrates and consequently modulate molecular motions within the matrix. Hydroxyl groups within the solid carbohydrate can be either free, not involved in hydrogen bonds or associated, hydrogen bonded to other hydroxyl groups (Liang. Corradini & Ludescher, 2014). The frequency of the OH stretch vibration in the region 3000-3600 cm^{-1} has been shown to be sensitive to the transformation between free and associated hydroxyls (Lutz & van der Maas, 1994) and thus provides an indicator of hydrogen bond strength in amorphous solid (Wolkers, Oliver, Tablin & Crowe, 2004). A higher OH stretching frequency indicates more free hydroxyls (Lutz & van der Maas, 1994), and thus presumably a more poorly packed hydrogen-bonded network.

The OH stretch shifted to higher frequency with increase in temperature in all samples, as illustrated by the spectra of starch-sucrose in Fig. 37A; the shift was accompanied by a decrease in the absorption bandwidth. The red shift in peak frequency was linear with temperature (Fig. 37B) in all starch-based matrices. The OH stretch frequency in the order starch-trehalose < starch-maltitol < starch-sucrose < starch-MC; the frequency in pure starch was comparable to starch-trehalose at low temperature and starch-MC at high. The rank order of network bonding in the matrixes with additives thus varied with temperature and followed an order of starch-MC < starch-sucrose < starch-maltitol < starch-trehalose.

For the starch-based matrices containing sugars, the hydrogen bond network in the starch matrix with maltitol, a smaller molecule possessing more free molecular volume which means that the hydroxyl in maltitol which is easy to form hydrogen bonds (Roussenova, Murith, Alam, Ubbink, 2010), was stronger than that with sucrose. However, the strongest hydrogen bond

network in starch-trehalose may reflect distinctive properties of trehalose. According to Phillips (Phillips, 2006), trehalose can form a kind of compact tandem sandwich structure in which the H atoms complete the covalent intramolecular network, so that the intermolecular hydrogen bonds can attach to all the carbon and oxygen atoms within this structure, except for the bridging oxygen. Thus, the intermolecular hydrogen bond network in this structure is very strong, whereas the hydrogen bond with molecules outside this structure is relatively weak. This conjecture is in accord with our results: though the molecular weight of trehalose is bigger than that of maltitol, the hydrogen bond network in the starch matrix with trehalose is much stronger due to the strong intermolecular hydrogen bond network among the trehalose molecules. Besides, the molecular mobility in the starch-trehalose matrix is the highest among the starch-sugar systems (Fig. 36) due to the comparatively weak interaction between trehalose and starch resulting from the structure of trehalose. The observation that the molecular mobility in the amorphous solids studied was not solely determined by T_g can also be found in the case of starch-methylcellulose matrix. Though the T_g of MC is the highest among the additives and it's presumable that T_g of starch-MC matrix is the highest among the homogenous mixture matrices (Gordon, Taylor, 1952), its molecular mobility is also the highest due to the limited restriction on the starch molecules from hydrogen bond network from added MC (Fig. 36).

Figure 38

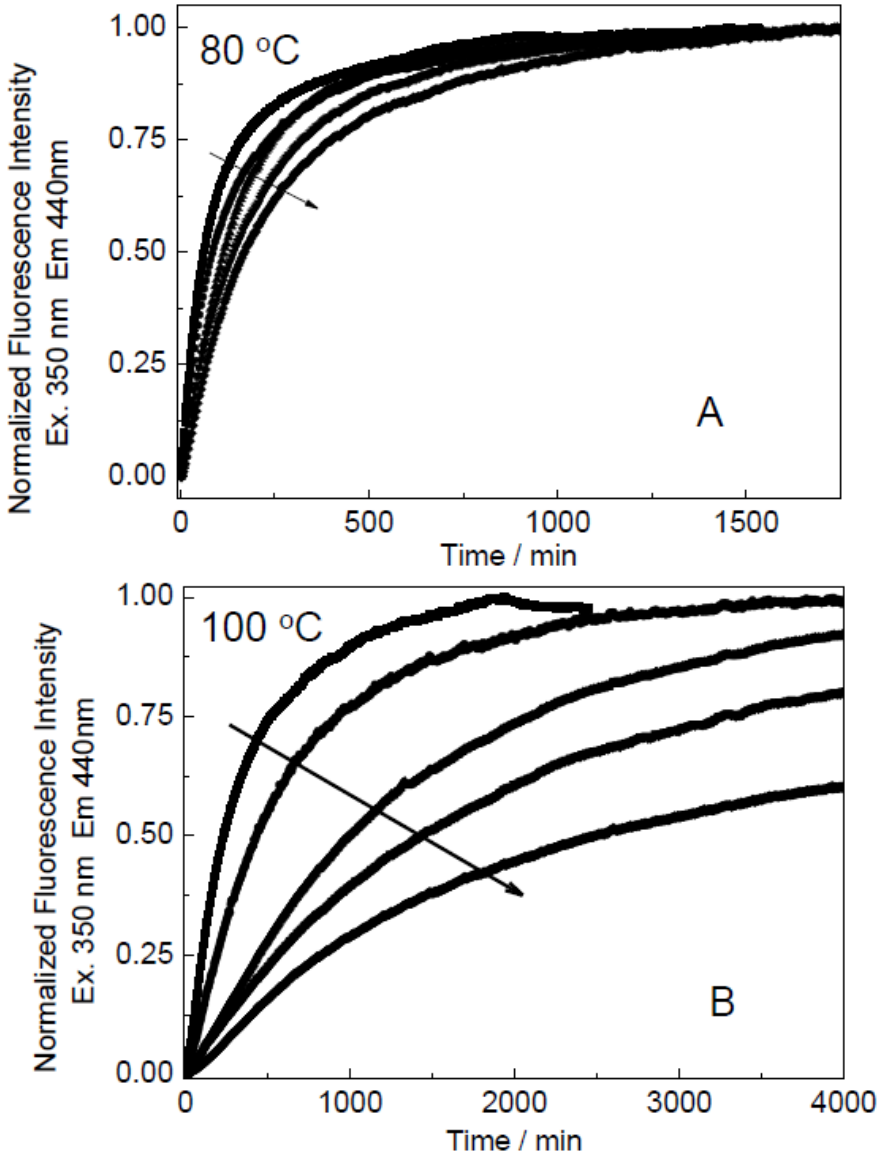

Figure 38: The normalized fluorescence intensity values at 80 ℃ (A) and 100 ℃ (B) from fluorescent compounds. Orientation of arrow: starch, starch-methylcellulose (MC), starch-maltitol, starch-sucrose, starch-trehalose.

Table 1

	Rate constants ($\times 10^{-3}$ min^{-1})	
	80 °C	100 °C
Starch	2.47±0.01	8.99±0.12
Starch-MC	1.37±0.02	7.69±0.18
Starch-maltitol	0.57±0.007	4.93±0.04
Starch-sucrose	0.47±0.008	4.56±0.01
Starch-trehalose	0.24±0.005	3.82±0.03

3.4. Non-enzymatic Browning Reaction

In this study, glucose and lysine were added to the starch-based matrixes to a final content of 1% to serve as reactants to enhance the browning reaction. The kinetics of the browning reaction were monitored by the increase in emission intensity with time due to formation of fluorescent compounds; fluorescence intensity is considered a valid indicator of the browning reaction under favorable conditions such as high temperature (Matiacevich, Santagapita & Buera, 2005). The browning reaction between starch and lysine was significant while for MC and lysine it is negligible based on preliminary fluorescence tests. Fluorescence kinetic traces at 80 ℃ and 100 ℃ are shown in Fig. 38 for starch matrixes with starch, starch-MC, starch-maltitol, starch-sucrose, and starch-trehalose.

The increase in fluorescence intensity in the systems studied here was fit to a zero-order kinetic model for the initial 150 minutes and rate constants for increase of fluorescence (emission at 440 nm and excitation at 350 nm) in the conditional temperature of 80 ^{o}C and 100 ^{o}C were determined; the R^2 value was ≥ 0.99 for all fits. These rate constants are summarized in Table 1. Based upon extrapolation of the glass transition temperature of malto-oligosaccharides with different degrees of polymerization, the T_g of dry amylopectin and amylose was estimated to be approximately 230 ℃ (Orford, Parker, Ring & Smith, 1989). Thus these values represent the rates of NBR in a glassy state considering that starch constitute 91% of matrix mass.

It is evident that rates of the browning reaction are slow at temperatures below T_g, due to slow reactant diffusion (Karmas, Buera & Karel, 1992). However, the rates in these mixed starch matrixes were significant below T_g, particularly for starch and starch-MC. The rates of NBR in the starch–sugar matrices varied inversely with the T_g's of added food additives. The NBR rate in

starch matrix was the highest, which could be expected given that the concentration of starch (98%), one of the reactants, was higher than its concentration in any of other mixed matrices (91%). However, the NBR rate for the starch-MC matrix was faster than that in any of the starch-sugar matrices, despite the additive with the highest T_g was added.

Non-enzymatic browning is probably the best studied example of diffusion-controlled chemical reactions in food systems. It is a good model for studying the effects of glass transition, molecular mobility, hydrogen bond network and interactions of compounds on the reaction kinetics, because the reaction mechanism includes several condensation steps that require the diffusion and collision of reactants (Namiki, 1988). Except for the matrix with trehalose, the rank for the rates of NBR in the mixed matrices consistents with the reverse rank for molecular mobility, which is greatly influenced by hydrogen bond strength as noted above. The region where the hydrogen bonds mainly distribute in the tandem trehalose sandwich structure can strongly trap each trehalose molecule by intensity hydrogen bond network. It can be speculated that small molecule like glucose could be grasped by trehalose (Karmas, Buera & Karel, 1992) and thus the interaction between lysine and glucose can be greatly hindered by trehalose, which will certainly have a restraining effect on the browning reaction. Thus, the rate of NBR inside the starch-trehalose matrix is the lowest even though the matrix mobility is the highest among the starch-sugar systems. The physical properties inside the food solid in the present work, e.g. molecular mobility, hydrogen bond network and interactions among the compounds, in fact influence the browning reaction in different ways.

4. Conclusion

We have studied the physical properties and the rate of NBR in food systems with compositions appropriate for daily application. The addition of sugar or methylcellulose considerably changed the hydrogen bond network, and further modulated the matrix mobility in the starch-based matrices. At temperatures below T_g, starch-based amorphous solids with sugar shows a decreased mobility compared with that containing methylcellulose. As for the samples with sugars, the matrix mobility was suggested to be determined by the molecular weight and T_g of the added sugar and the interaction among the compounds. Although the fundamental concept of glass transition is widely accepted, it has not been fully applied to research on NBR in amorphous solids. The rate of NBR for lysine with glucose or starch seems to be determined by matrix mobility, whereas interaction between the compounds also plays an important role.

References

Ajandouz, E. H., Puigserver, A. (1999). Nonenzymatic browning reaction of essential amino acids: effect of pH on caramelization and maillard reaction kinetics. *Journal of Agricultural and Food Chemistry*, 47, 1786-1793.

Bencz ́edi, D., Tomka, I., Escher, F. (1998). Thermodynamics of amorphous starch-water systems 1: volume fluctuations. *Macromolecules*, 31, 3055-3061.

Burin, L., Buera, M. P., Hough, G., Chirife, J. (2002). Thermal resistance of β-galactosidase in dehydrated dairy model systems as affected by physical and chemical changes. *Food Chemistry*, 76, 423-430.

DUCHOWICZ, R., FERRER, M. L., ACUÑA, A. U. (1998). KINETIC SPECTROSCOPY OF ERYTHROSINE PHOSPHORESCENCE AND DELAYED FLUORESCENCE IN AQUEOUS SOLUTION AT ROOM TEMPERATURE. *JOURNAL OF PHOTOCHEMISTRY AND PHOTOBIOLOGY*, 68, 494-501.

Elke, A., Fabio, D. B. (2011). Gluten-Free Cereal Products and Beverages (pp. 109), London, Elsevier.

Gabarra, P., Hartel, R. W. (2008).Corn syrup solids and their saccharide fractions affect crystallization of amorphous sucrose. *Journal of Food Science*, 63, 523-529.

Gaudin, S., Lourdin, D., Le Botlan, D, Ilari, J. L., Colonna, P. (1999). Plasticization and mobility in starch-sorbitol films. *Journal of Cereal Sci*ence, 29, 273–284.

Gómez-Carracedo, A., Alvarez-Lorenzo, C., Gómez-Amoza, J. L., Concheiro, A. (2003). Chemical structure and glass transition temperature of non-ionic cellulose ethers DSC, TMDSC oscillatory rheometry study. *Journal of Thermal Analysis and Calorimetry*, 73, 587-596.

Gordon, M., Taylor, J. S. (1952). Ideal copolymers and the second-order transitions of synthetic rubbers. 1. Non-crystalline copolymers. *Journal of applied chemistry*, 2, 493-500.

Karmas, R., Buera, M. P., Karel, M. (1992). Effect of glass transition on rates of nonenzymatic browning in food systems. *Journal of Agricultural and Food Chemistry***,** 40, 873-879.

Kawai, K., Hagiwara, T., Takai, R., Suzuki, T. (2004). Maillard reaction rate in various matrices. *Bioscience, Biotechnology, and Biochemistry*, 68, 2285-2288.

Leloup, V. M., Colonna, P., Ring, S. C., Roberts, K., Wells, B. (1992). Microstructure of amylose gel. *Carbohydrate Polymers*, 18,189-197.

Liang, J., Ludescher, R. D. (2011).Antioxidant modulate molecular mobility, oxygen permeability, and microstructure in zein films. *Journal of Agricultural and Food Chemistry*, 59, 13173-13180.

Liang. J., Corradini, M.G., Ludescher, R.D. (2014) Influence of antioxidant structure on local molecular mobility in amorphous sucrose. *Carbohydrate Research*, 383, 14-20.

Lievonen, S. M., Laaksonen, T. J., Roos, Y. H. (1998). Glass transition and reaction rates: nonenzymatic browning in glassy and liquid systems. *Journal of Agricultural and Food Chemistry***,** 46, 2778-2784.

Lindsey, C. P., Patterson, G. D. (1980). Detailed comparison of the Williams-Watts and Cole-Davidson functions. *Journal of Physical Chemistry*, 2, 3348-3357.

Lutz, E. T. G., van der Maas, J. H. (1994). Hydrogen bonds in crystalline carbohydrates: a variable temperature FT-IR study. *Journal of Molecular Structure*, 324, 123-132.

Lourdin, D., Bizot, H., Colonna, P. (1997). Antiplasticization in starch–glycerol films. *Journal of Applied Polymer Science*, 63, 1047-1053.

Matiacevich, S. B., Santagapita, P. R., Buera, M. P. (2005).Fluorescence from the maillard reaction and its potential applications in food science. *Critical Reviews in Food Science and Nutrition* , 45,483-495.

Namiki, M. (1988). Chemistry of maillard reactions: recent studies on the browning reaction mechanism and the development of antioxidants and mutagens. *Advances in Food Research*, 32, 116-184.

Noel, T. R., Parker, R., Ring, S. G. (2000). Effect of molecular structure and water content on the dielectric relaxation behavior of amorphous low molecular weight carbohydrates above and below their glass transition. *Carbohydrate Research*, 10, 839-845.

Noel, T. R., Ring, S. G., Whittam, M. A. (1990). Glass transitions in low-moisture foods. *Trends in Food Science & Technology*, 1, 62-67.

Obrzut, J., Anopchenko, A., Douglas, J.F., Rust, B.W. (2010).Relaxation and antiplasticization measurements in trehalose-glycerol mixtures—A model formulation for protein preservation. *Journal of Non-Crystalline Solids*, 356, 777-781.

Orford, P. D., Parker, R., Ring, S. G. ,Smith, A. C. (1989).Effect of water as a diluent on the glass transition behaviour of malto-oligosaccharides, amylose and amylopectin. *International Journal of Biological Macromolecules*, 11, 91-96.

Partanen, R., Marie, V., MacNaughtan, W., Forssell, P., Farhat, I. (2004).^{1}H NMR study of amylose films plasticized by glycerol and water. *Carbohydrate Polymers*, 56, 147-155.

Pravinata, L. C., You, Y. M., Ludescher, R. D. (2005). Erythrosin B phosphorescence monitors molecular mobility and dynamic site heyerogeneity in amorphous sucrose. *Biophysics Journal*, 88, 3551-3561.

Phillips, J. C. (2006). Ideally glassy hydrogen-bonded networks. *Physics Review*, 73, 024210-1-024210-10.

Roos, Y. (1993).Melting and glass transitions of low molecular weight carbohydrates. *Carbohydrate Res*earch, 238, 39-48.

Roos, Y. H., Himberg, M. J. (1994). Nonenzymatic browning behavior, as related to glass transition, of a food model at chilling temperature. *Journal of Agricultural and Food Chemistry*, 42, 893-898.

Roussenova, M., Murith, M., Alam, A., Ubbink, J. (2010), Plasticization, antiplasticization, and molecular packing in amorphous carbohydrate-glycerol matrices. *Biomacromolecules*, 11, 3237-3247.

Shirke, S., Takhistov, P., Ludescher, R. D. (2005). Molecular mobility in amorphous maltose and maltitol from phosphorescence of Erythrosin B. *Journal of Physical Chemistry B*, 109, 16119-16126.

Shirke, S., Ludescher, R. D. (2005). Molecular mobility and the glass transition in amorphous glucose, maltose, and maltotriose. *Carbohydrate Research*, 240, 2654-2660.

Sussich, F., Cesàro, A. (2008).Trehalose amorphization and recrystallization. *Carbohydrate Research*, 343, 2667-2674.

Talja, R. A. (2007). Preparation and characterization of potato starch films plasticized with polyols. *Ph.D. thesis*. Department of Food Technology, University of Helsinki.

Wolkers, W. F., Oliver, A. E., Tablin, F., Crowe, J. H. (2004). A fourier-transform infrared spectroscopy study of sugar glasses. *Carbohydrate Research*, 339, 1077-1085.

You, Y., Ludescher, R. D. (2008).Effect of gelatin on molecular mobility in amorphous sucrose detected by erythrosin B phosphorescence. *Carbohydrate Research*, 343, 2657-2666.

You, Y., Ludescher, R. D. (2009).The effect of xanthan on molecular mobility in amorphous sucrose detected by erythrosin B phosphorescence. *Journal of Agricultural and Food Chemistry*, 57, 709-716.

You, Y. M., Ludescher, R. D. (2010). The effect of molecular size on molecular mobility in amorphous oligosaccharides. *Food Biophysics*, 5, 82-93

You, Y. M., Ludescher, R. D. (2011). Effect of starch on the molecular mobility of amorphous sucrose. *Journal of Agricultural and Food Chemistry*, 59, 3340-3347.

Chapter VII: Summary and Future Work

1. Summary

In this work, use spectroscopic and other physical techniques to investigate how the food additives modulate the molecular mobility, local structure, strength of hydrogen bond, and rates of chemical reaction within amorphous food solid matrices. It builds on the previous work in Dr. Ludescher's lab indicating that composite sugar matrixes can greatly influence the physical properties of amorphous food solids and some food addtives with small molecular weights (glycerol and sucrose; maltose and maltitol; lactose and lactitol) could lower the rates of molecular mobility in carbohydrate matrixes (Shirke and Ludescher, 2005; Lukasik and Ludescher, 2006; You and Ludescher, 2007; You and Ludescher, 2009). The latter phenomenon, comparable to the well-known process of anti-plasticization seen in synthetic polymers, appears to be wide-spread in biomaterials and raises the enticing possibility that judicious manipulation of food composition may dramatically enhance the stability of foods, food ingredients, and encapsulation matrixes containing extensive amorphous regions. A detailed study of the effect of composition on molecular mobility, local structure, and the rates of chemical reaction and physical change in amorphous sugars and carbohydrates is thus warranted.

Luminescence from triplet probe Ery B and tryptophan provide spectroscopic characteristics such as lifetime and emission energy that are sensitive to molecular mobility of local environment and oxygen diffusion. Measurements of emission energy and lifetime were made to investigate the temperature- and composition-dependence of molecular mobility and oxygen diffusion in amorphous carbohydrate and protein matrices. In those matrices, the molecular mobility (both dipolar relaxation and collisional quenching) increased gradually below and

dramatically close and above the T_g; the distribution of emission energy and lifetime provided evidence of dynamic site heterogeneity in amorphous biomaterials.

Food additives like plasticizer (glycerol), sugars (glucose, matitol, and sucrose), antioxidants (gallic acid and methyl, propyl and octyl gallate) and polymers (methyl cellulose) were selected to investigate how variation in molecule nature influences physicochemical properties in amorphous food matrices, and the relation between physicochemical factors like T_g, microstructure, oxygen diffusion, browning reaction, hydrogen bond, and molecular mobility were systemically studied.

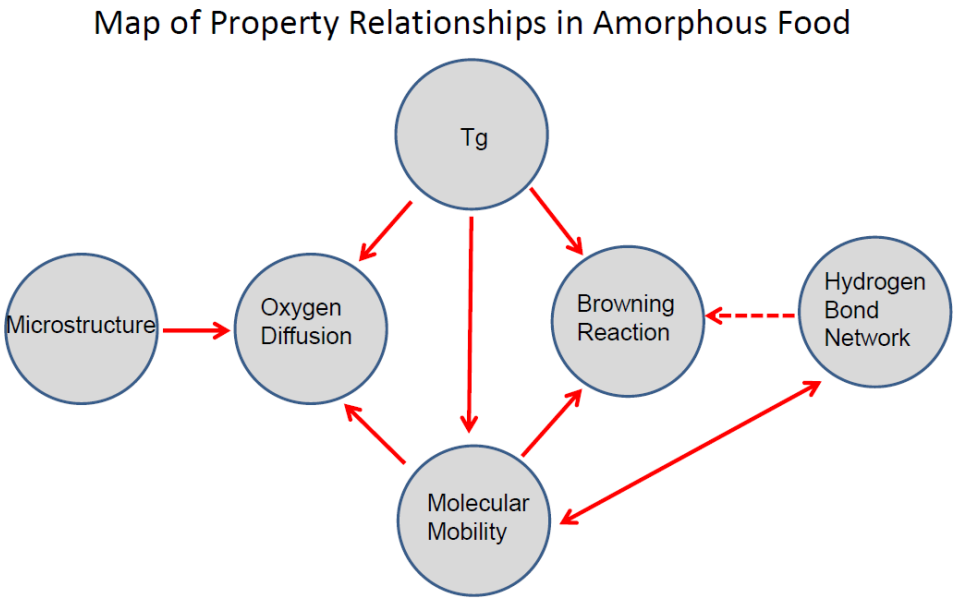

(a) Influence of antioxidants

The effect of the antioxidants gallic acid and methyl, propyl and octyl gallate on the molecular mobility and hydrogen bond network in sucrose-based films was studied. Using tryptophan amino acid as a luminescent probe dispersed in the films, Local molecular mobility increased in the following order: sucrose < sucrose-octyl gallate < sucrose-propyl gallate ⩽ sucrose-methyl gallate ⩽ sucrose-gallic acid. The antioxidants also modulated the activation

energy for matrix motions that quench the tryptophan phosphorescence in a structure-dependent manner. IR measurements as a function of temperature indicated that hydrogen bond strength in these films followed a rank order (sucrose-methyl gallate > sucrose-gallic acid > sucrose-propyl gallate > sucrose > sucrose-octyl gallate) that was nearly the reverse of that seen in matrix mobility. Analysis of the differential effects of the antioxidants suggests that the presence of the hydroxyl benzoyl head group increased matrix molecular mobility and hydrogen bond strength while the saturated carbon chain decreased mobility and bond strength. The influence of the carboxyl group on film properties was comparable to that of the formyloxy group. These results indicate that the addition of specific functional ingredients such as antioxidants may significantly affect the physical properties and consequently functional properties of edible films in ways that might condition their use. The observed changes are closely related to the chemical structure of the added species.

(b) Influence of glycerol

The effect of glycerol on the molecular mobility, oxygen diffusion and hydrogen bonding in amorphous glucose, starch and zein matrices was studied. Erythrosin B (Ery B) was used to spectrally characterize the temperature dependence of mobility in glucose/glycerol and zein/glycerol films from 100 ℃ down to -10 ℃. When normalized to glass-transition temperature (T_g), the lifetime and stretching exponent of Ery B and the value of k_{TS0} over the range of T-T_g from -50 ℃ to 91 ℃ were comparable for glucose matrixes at all glycerol contents. These data demonstrate that both the average rate of matrix mobility and the width of the distribution of matrix mobility rates around the glass transition were largely unaffected by glycerol. The IR hydrogen bond bandwidth increased at higher glycerol content, suggesting that the strength of the bond became more widely distributed with the added glycerol. An

increase with temperature in the hydrogen bond peak frequency indicated the transformation of associated hydroxyl to free hydroxyl. These results support a model in which glycerol plasticizes the glucose matrix across the entire range of concentrations while providing no evidence for the antiplasticization seen in other sugar matrixes.

In the zein films, dipolar relaxation around the triplet state of Ery B was weakened and the extent of relaxation was decreased by adding glycerol at low concentration ($\leqslant$ 10%), indicating the role of antiplasticizer in zein films at this concentration range. Consistently, measurements of the rate of non-radiative decay from the Ery B triplet state indicated that glycerol only performed as a plasticizer and increased the local mobility of the zein matrix at and above ~20 wt %, while for the films with glycerol at the content $\leqslant$20 wt %, the local mobility remained nearly constant or only slightly increased compared with that in the pure zein. Though there is a transition from antiplasticizer to plasticizer at higher content, glycerol dramatically suppressed the oxygen permeability of the film in the whole concentration range tested, even in the antiplasticizer region at low concentrations ($\leqslant$ 10%). AFM images indicated that glycerol induced aggregation of zein complexes, which could lead to a more condensed film. These results indicate how the addition of glycerol to zein films could affect the physical properties, structure and thus functional properties in ways that influence their eventual use.

In starch films, dipolar relaxation around the triplet state of Ery B was enhanced by addition of glycerol and the extent of relaxation increased at low and intermediate but decreased at higher temperature. The glycerol content-dependent onset temperature for this transition was 70 ℃ for pure starch and decreased to 40 ℃ for a matrix with 30% glycerol. Measurements of the rate of non-radiative decay from the Ery B triplet state indicated that glycerol plasticized the starch

matrix above ~10 wt. % while at lower content glycerol acted as an antiplastizer to increase the matrix molecular mobility. These matrix properties were related to glycerol-dependent increases in hydrogen bond strength as measured by IR and AFM imaging studies related mobility changes to the effect of glycerol on the microstructure of the starch films.

(c) Influence of sugars and methylcellulose

Effect of non-reducing sugars or methylcellulose on the physical properties and rates of non-enzymatic browning (NBR) in starch-based glassy matrices were studied using the methods of luminescence and FTIR. Data on the phosphorescence emission energy and lifetime from erythrosin B dispersed in the matrices indicated that sugars decreased starch matrix mobility in a T_g-dependent manner, except for trehalose that interacted with starch in a unique mode, while methylcellulose, the additive with the highest T_g, increase the molecular mobility. Using FTIR we found that methylcellulose decreased the strength of hydrogen bond network and sugars enhanced the hydrogen bond strength by the rank: trehalose > maltitol > sucrose. Comparing those changes with the rate of NBRs, we suggest that NBRs are primarily influenced by matrix mobility, which is modulated by the hydrogen bond network, and interactions among components.

2. Future work

There is still one extremely important question we want to resolve: how could the interaction of sugars with interface of protein dispersed in the sugar matrices influence the properties of mixed amorphous solid. Those physical characters include molecular mobility and conformational change of protein, hydrogen bond network and *T*g of sugar/protein matrices. The techniques we will use including luminescence measurement, DSC, and FTIR.

The addition of sugars to protein matrices can be very beneficial. Sugars can serve as plasticizers, stabilizers, and protectants for protein matrices (Koreyoshi, Tomohiro, Takaharu & Kazuhiro, 2003). The specific sugar-protein interactions are generally thought to prevent conformational changes in the protein during dehydrate and storage (Crowe, Crowe, Carpenter & Aurell, 1987). Sugar-based foods mixed with protein often exist in solid, dried matrices and are subjected to high temperature in some cases. The induced changes of molecular mobility and hydrogen bond network will greatly influence the reaction inside the sugar/protein matrices. Temperature is one of the main factors determining the stability of proteins, and thus, the degree of protein conformational changes, which is a primary degradation pathway of protein-based matrices (Manning, Patel & Borchardt, 1989).

Fourier transform infrared (FTIR) spectroscopy is a frequently used technique to analyze secondary protein structure and hydrogen bond network in the solid matrix. IR absorption bands, corresponding to C=O (amide I band), N-H (amide II band), and C-N (amide III band) of peptide linkages, are resolved into multiple component bands corresponding to different secondary structure (Koreyoshi, Ken-Ichi, Toru, Yoshinobu & Nakanishi, 2009). Hydrogen bonds are the primary intermolecular forces that maintain the state of the amorphous sugar matrix. Hydroxyl groups in a carbohydrate solid can be either associated, hydrogen bonded to other hydroxyl groups, or free, not involved in hydrogen bonds. The vibrational frequency of both types of hydroxyls are distributed in the frequency range 3000-3600 cm-1, while the frequency of free hydroxyls extends primarily into the higher frequency region (Kondo, 2007). Thus, when associated hydroxyls change to free hydroxyls, the hydroxyl absorbance in this region will shift to higher frequency. By controlling the sample temperature, changes in secondary structures of

proteins embedded in dried solids and the hydrogen bond network due to alterations in temperature can be analyzed.

The phosphorescence of Trp residues in protein can provide an exquisitely sensitive monitor of protein conformation. In a homogeneous protein site the spectrum exhibits a well resolved vibronic band as narrow as 3.8-3.9 nm. The scope of this band ranges from 403 to 420 nm depending on the polarity of neighbouring side chains (Gabellieri, Rahuel-Clermont, Branlant & Strambini, 1997). Perturbations of the structure that increase the heterogeneighty of the chromophore's environment will be characterized by shifts and loss in resolutions of the spectrtrum. The intrinsic lifetime, on the other hand, is governed principally by the local flexibility of the polypeptide (Edi Gabellieri & Giovanni, 2000). Thus we can measure the spectra and lifetime of phosphorescence from Trp to detect the subtle changes in second structure and molecular mobility in the protein complex that is induced by binding of substrates/allosteric effectors and change of environmental temperature.

In the future research, we will prepare for the amorphous sugar solid by mixing protein in the sugar film forming solution and dehydrate the solution in desiccator with 0% moisture content. The dehydrated non-reducing sugar / protein solid contain sugars with different molecular weight and and BSA will be measured with a temperature –scanning Fourier transform infrared (TS-FTIR) using a temperature-controlled FTIR spectrometer. The samples will be heated gradually and the IR spectra of sample will be measured at various temperatures. The secondary protein structures and strength of of hydrogen bond at different temperatures will be determined by analyzing amide I bands in the IR spectra and the hydroxyl band above 3000 cm^{-1} respectively. The phosphorescence from Trp will be used to probe the conformational state of BSA. By detect the variations in the lifetime and spectra of phosphorescence from Trp, we mean to know the

change of conformation and molecular mobility induced by interaction of sugars with protein. Because Tg ́s are important for this change, the Tg ́s of the of sugar/protein matrices will be measured by DSC.

The successful completion of this research will provide a detailed understanding how the perturbations of molecular mobility and conformation can be induced by intact of protein interface with sugar molecules and guidance in choice of sugar stabilizers for the prevention of protein degradation and for improvement of nature of usage for biomaterial film in food industry.

References

Lukasik, K. V., Ludescher, R. D. (2006) Molecular mobility in water and glycerol plasticized cold- and hot-cast gelatin films. *Food Hydrocolloid.* 20, 96-105.

Shirke, S., Takhistov, P., Ludescher, R. D. (2005) Molecular mobility in amorphous maltose and maltitol from phosphorescence of Erythrosin B. *J. Physical Chemistry B*, 109, 16119-16126.

You, Y. M., Ludescher, R. D. (2007) The effect of glycerol on molecular mobility in amorphous sucrose detected by phosphorescence of erythrosine B. *Food Biophysics*, 2, 133-145.

You, Y. M., Ludescher, R. D. (2009) Effect of xanthan on the molecular mobility of amorphous sucrose detected by erythrosin B phosphorescence. *Journal of Agriculture and Food Chemistry*, 57, 709-716.

Koreyoshi, I., Tomohiro, O., Takaharu, S., Kazuhiro, N. (2003) Effects of types of sugar on the stabilization of protein in the dried state. *Journal of Pharmaceutical Sciences*, 92, 266-274.

Crowe, J.H., Crowe, L.M., Carpenter, J. F., Aurell, W. C. (1987) Stabilization of dry phospholipid bilayers and proteins by sugars. *Biochemistry Journal*, 242, 1–10.

Manning, M.C., Patel, K., Borchardt, R.T. (1989) Stability of protein pharmaceuticals. *Pharmaceutical Research*, 8, 903-918.

Koreyoshi, I., Ken-Ichi, O., Toru, Y., Yoshinobu, M., Nakanishi, K. (2009) Temperature scanning FTIR analysis of secondary structure of proteins embedded in amorphous sugar matrix. *Journal of Pharmaceutical Science*, 98, 3088-3098.

Kondo, T. (1997) The assignment of IR absorption bands due to free hydroxyl groups in cellulose. *Cellulose,* 4, 281-292.

Gabellieri, E., Rahuel-Clermont, S., Branlant, G., Strambini, G.B. (1996) Effects of NAD+ binding on the luminescence of tryptophans 84 and 310 of glyceraldehyde-3-phosphate dehydrogenase from Bacillus stearothermophilus. *Biochemistry*, 35, 12549-12559.

Edi Gabellieri, S., Giovanni, B. S. (2000) Tryptophan phosphorescence as a monitor of protein conformation in molecular films. *Biosensors and Bioelectronics,* 15, 483-490.